

Benjamin Igbodo

**IMPLEMENTATION OF STANDARD METHODS FOR PARAMETERS ROUTINELY
MONITORED IN WASTEWATER TREATMENT PLANTS AND APPLICATION IN
BIOAUGMENTATION WITH *MYCOLICIBACTERIUM* SP. IN GRANULAR SLUDGE
REACTORS**



UAAlg

UNIVERSIDADE DO ALGARVE

Faculdade de Ciências e Tecnologia

2023

Benjamin Igbodo

**IMPLEMENTATION OF STANDARD METHODS FOR PARAMETERS ROUTINELY
MONITORED IN WASTEWATER TREATMENT PLANTS AND APPLICATION IN
BIOAUGMENTATION WITH *MYCOLICIBACTERIUM* SP. IN GRANULAR SLUDGE
REACTORS**

Mestrado *Erasmus Mundus* em Qualidade em Análises

Trabalho efetuado sob a orientação de:

Prof. Maria Clara Costa (University of Algarve)

Dr. Jorge Carliar (Centre of Marine Sciences of Algarve)



UAAlg

UNIVERSIDADE DO ALGARVE

Faculdade de Ciências e Tecnologia

2023

**IMPLEMENTATION OF STANDARD METHODS FOR PARAMETERS ROUTINELY
MONITORED IN WASTEWATER TREATMENT PLANTS AND APPLICATION IN
BIOAUGMENTATION WITH *MYCOLICIBACTERIUM* SP. IN GRANULAR SLUDGE
REACTORS**

Declaration of Authorship

I declare that I am the author of this work, which is original. The work cites other authors and works, which are adequately referred in the text and are listed in the bibliography.

Signature

Date

Name: Benjamin Igbodo

Copyright on behalf of Benjamin Igbodo, and the University of Algarve, “The University of Algarve reserves the right to, in accordance with the provisions of the Copyright Law and Code, archive, reproduce, and publish this work in any medium, as well as to disseminate this work through academic repositories and allow it to be copied and distributed for educational, research, and non-commercial purposes, while ensuring credit is given to the work’s author and publisher.”

Funding

This work is financed by Portuguese national funds through FCT – Fundação para a Ciência e a Tecnologia, I.P., within the scope of the project PTDC/CTA-AMB/7782/2020.

Acknowledgement

I wish to extend my gratitude to God almighty and the European Commission for the scholarship of my master's program; this work would not have been possible without their financial support. I am also grateful to the entire staff of EMQAL consortium, University of Bergen Norway, University of Algarve in Portugal, the Centre of Marine Sciences (CCMAR), and the research project management team for their indispensable forbearance and feedback which was instrumental in forging my interesting academic term. Additionally, this endeavor would not have been successful without the selfless support from the following individual who provided knowledge and expertise for my research: Dr. Jorge Daniel Dias Carlier, Prof. Maria Clara Semedo da Silva Costa, the company Águas do Algarve, S.A. (AdA) and Eng. Patrício Fontinha for helping with collection of the granular sludge sample, and Dr. António Martins who authorized and made possible the collection and finally Prof. Bjorn Grung the EMQAL program director.

Furthermore, I am very grateful to my laboratory colleagues who inspired me and impacted me positively. Thanks also go to the members of my cohort especially Joachim Arikibe, Janet Amanze, Abdullah Ismail, Alba Gascon Nicolas, and Ismaiel Fatma for their moral support.

Lastly, I will be remiss in not mentioning my family, especially my wife Mrs. Blessing Oghale Igbodo, my daughter and my parents whose prayers and emotional support have kept my spirit and motivation high during this endeavor.

Dedication

I dedicate this thesis to my father and mother, Mr. and Mrs. Igbodo, and my wife Mrs. Blessing Oghale Igbodo.

Abstract

The effective treatment of domestic wastewater is pivotal for the health and sanitation status of water resources and wastewater reclamation campaigns. Thus, this study was aimed at evaluating the performance of Aerobic granular Sludge (AGS) in the treatment of synthetic wastewater during a bacteria bioaugmentation (*Mycolicibacterium spp* strain) experiment using laboratory-scale Sequencing Batch Reactors (SBRs). The routine parameters evaluated using UV-visible spectrophotometry methods were Total Nitrogen (TN), ammonia nitrogen ($\text{NH}_3\text{-N}$), nitrate nitrogen ($\text{NO}_3^-\text{-N}$), phosphate phosphorus ($\text{PO}_4^{3-}\text{-P}$) and Chemical Oxygen Demand (COD), on samples from the influents and effluents of the SBRs. Nitrite nitrogen ($\text{NO}_2^-\text{-N}$) was evaluated by mass balance and pH was measured using a benchtop pH meter. The individual standard calibration curves for the parameters had regression coefficients > 0.995 and the LOD (for qualitative analysis) and LOQ (for quantitative analysis) values were compatible with the concentrations of the samples analyzed while the validation process (using reference materials) yielded relative accuracy $> 94\%$. The SBR effluent samples had concentrations of TN > 20 mg/L since effective nitrification but incomplete denitrification was achieved as indicated by $\text{NH}_3\text{-N}$ usually < 1 mg/L (except for two days with lower aeration periods) and $\text{NO}_3^-\text{-N}$ generally around 20 mg/L (or below 10 mg/L just during acclimatation and at the two days with less aeration), while NO_2^- concentration was in “counter cycle” with NO_3^- . The COD dropped from around 1000 to < 40 mg/L O_2 , showing effective treatment of organic compounds, although, dephosphatation was not achieved and phosphorus was similar in the influent and effluent samples, ranging between 78 – 128 mg/L. The pH conditions were good for domestic wastewater bio-treatment, ranging between 7.3 – 7.8 in the SBR. Indeed, overall, the SBR conditions favored the activities of Ammonia Oxidizing Bacteria (AOB) and Nitrites Oxidizing Bacteria (NOB) and other microorganisms in the AGS, regardless of the bioaugmentation experiment, and thus the wastewater was treated in terms of ammonia, nitrites, and organics removal. Yet, either in the bioaugmented or in the control reactors, the conditions did not favor the Denitrifying Polyphosphate Accumulating bacteria (DPB) activity, the group of Phosphorus Accumulating Organisms (PAOs) usually involved in the removal of P and N in SBRs. Lack of anaerobic or anoxic conditions was suggested as a possible cause of this incomplete treatment. In what concerns Paracetamol removal, the results showed a slightly faster removal of this drug and a very evident faster removal of its transformation product hydroquinone in the bioreactors bioaugmented with the bacterial strain *Mycolicibacterium aubagnense* HPB1.1 in comparison to the non-bioaugmented bioreactors.

Keywords: Municipal Wastewater Treatment; Trueness of measurements; Sequencing Batch Reactor; Bioaugmentation; Paracetamol removal; Hydroquinone removal

Resumo

O tratamento eficaz de águas residuais domésticas é fundamental para o estado de saúde e saneamento dos recursos hídricos e campanhas de recuperação de águas residuais. Assim, este estudo teve como objetivo avaliar o desempenho de lama granular aeróbica (LGA) no tratamento de efluentes sintéticos durante uma experiência de bioaumentação de bactérias (uma estirpe de *Mycolicibacterium* sp.) usando reatores em Batelada Sequencial (RBS) em escala laboratorial. Os parâmetros de rotina avaliados usando métodos de espectrofotometria UV-visível foram nitrogénio Total (TN), nitrogénio amoniacal (NH_3 - N), nitrogénio de nitrato (NO_3^- - N), fósforo de fosfato (PO_4^{3-} - P) e Carência Química de Oxigénio (CQO), em amostras dos afluentes e efluentes dos RBS. O nitrogénio de nitrito (NO_2^- - N) foi avaliado por balanço de massa e o pH foi medido usando um medidor de pH de bancada. As curvas de calibração padrão para os parâmetros analisados tiveram coeficientes de regressão $> 0,995$ e valores de LOD e LOQ compatíveis com as concentrações das amostras que se pretendem analisar, enquanto o processo de validação (usando materiais de referência) revelou precisão relativa $> 94\%$. As amostras de efluente do RBS apresentaram concentrações de TN > 20 mg/L uma vez que foi alcançada nitrificação efetiva, mas a desnitrificação foi incompleta, conforme indicado por NH_3 - N geralmente < 1 mg/L (exceto por dois dias com períodos de arejamento mais baixos) e NO_3^- - N geralmente em torno de 20 mg/L (ou abaixo de 10 mg/L apenas durante a aclimação e nos dois dias com menos arejamento), enquanto a concentração de NO_2^- - N estava em “contraciclo” com NO_3^- - N. A CQO caiu de cerca de 1000 para < 40 mg/L O_2 , mostrando tratamento eficaz de compostos orgânicos, porém, a desfosfatação não foi alcançada e o PO_4^{3-} - P foi semelhante nas amostras de afluente e efluente, variando entre 78 – 128 mg/L. As condições de pH foram boas para o biotratamento de efluentes domésticos, variando entre 7,3 – 7,8 nos RBS. De facto, em geral, as condições dos RBS favoreceram as atividades de Bactérias Oxidantes de Amónia e Bactérias Oxidantes de Nitritos assim como de outros microrganismos da LGA, independentemente da experiência de bioaumentação, e assim as águas residuais foram tratadas em termos remoção de amónia, nitritos e orgânicos. No entanto, tanto nos reatores bioaumentados quanto nos reatores controlo, as condições não favoreceram a atividade das Bactérias Desnitrificantes Acumuladoras de Polifosfato (DPAB), grupo de Organismos Acumuladores de Fósforo (PAO) usualmente envolvidos na remoção de P e N em RBS. A falta de condições anaeróbicas ou anóxicas foi sugerida como uma possível causa desse tratamento incompleto. No que respeita à remoção do Paracetamol, os resultados mostraram uma remoção ligeiramente mais rápida deste fármaco e uma remoção muito mais rápida do seu produto de transformação hidroquinona nos biorreatores bioaumentados com a estirpe

bacteriana *Mycolicibacterium aubagnense* HPB1.1 em comparação com os bioreatores sem bioaumentação.

Palavras-chave: Tratamento de efluentes municipais; Veracidade das medições; Reatores em batelada sequencial; Bioaumentação; Remoção de paracetamol; Remoção de hidroquinona

Table of Contents

Declaration of Authorship	i
Funding	ii
Acknowledgement	ii
Dedication	iii
Abstract.....	iv
Resumo	vi
List of Figures	xi
List of Tables	xiii
List of abbreviations	xv
1. Introduction	1
1.1. Components of Domestic Wastewater.....	1
1.2. Reasons to treat Domestic Wastewater.....	5
1.3. Stages of wastewater treatments.....	9
1.3.1. The Primary Treatment Stage.....	10
1.3.2. The Secondary Treatment strategy.....	10
1.3.3. Bacterial growth during STP.....	13
1.4. Tertiary Treatment Strategy.....	15
1.5. Wastewater Activated Sludge morphology and microorganism communities.....	16
1.5.1. Flocculent Activated Sludge.....	17
1.5.2. Aerobic Granular Sludge	19
1.6. The emerging Concept of Bioaugmentation Strategies of Batch Reactors.....	22
1.7. Paracetamol removal in WWTPs.....	23
1.8. Objective	23
2. Materials and Methods	24
2.1. Evaluation of methods for wastewater analysis.....	24
2.1.2. Ammonia nitrogen method and calibration Standards	24
2.1.3. Total nitrogen method and calibration standards	25
2.1.4. Nitrate nitrogen method and calibration standards	25
2.1.5. Phosphate-phosphorus method and calibration standards	25
2.1.6. Chemical Oxygen Demand Standard.....	26
2.2. Calibration Curves construction	26
2.3. Precision, accuracy, and trueness.....	27
2.4. Bioreactor setup and operational conditions	29
2.5. Characterization of Granular Sludge used in the experiment.....	31

2.5.1. Sludge Volume Index and Mixed Liquor Suspended Solids	31
2.5.2. Morphological characteristics.....	32
2.5.3. Bioaugmentation and Paracetamol removal	32
3. Results.....	34
3.1. Calibration curves and trueness of analytical methods for wastewater analysis.....	34
3.1.1. Ammonium Nitrogen method	34
3.1.2. Total Nitrogen method.....	40
3.1.3. Nitrate Nitrogen method.....	43
3.1.4. Phosphate-phosphorus method	46
3.1.5. Chemical Oxygen Demand method	49
3.2. The performance of the bioreactor on wastewater treatment.....	52
3.2.1. Total Nitrogen in Bioreactors.....	52
3.2.2. Ammonia Nitrogen in Bioreactors.....	53
3.2.4. Nitrate Nitrogen in Bioreactors.....	54
3.2.5. Chemical Oxygen Demand (COD) in Bioreactors.....	55
3.2.5. Phosphate-Phosphorus in Bioreactors	56
3.2.6. pH conditions in the bioreactors.....	57
3.3. Characterization of granular sludge used in the experiment.....	58
3.4. The results of paracetamol removal after bioaugmentation.	59
4. Discussion	64
4.1. Calibration curves and trueness of analytical methods for wastewater analysis.....	64
4.1.1. Total nitrogen standard calibration curve	64
4.1.2. Ammonium Standard Calibration Curve.....	65
4.1.3. The Nitrate Nitrogen Standard Curve.....	67
4.1.4. Phosphate-Phosphorus Standard Curve and Validation Results.....	69
4.1.5. COD Calibration Curve and validation result.	70
4.2. SBR bioreactors.....	71
4.2.1. Total Nitrogen, Ammonia and Nitrates.....	71
4.2.2. COD	73
4.2.3. Phosphate-phosphorus	75
4.3. pH.....	76
4.3.1 Role of pH in Total nitrogen removal	76
4.3.2. Role of pH in Phosphorus removal	78
4.3.3. Role of pH in COD removal.....	79
4.4. The removal of Paracetamol after bioaugmentation	79
4.5. Conclusions	80

4.6. Future prospects.....	81
5. References.....	82

List of Figures

Figure 1: Typical Source of Domestic Wastewater	2
Figure 2: Chart depicting wastewater characteristics.....	3
Figure 3: Schematics depicting the major sources of phosphorus.....	8
Figure 4: Flow chart depicting a typical WWTP arrangement.....	11
Figure 5: Bacteria growth curve illustration.....	14
Figure 6: Representation showing (A) conventional Floc and (B) Granular Sludge.....	17
Figure 7: Schematics depicting the typical activated sludge flocs structure.....	18
Figure 8: The illustration depicting sludge age process.....	19
Figure 9: Schematics showing aerobic granule formation mechanism and process	20
Figure 10: Graphical illustrations of aerobic granular sludge.....	21
Figure 11: Schematics showing the bioreactor setup.....	31
Figure 12: LCK 304 Ammonium Nitrogen calibration curve plot and residual plot.....	35
Figure 13: Ammonia nitrogen (Salicylate method) calibration curve and residual plot.....	38
Figure 14: Total Nitrogen calibration curve plot and residual plot.....	41
Figure 15: Nitrate Nitrogen calibration curve plot and residual plot.....	44
Figure 16: Phosphate-Phosphorus calibration curve plot and residual plot.....	47
Figure 17: Chemical oxygen demand calibration curve plot and residual plot.....	50
Figure 18: Graph showing total nitrogen results from test reactors and control reactors.....	53
Figure 19: Graph showing ammonia nitrogen results from test reactors and control reactors.....	54
Figure 20: Graph showing nitrite nitrogen results from test reactors and control reactors.....	55
Figure 21: Graph showing nitrate nitrogen results from test reactors and control reactors.....	55
Figure 22: Graph showing COD results from test reactors and control reactors.....	56

Figure 23: Graph showing phosphate-phosphorus results from test reactors and control reactors.....	57
Figure 24: Graph showing the bioreactors pH results for test reactors and control reactors.....	58
Figure 25: The morphological observation of granular sludge under a Leica Zoom 2000 Magnifier (x 7)	59
Figure 26: Pie chart statistical representation aspects and shape of the observed granules.....	60
Figure 27: Calibration curve obtained for Paracetamol by HPLC analysis.....	61
Figure 28: Calibration curve obtained for Hydroquinone by HPLC analysis.....	62
Figure 29: Graph showing the evolution of paracetamol during the first cycle aeration period.....	63
Figure 30: Graph showing the evolution of paracetamol during the second cycle aeration period.....	63
Figure 31: Graph showing the evolution of hydroquinone during the first cycle aeration period.....	64
Figure 32: Graph showing the evolution of hydroquinone during the second cycle aeration period.....	64

List of Tables

Table 1.1: The typical composition of untreated domestic wastewater	4
Table 1.2: Examples of bacteria in biological wastewater and their application in WWTPs.....	12
Table 1.3: The physical characteristics of floc and granular activated sludge	17
Table 2.4: Standard reference materials concentrations	28
Table 2.5a: Time of each phase during the SBR cycles, throughout the operation, and minimal imposed settling velocity in the different operation stages	30
Table 2.5b: Synthetic sewage preparation and composition	30
Table 3.6a: The data set for the Ammonium Nitrogen indophenol blue method (LCK 304, HACH) standard calibration curve	36
Table 3.6b: The data sets for the Ammonium-Nitrogen indophenol blue method (LCK 304, HACH) parameters of trueness based on analysis of 1 mg/L ammonia nitrogen Reference Material	37
Table 3.7a: The data sets for the Ammonia- Nitrogen Salicylate method (method 8155, HACH) standard calibration curve.....	39
Table 3.7b: The data sets for the Ammonia-Nitrogen Salicylate method (method 8155, HACH) parameters of trueness based on analysis of 0.25 mg/L ammonia nitrogen Reference Material	40
Table 3.8a: The data set for the Total Nitrogen method (10072, HACH) standard calibration curve.....	42
Table 3.8b: The data sets for the total nitrogen method (10072, HACH) parameters of trueness based on the analysis of low range (7 mg / L nitrogen) and high range (50 mg / L nitrogen) standard reference materials	43
Table 3.9a: The data sets for the Nitrate Nitrogen cadmium reduction method (8039, HACH) standard calibration curve	45
Table 3.9b: The data sets for the nitrate nitrogen cadmium reduction method (8039, HACH) parameters of trueness based on the analysis of low range (6 mg / L nitrate nitrogen) and high range (25 mg / L nitrate nitrogen) standard reference materials	46

Table 3.10a: The data sets for the Phosphate-phosphorus ascorbic acid method (8048, HACH) standard calibration curve48

Table 3.10b: The data sets for the phosphate-phosphorus ascorbic acid method (8048, HACH) parameters of trueness based on analysis of 1 mg / L phosphate phosphorus standard reference material49

Table 3.11a: The data sets for the chemical oxygen demand dichromate method (LCI – 400, HACH) standard calibration curve51

Table 3.11b: The data sets for the chemical oxygen demand dichromate method (LCI – 400, HACH) parameters of trueness based on analysis of 500 mg / L O₂ reference standard material.52

List of abbreviations

AGS	Aerobic granular Sludge
AND	Alternating Nitrification and Denitrification
ANOVA	Analysis of Variance
AOB	Ammonia Oxidizing Bacteria
APHA	American Public Health Association
ASFs	Activated Sludge Floes
AWWA	American Water Works Association
BOD	Biochemical Oxygen Demand
CBOD	Carbonaceous Biochemical Oxygen Demand
COD	Chemical Oxygen Demand
COD	Chemical Oxygen Demand
DPB	Denitrifying Polyphosphate Accumulating Bacteria
EBPR	Enhanced Biological Phosphorus Removal
EPS	Extracellular Polymeric Substances
FAS	Flocculent Activated Sludge
FSCC	Final Standard Calibration Curve
GAO	Glycogen-Accumulating Organisms
LOD	Limit of Detection
LOQ	Limit of Quantification
MLSS	Mixed Liquor Suspended Solids
NBOD	Nitrogenous Biochemical Oxygen Demand
NH ₃ - N	Ammonia nitrogen
NO ₃ – N	Nitrate nitrogen
NOB	Nitrites Oxidizing Bacteria
PAO	Polyphosphate-Accumulating Organisms
PAOs	Phosphorus Accumulating Organisms
PES	Polyethersulfone
PHA	Poly- β -hydroxyalkanoates

PO ₄ – P	- Phosphate phosphorus
PTP	Primary Treatment Phase
PVC tube	- Polyvinyl chloride tube
SBRs	Sequencing Batch Reactors
SND	Simultaneous Nitrification and Denitrification
SRM	Standard Reference Materials
SS	Sum of squares
STP	Secondary Treatment Phase
SV	Sludge Volume
SVI	Sludge Volume Index
TN	Total Nitrogen
TOC	Total Organic Carbon
VFA	Volatile Fatty Acid
VOC	Volatile Organic Compounds
WEF	Water Environment Federation
WWTP	Wastewater Treatment Plant

1.0. Introduction

The concept domestic wastewater treatment has in recent decades experienced a surge globally due to its pivotal role in agriculture, environment, and public health concerns (Burdon *et al.*, 2019; Rodriguez-Mozaz *et al.*, 2020; O'Brien *et al.*, 2019). In fact, several institutions such as UNICEF, WHO and the European union amongst others have advocated and emphasized the relevance of domestic wastewater treatment in proportionality to their use in agriculture as well as environmental and public health concerns (Pellegrini *et al.*, 2020; Gutberlet *et al.*, 2020; Boom Carcamo *et al.*, 2022).

Consequently, in developed countries for instance the domestic wastewater treatment and reuse campaign as a mechanism for conserving the limited freshwater resource and safeguarding the aquatic environment have gained prominence and has thus, propelled research scientists, industries, and governmental organizations to initiate several treatment and safe disposal mechanisms, research funding packages and regulatory guidelines in a bid to curtail any adverse effects that may ensue from wastewater management and disposal. Conversely, many developing countries in Africa, Asia, and Latin America use untreated domestic wastewater for its agricultural, and environmental practices with less attention paid to its public health adverse implications as well as lacking the technical-know-how and economic enablement in implementing state-of -the-art wastewater treatment plants and reclamation measures in parallel with the practices in developed countries (Akhkha *et al.*, 2019; Kalpy *et al.*, 2020).

However, series of publications have postulated certain rational encouraging the use of untreated domestic wastewater and its resource for agricultural activities to be chiefly due to the rich variety of nutrients resident in wastewater in the form of nitrogen, phosphorus, potassium, and sulfur (Krogh *et al.*, 2018; Symonds *et al.*, 2019; Bracher *et al.*, 2020; Thiruchelva *et al.*, 2020). These nutrients represent a readily available alternative for farmers to use as fertilizers as well as reducing the cost of crop production. Nevertheless, additional studies have linked the use of untreated wastewater for agricultural practices and the environment to certain health related issues such as cholera, typhoid fever, hepatitis A, and food poisoning in these regions (Huang *et al.*, 2019; Contreras *et al.*, 2020; Lee *et al.*, 2021; Hiruy *et al.*, 2022).

1.1. Components of Domestic Wastewater

Over the years, researchers have asserted the strength and composition of wastewater tends to change significantly enough on an hourly, daily, and seasonal basis across the globe (Abdel-

Aal *et al.*, 2018; Golzar *et al.*, 2020; Sutherland *et al.*, 2021; Hamoda *et al.*, 2021) and these compositions are directly proportional to the natural environment, the diets and lifestyle of the inhabitants figure 1, as well as the *per capita* water usage (Drozdova *et al.*, 2018; Pluciennik-Koropczuk *et al.*, 2021; Shao *et al.*, 2021).

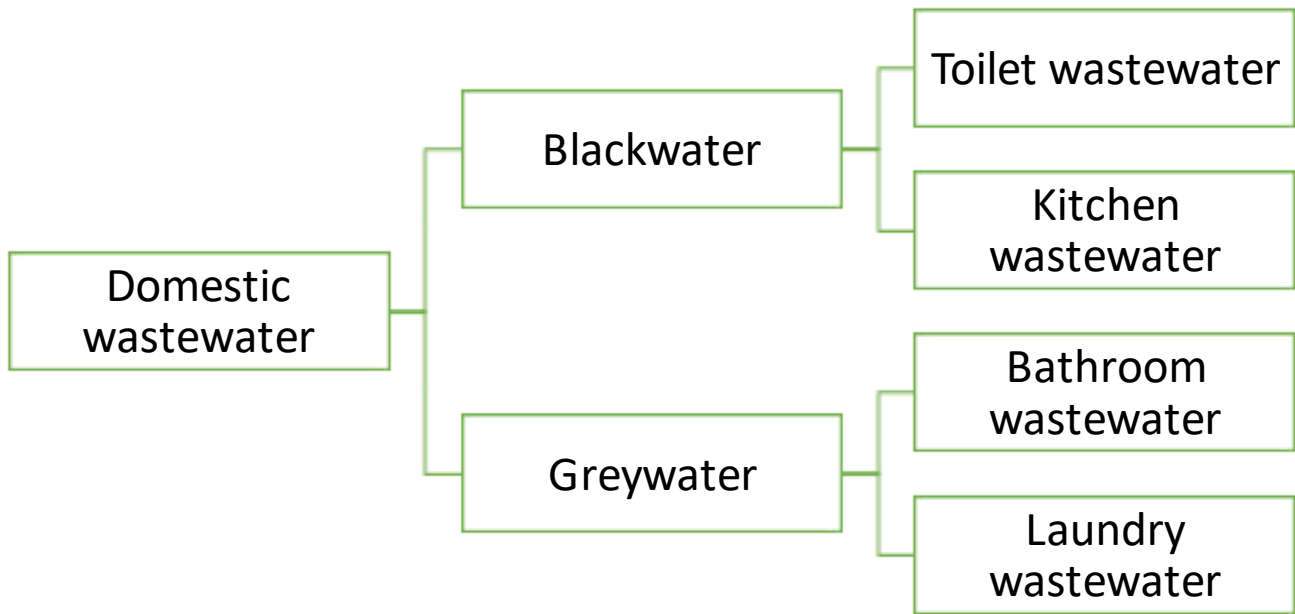
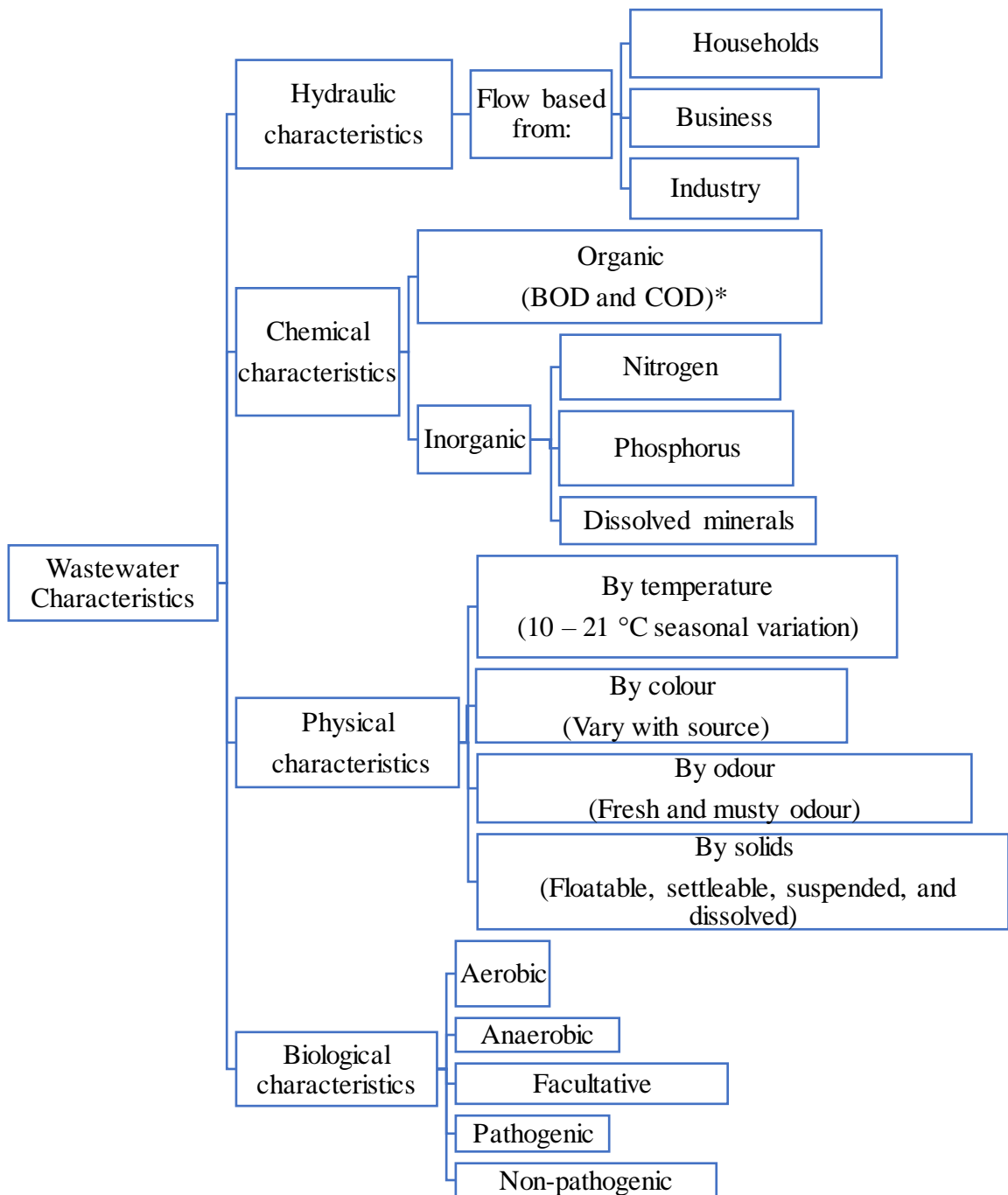


Figure 1: Typical source of domestic wastewater. Domestic wastewater contains 99.9 % water and 0.1 % of organic, inorganic solids and some microorganisms (Feigin *et al.*, 1991). Blackwater constitute contaminated water with toxic chemicals and excrement while greywater comprise used water devoid of toxic chemicals and excrement (Dorji *et al.*, 2022).

Wastewater can be characterized according to several parameters as illustrated in figure 2 and the important categorization include suspended solids, organic load (Sgroi *et al.*, 2018; Zhou *et al.*, 2019), inorganic nutrients (Kekedy-Nagy *et al.*, 2022; Verma *et al.*, 2022), and pathogens (Atif *et al.*, 2018) in water. Based on physical observations of domestic wastewater, it can be said they are often characterized with dissolved solids (about 70 %) which can be precipitated chemically and via biological processes while suspended solids (about 30 %) have been reported to result in the formation of sludge deposits as well as anaerobic conditions when introduced to the environment (Cetin *et al.*, 2018; Gurung *et al.*, 2019).



*BOD: Biochemical Oxygen Demand

*COD: Chemical Oxygen Demand

Figure 2: Chart depicting wastewater characteristics.

Wastewater is composed of organic and inorganic chemicals in a ratio of about 70: 30 % respectively (Masoner *et al.*, 2019; Mehdaoui *et al.*, 2022). Certain research studies have reported the organic component of wastewater to comprise primarily of about 25 % carbohydrates, 65 % proteins, and 10 % fats which reflect the dietary composition of the inhabitants (Gonzalez-Balderas *et al.*, 2020; Cardoso *et al.*, 2020; Noguchi *et al.*, 2021).

Similarly, reports have also posited the inorganic composition of wastewater to be made of heavy metals, nitrogen, phosphorus, pH, sulfur, chlorides, alkalinity, and toxic compounds amongst others (Anh *et al.*, 2021; Hag *et al.*, 2021; Verma *et al.*, 2022; Forouzanmehr *et al.*, 2022). Certain gases: hydrogen sulphide, methane, ammonia, oxygen, carbon dioxide, and nitrogen have been postulated to commonly dissolve in wastewater (Persson *et al.*, 2021; Despot *et al.*, 2021) and other research have asserted the decomposition of organic matter *in situ* in wastewater to often result in production of hydrogen sulfide, methane, and ammonia gases (Nunes *et al.*, 2021; Rolewicz *et al.*, 2021).

The diverse communities of microorganisms present in wastewater include bacteria, viruses, fungi, and protozoa. The common bacteria community includes aerobic bacteria (*Acinetobacter*, *Pseudomonas*, and *Aeromonas*) and Anaerobic bacteria (*Clostridium*, *Methanosarcina*, and *Desulfovibrio*) (Shi *et al.*, 2022; Machnicka *et al.*, 2022). The common viruses found in wastewater include viral pathogens (Korajkic *et al.*, 2022), enteric viruses such as norovirus and adenovirus (Hoque *et al.*, 2023) while the common fungi community found in wastewater includes *Aspergillus*, *Candida*, and *Penicillium* (Ezeonuegbu *et al.*, 2022; Padri *et al.*, 2022). The common protozoa community found in wastewater includes ciliates (*Paramecium*), amoebae (*Acanthamoeba*) and flagellates (*Euglena*) (Johansen *et al.*, 2022). Overall, the presence of these communities in wastewater tends to support the scientific publications asserting the vast pathogenic organisms resident in a given wastewater deposit to have predominantly emanated from humans either infected or carriers of certain diseases (Yan *et al.*, 2018 Thompson *et al.*, 2020; Oeschger *et al.*, 2021). For example, the quantity of concentrated fecal coliforms in raw wastewater composition runs in several hundred thousand to tens of million per 100 mL of sample (Sbahi *et al.*, 2020; Sadek *et al.*, 2021; Miller *et al.*, 2022; Giraldo *et al.*, 2022). Table 1 shows examples of typical characterization of untreated domestic wastewater.

Table 1: The typical composition of untreated domestic wastewater

Analysis Parameters	Unit	Domestic Wastewater Typical Estimated Concentration		
		Concentrated	Moderate	Diluted
Solids, Total (TS)	mg/L	1200	720	350
Suspended Solids (SS)		350	220	100
Fixed	mg/L	75	55	20

Volatile		275	165	80
Settleable Solids	ml/L	20	10	5
BOD (5 – day, 20 ° C)	mg/L	400	220	100
TOC *	mg/L	290	160	80
COD	mg/L	1000	500	250
Nitrogen, Total (TN)		85	40	20
Organic	mg/L	35	15	8
Free ammonia		50	25	12
Phosphorus, Total (P)		15	8	4
Organic	mg/L	5	3	1
Inorganic		10	5	3
Chloride	mg/L	100	50	30
Sulphate	mg/L	50	30	20
Alkalinity (as CaCO ₃)	mg/L	200	100	37
Conductivity	mg/L	66	55	38.5
Grease, Fats and oil	mg/L	150	100	50
Total Coliform	No/100 ml	10 ⁸ – 10 ⁹	10 ⁷ – 10 ⁸	10 ⁶ – 10 ⁷
VOC*	mg/L	> 400	100 – 400	< 100

* TOC: Total Organic Carbon; * VOC: Volatile Organic Compounds. (Sudiarto *et al.*, 2019; Aragon *et al.*, 2020; Odedishemi *et al.*, 2021)

Nutrients (typically nitrogen and phosphorus) removal constitute an integral part of wastewater treatments and their concentration levels in the effluent are an indicator of the health of the process (Restivo *et al.*, 2021). Insights from research suggest Nitrogen – N in wastewater to exist in organic forms (urea, amino acids, nucleic acids, and amino sugars), ammonia form – NH₄⁺, nitrate form – NO₃⁻, and Nitrite forms – NO₂⁻ (Daneshvar *et al.*, 2018; Chauhan *et al.*, 2020; Mukimin *et al.*, 2022).

Similarly, Phosphorus – P, in wastewater have been postulated to exist in organic forms such as organophosphates, in polyphosphate forms formed of linked PO₄ (phosphate) units, and in phosphate or orthophosphate form – PO₄³⁻ (Gutierrez *et al.*, 2020; Lavrinovics *et al.*, 2022). However, further reports emphasized that certain untreated wastewaters may contain innumerable varieties of constituents forming a separate category of parameters from those

enumerated in (table 1) such as pesticides, pharmaceuticals, and personal care products amongst others (Kumar *et al.*, 2019; Matheus *et al.*, 2020).

1.2. Reasons to treat Domestic Wastewater

The concentrations of COD, Total Nitrogen, Nitrate - Nitrogen, Nitrite - Nitrogen, ammonia - nitrogen, and Phosphate - Phosphorus are parameters often analyzed during water analysis and wastewater treatment and in some instance additional parameters such as BOD, the quantification of suspended solids is also ascertained.

The detection and removal of these aforementioned parameters is necessary to restore and maintain the chemical, physical and biological integrity of water residue rendering the water toxic-substance free and fit for use in agricultural purposes, environmental discharge and onward treatment for use as drinkable water in homes. In the case of environmental discharges, the removal of nutrients in wastewater is necessary because they can overwhelm the natural processes of recovery and cause severe problems in affected ecosystems (Rani *et al.*, 2021; Tadda *et al.*, 2021).

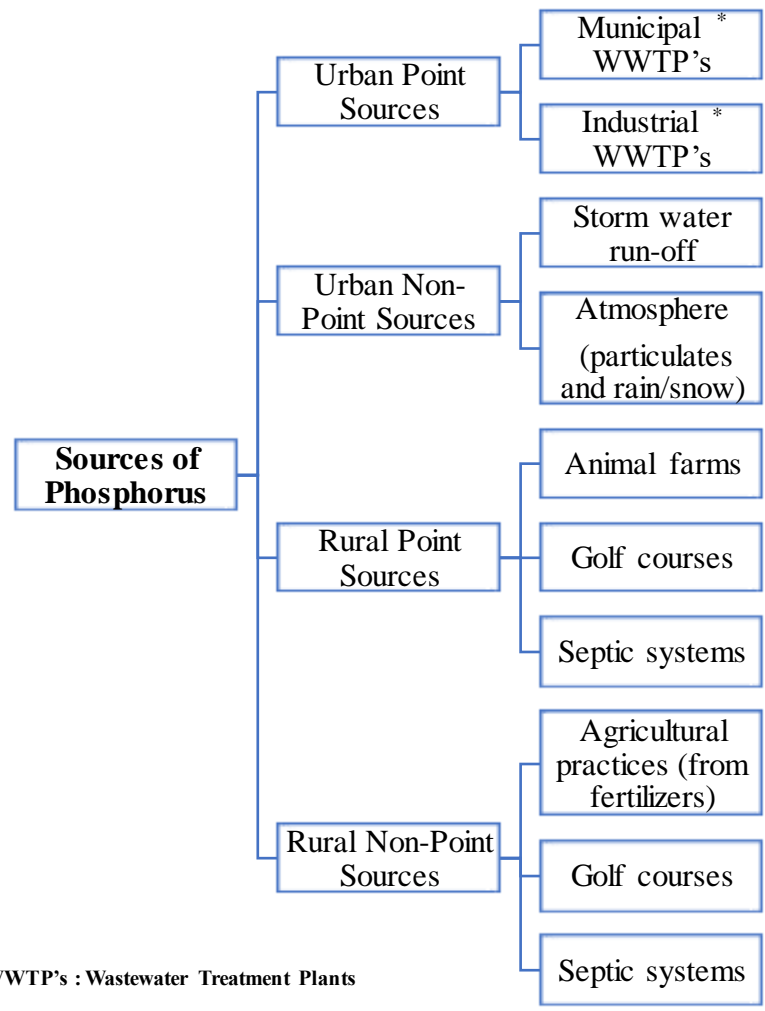
Ammonia has been reported to contribute to about 60 % of nitrogen sources for organisms (Pereira *et al.*, 2021), while the remaining 40 % constitute contributions from organic nitrogen sources (amino acids, proteins, and urea). However, ammonia at concentrations greater than 0.2 mg/L have been postulated to be toxic to aquatic fishes and thus tends to exert BOD on receiving water bodies (Subhashree *et al.*, 2020). Moreover, the removal of ammonia from wastewater during the biological wastewater treatments is necessary because high concentration of ammonia depletes oxygen demand, thereby resulting in insufficient nutrients for bacteria which could also impair their ability to grow (Akizuki *et al.*, 2019; Abeysiriwardana *et al.*, 2019). The BOD₅ (the five – day BOD test indicated in table 1) exists in the Carbonaceous form (CBOD) and the Nitrogenous form (NBOD), such that some microorganisms in wastewater use oxygen to break-down the carbonaceous organic materials in carbon-dioxide and nitrifying organisms oxidize ammonia to nitrites and then to nitrates. Thus, increased nitrification exerts oxygen demand by consuming oxygen from wastewater (Young and Vanrolleghem, 2021).

Research works have shown nitrite – NO_2^- to cause wastewater toxicity in receiving waters and subsequently nitrate – NO_3^- contamination of groundwater (Scholes *et al.*, 2019; Bashandy *et al.*, 2020; John *et al.*, 2020). Nitrites are toxic to aquatic organisms at high concentrations capable of causing damage to fish skins, gills and increase the chances for bacterial infections

and success of parasitic organisms (Nikel *et al.*, 2021). In recent decades, scientific reports have suggested the possible link between the concentration of nitrite and nitrate in drinkable water to blue baby syndrome in infants below twelve months of age (Aswin *et al.*, 2020; Saikia *et al.*, 2021). Nitrites are in general less toxic in comparison with ammonia in aquatic wastewater environments, however, even in low level concentrations it could cause certain stress-related issues (Zorgoni *et al.*, 2020). The increase in the toxicity levels induced by nitrites (NO_2) in receiving water bodies results in groundwater contamination by nitrate (NO_3^-) because once nitrate-containing substances enter the soil, they undergo a process called leaching and since nitrate are highly soluble in water and does not bind strongly to soil particles, it can infiltrate the deep water in the soil and eventually reach the groundwater. Thus, nitrate represents one of the major surface and groundwater contaminants resulting from natural processes such as leakage from fertilized soil, animal waste run-off from dairies and feedlots, wastewater, septic systems, urban drainage, and landfills. Moreover, nitrates (and phosphorus-phosphates, PO_4^{3-}) act as fertilizers and have been reported to promote greater than normal algae growth in several receiving water bodies giving rise to a phenomenon known as eutrophication - where receiving water bodies are progressively enriched with nutrients (nitrogen and phosphorus) causing the exponential growth of aquatic plants (both phytoplankton and macrophytes). Eutrophication has been argued to confer heightened environmental concerns as it deteriorates water quality, depletes dissolved oxygen in the receiving water bodies and in extreme situations designated as dead zones which are incapable of supporting life (Andersen *et al.*, 2019; Farahani *et al.* 2019).

Orthophosphates and polyphosphates constitute the common forms of phosphorus in aqueous solutions such as wastewater (Hoxha *et al.*, 2022). They cause decrease recreational and conservation value of an impoundment as well as loss of livestock and in extreme cases confer lethal effects of algal toxins on drinking water (Bawiec, 2018). Total phosphorus concentrations in wastewater (table 1) have been postulated to vary (6 -10 mg/L) in proportion to the individual concentration of the organic (1 – 5 mg/L) and inorganic composition from its source (figure 3). Researchers have further argued the daily individual phosphorus contribution from the inhabitants in certain societies could range between 0.65 – 4.80 g/inhabitant per day and on average 2.18 g (Omwene *et al.*, 2018; Sudiarto *et al.*, 2019b). Thus, the control of phosphorus discharged from municipal and industrial WWTP's has been deemed essential in preventing eutrophication of surface waters. Phosphorus represents one of the main constituents of synthetic detergents, corrosion inhibitors (used in drinking water pipe preservation), and human

waste (Murrell *et al.*, 2020; Phuong *et al.*, 2022). However, current trends suggest the phosphorus limit in these influents have plummeted as low as between 2.0 – 0.01 mg/L probably due to the practice of treating wastewater at the source (as illustrated in figure 3) using best management practices and pretreatment programs. Orthophosphates and polyphosphates constitute the common forms of phosphorus in aqueous solutions such as wastewater (Hoxha *et al.*, 2022).



Original chart developed using ppt.

Figure 3: Schematics depicting the major sources of phosphorus.

Orthophosphate, the dissolved forms of phosphorus in water, are readily available for consumption and biological metabolism without further breakdown by plants and algae which has informed the notion that phosphorus is a limiting nutrient for organisms in wastewater (Roots *et al.*, 2020). Polyphosphates in water (undergo hydrolysis and reverse back to orthophosphate) are composed of two or more phosphorus atoms like oxygen and hydrogen

atoms and are bound to complex molecules in wastewater (Li *et al.*, 2018). Conventionally, scientists employ certain effective management practices and pretreatment programs to remove phosphorus from wastewater and these include biological and chemical methods of phosphorus removal. Biological phosphorus removal may involve the use of certain bacteria to store higher levels of phosphorus than normal (*Acinetobacter*), while the excess phosphorus is stored as polyphosphates in other kinds of microbes such as polyphosphate bacteria (Fernando *et al.*, 2019; Bertanza *et al.*, 2020). Chemical treatments to remove phosphorus have been reported to be the most used method to meet effluent concentrations at least below 1.0 mg / L (Kazadi *et al.*, 2019).

High COD concentrations (as shown in table 1) in wastewater samples suggest the presence of high levels of oxidizable materials (substances that can undergo chemical reaction with oxygen) which result in reduced dissolved oxygen levels and thus affect the water quality, environmental integrity, and aquatic lifeforms. The evaluation of COD during wastewater treatments can be useful to ascertain the concentrations of oxidizable pollutants in wastewater and it could also assist in analyzing the effectiveness of wastewater treatment processes as well as provide insights into the effect of wastewater disposed on the environment (tributaries and streams) and finally could serve as an index for determining the overall water quality (Phanwilai *et al.*, 2020; Abu-Reesh *et al.*, 2020).

The discharge of wastewater with high organic load to receiving waters could cause oxygen depletion (resulting in BOD), disruption to the balance of aquatic ecosystems, nutrient imbalances (contributing to eutrophication), and amplified toxicity amongst others. For instance, when bacteria and other microorganisms consume organic matter via aerobic respiration, oxygen is depleted, and this could cause hypoxia or anoxia which can harm aquatic organisms who primarily rely on oxygen for their survival (Merbouh *et al.*, 2022; Khumalo *et al.*, 2022).

1.3. Stages of wastewater treatments

Several advances have been recorded in WWTP processes with the emergence of certain methodological approaches involving four major treatment strategies: primary (solid removal), secondary (bacterial decomposition), and tertiary (extra polishing processes). The wastewater treatment plant is designed to treat wastewater such that the effluent does not pose any harm to the receiving water bodies (Salmi *et al.*, 2021). The wastewater channeled to the WWTP is routinely subjected to a series of physical, chemical, and biological processes in a bid to

eradicate nutrients and pollutants resident in the wastewater (Martinez *et al.*, 2018; Ahmed *et al.*, 2021).

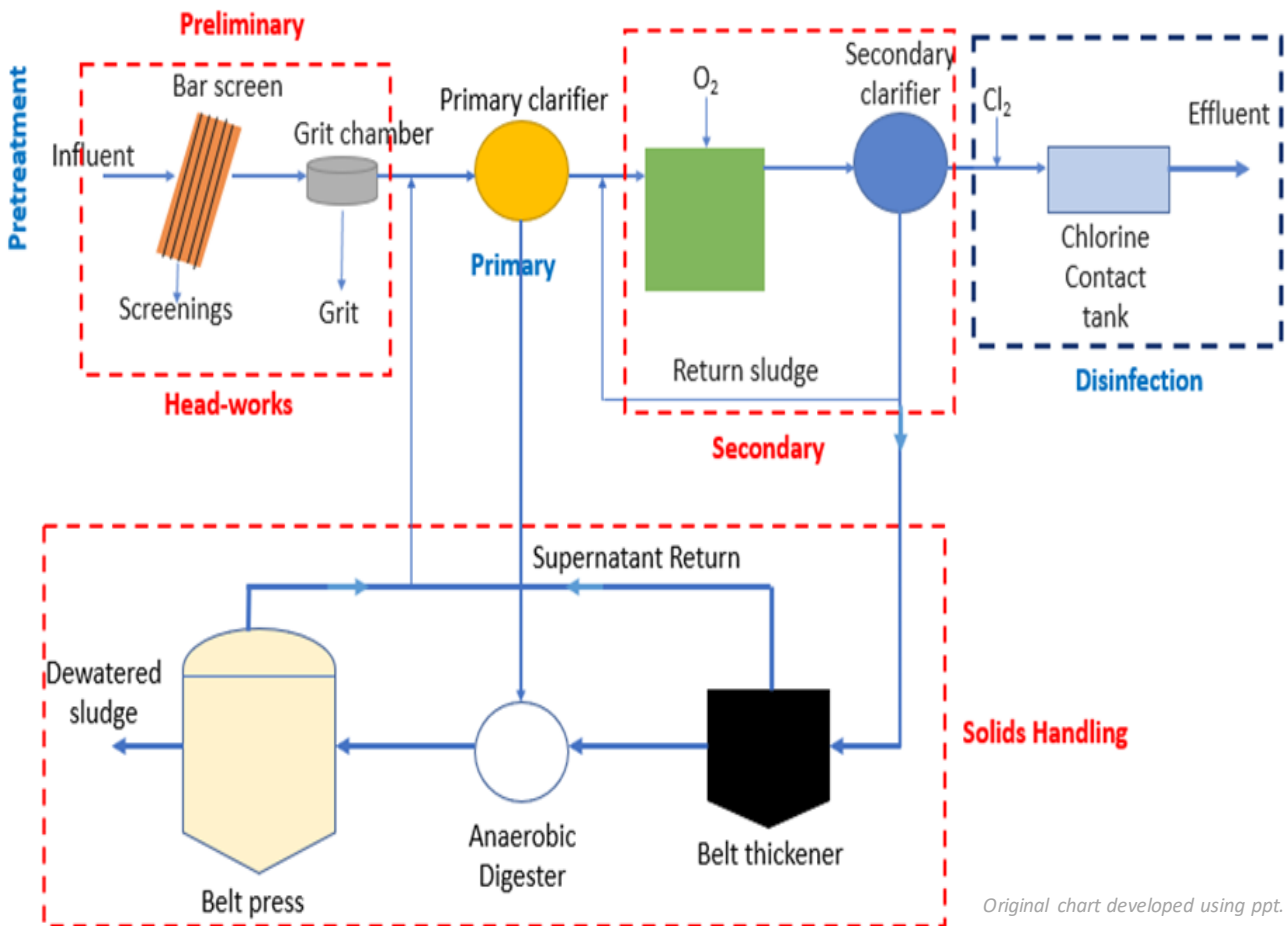
1.3.1. The Primary Treatment Stage

The preliminary treatment phase (the screening phase as shown in figure 4) is regarded as the first step in wastewater treatment strategy to prepare the water for purification by sieving and eradicating objects capable of damaging the WWTP (Ziajahromi *et al.*, 2021). At this stage, large and medium-sized solids wastes are segregated using thick screens and sieves and subsequently, grease and sand particles are removed.

The Primary Treatment Phase (PTP) as illustrated in figure 4 begins with the storage of wastewater in tanks or basins in a bid to allow settleable solids (sludge) to settle to the bottom and with the aid of gravity, oil, and lighter substances (floatable) segregate and rise to the top layer (Orhon *et al.*, 2020; Zhao *et al.*, 2020). The primary treatment phase is aimed at eliminating certain aspects of the grits in the wastewater as well as achieving the flow homogenization and eradication of organic matter in the wastewater (Muriuki *et al.*, 2020; Sun *et al.*; 2021). These solid layers are removed, and the liquid is channeled to the secondary treatment phase. The wastewater sludge can be treated via sludge digestion separately (solid handling process in figure 4 below). The process of sedimentation of solids and elimination of phosphorus during PTP (Chen *et al.*, 2021; Sheik *et al.*, 2021) can be improved via the introduction of certain chemicals such as coagulants (iron or aluminum salt) and flocculants (aluminum sulfate or alum, ferric chloride, and ferric sulfate) (Rossi *et al.*, 2018).

1.3.2. The Secondary Treatment strategy.

The Secondary Treatment Phase (STP) is essential for the removal of organic matter and nutrients (such as nitrogen and phosphorus) from wastewater (Aves *et al.*, 2022; Van Gijn *et al.*, 2021). The secondary treatment phase is mainly dominated by biological processes where the utilization of bacteria (mostly aerobic bacteria) and microorganisms are routinely employed to degrade and eliminate the organic matter (such as sugar, fats amongst others) and different nutrients present in wastewaters (Lakshminarasimman *et al.*, 2018; Honda *et al.*, 2020; Mishra *et al.*, 2020; Bustos – Torrones *et al.*, 2022).



Original chart developed using ppt.

Figure 4: Flow chart depicting a typical WWTP arrangement. The preliminary process involves removal of large particles and grits from the influent to avoid damage to the pumps, valves, and other equipment facilities. The primary clarifier separates solid organic matter from the wastewater while the secondary clarifier eliminates any residual organic sediment by allowing the sediments to settle-out of treated water flow. The disinfection (chlorination) process involves the addition of chlorine to kill any remaining bacteria in the contact chamber. At the effluent disposal phase, clean water is reintroduced to the environment (Diagram adapted from: Farahbakhsh *et al.*, 2020; Jasim *et al.*, 2020).

Certain STPs fitted with fixed films systems grow their bacteria on filters to treat wastewater while suspended growth systems use activated sludge where the decomposing bacteria tends to mix directly into the wastewater and the water is adequately mixed with air to facilitate decomposition and provide oxygen for critical bacterial growth. Some examples of bacteria commonly found in biological wastewater treatment are shown in table 2 below.

Table 2: Examples of bacteria in biological wastewater and their application in WWTPs.

Species	Genre	Process involved	Reference
Achromobacter	Bacteria	Biofilters and activated sludge	Meena <i>et al.</i> , 2021 ; Sun <i>et al.</i> , 2022.
Acinetobacter	Bacteria	Biological phosphorus removal	Russel <i>et al.</i> , 2020.
Alcaligenes	Bacteria	Biofilters, activated sludge and sludge	Boonnorat <i>et al.</i> , 2021.
Desulfovibrio	Bacteria	Sludge digesters	Huang <i>et al.</i> , 2020.
Flavobacterium	Bacteria	Activated sludge, biofilters, sludge digester	Wang <i>et al.</i> , 2020.
*GAO	Bacteria	Biological phosphorus removal	Dan <i>et al.</i> , 2021.
Gordonia	Bacteria	Activated Sludge	Garg <i>et al.</i> , 2021.
Micrococcus	Bacteria	Activated sludge and biofilters	Morones – Esquivel <i>et al.</i> , 2022.
Microtrix	Bacteria	Nitrification	Nierychlo <i>et al.</i> , 2021.
Nitrobacter	Bacteria	Nitrification	Dang <i>et al.</i> , 2022.
Nitrosomonas	Bacteria	Nitrification	Sedlacek <i>et al.</i> , 2020.
*PAO	Bacteria	Biological phosphorus removal	Andreadakis <i>et al.</i> , 2021.
Pseudomonas	Bacteria	Denitrification	Sur <i>et al.</i> , 2019.
Sphaerotilus	Bacteria	Activated Sludge	Lu <i>et al.</i> , 2023.
Zoogloea	Bacteria	Activated Sludge and biofilters	Zhou <i>et al.</i> , 2022.

*GAO: Glycogen-Accumulating Organisms, *PAO: Polyphosphate-Accumulating Organisms.

1.3.2.1. Bacteria metabolisms during STPs.

Bacteria are mainly in the size range between 0.5 to 5 μm and are often in cocci, vibrio, and spirilla forms (Moh *et al.*, 2021). Bacteria accounts for about 90 % of the microorganisms in wastewater and aerobic bacteria are predominant in biological wastewater treatment strategies such as activated sludge and altering filters (Leong *et al.*, 2019; Osinska *et al.*, 2019; Stiborova *et al.*, 2020). The aerobic bacteria break down wastewater contaminants to produce energy for their growth and reproduction (Pachiega *et al.*, 2019; Ma *et al.*, 2020; Hu *et al.*, 2020). The aerobic bioconversion of organic matters tends to be rapid and biochemically efficient resulting in highly oxidized compound productions such as carbon dioxide and water (Smolinski *et al.*, 2019; Shahid *et al.*, 2021). Anaerobic bacteria produce alternative energy source (biogas) to fuel the wastewater treatment process (shown in figure 4) by deriving their oxygen from food

source and breakdown of sludge in the wastewater to produce methane gas which is used as energy (Jiraprasertwong *et al.*, 2019; Paddock *et al.*, 2020). In certain instances, anaerobic bacteria can be used to lower the concentration of phosphorus in the effluent (Iannacone *et al.*, 2019; De Graaff *et al.*, 2020; Bankston *et al.* 2020). Facultative bacteria have been reported to hold certain capabilities enabling them to alternate between aerobic and anaerobic forms of bacteria in response to their environment and although they prefer oxygen (Hembach *et al.*, 2019; Chen *et al.*, 2022).

In food and agricultural biological wastewater treatment, proteins are conventionally degraded anaerobically into amino acids and carbohydrates (like aerobic degradation), alcohols, organic acids, methane, hydrogen sulphide, phenol, and indole (Chen *et al.*, 2019; Izydorczyk *et al.*, 2021; Kusmayadi *et al.*, 2022; Yekta *et al.*, 2019). Research investigations have asserted bacteria to consume biodegradable organic materials, proteins, carbohydrates, and fats via adsorption and absorption (Khraisheh *et al.*, 2020; Zheng *et al.*, 2021). During adsorption, the bacteria typically stick to the food particle and secrete enzymes (either proteolytic or hydrolytic enzymes) in a bid to dissolve the food particle into smaller units which are permeable through the cell wall of the bacteria (Pajerski *et al.*, 2019; Lopez-Ramon *et al.*, 2019; Dehghani *et al.*, 2021). While during absorption, the smaller dissolved food particles get into the cell membrane (Tamayo *et al.*, 2020; Heidary *et al.*, 2020). The bacteria cell composition is made up of about 80 % water and 20 % dry matter (and approximately 90 % of the dry matter in bacteria is organic) and the inorganic compound constituents of bacteria cells are about 50 % phosphorus, 15 % sulphur, 11 % sodium, 9 % calcium, 8 % magnesium, 6 % potassium, and 1 % iron (Sedlacek *et al.*, 2019; Carmo *et al.*, 2019; Seghiri *et al.*, 2019; Umezawa *et al.*, 2020). The combination of these inorganic elements is essential for microbial growth under the right pH conditions in an environment. Most bacteria activities are greatly imparted in pH conditions above 9.5 or below 4.0 and perform optimally in pH ranging between 6.5 and 7.5 (Garcia – Depraect *et al.*, 2019; Yuan *et al.*, 2020; Choudhury *et al.*, 2021).

1.3.3. Bacterial growth during STP

The mixed liquor (comprising the mixture of microorganisms and wastewater) in the aeration tank of STP (figure 4) provides bacteria the conditions necessary to undertake mainly five phases of growth as illustrated in figure 5.

During the lag phase, there is no quantifiable increase in bacteria population and the situated bacteria undergo certain adaptation process to the environment and later trigger the manufacturing of enzymes to digest nutrients (Stumpf *et al.*, 2020). Thus, the lag phase has

been postulated to be pivotal in initiating the bacteria growth phase since bacteria require the appropriate enzyme to ensure the breakdown of nutrients proportionate to their conditions (Hamill *et al.*, 2020). However, there is lack of full understanding to the questions of the duration of the lag phase since they vary according to the bacteria species and as well as the composition of the media, temperature, and the size of the inoculation bacteria sample (Chaturvedi *et al.*, 2021; Del Angel *et al.*, 2021).

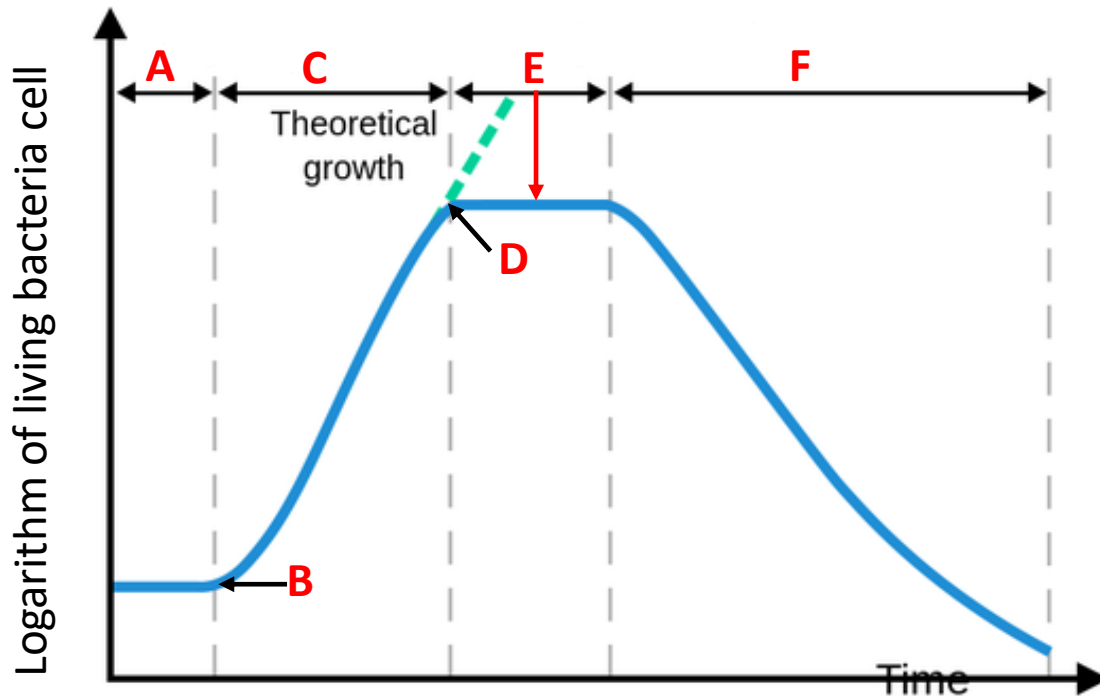


Figure 5: Bacteria growth curve illustration. (A) Lag phase, (B) Accelerating growth phase, (C) Log phase – exponential phase, (D) Declining growth phase, (E) Stationary phase, (F) Death phase.

Curve adapted from <https://theory.labster.com/bacterial-growth-curve/>.

The accelerating growth phase represents the phase at which bacteria commence their growth. Thereafter, almost immediately, the growth phase (denoted as letter C in figure 5) becomes conspicuous with bacteria growth and effective reproduction characterized by cell doubling continuing at a constant rate, so plotting the natural logarithm of cell number against time produces a linear function. This phase has been reported to represent the ideal stage at which samples extraction for inoculating fresh cultures should be obtained, and the bacteria replicating time can be ascertained by the standard practice of measuring the bacteria cell population at different intervals (Eladel *et al.*, 2019; Nawkardar *et al.*, 2019; Cardoso *et al.*, 2021; Singh *et al.*, 2021).

In an enclosed system, an increase in bacteria growth tends to prompt the decrease in available organic and inorganic nutrients resulting in situations where the bacteria begin to compete for nutrients thereby triggering the declining growth pattern of the bacteria (denoted as E in figure 5) due to the limited available nutrients for energy production and cell maintenance (Nguyen *et al.*, 2019; Bensaida *et al.*, 2021; Liu *et al.*, 2023). Overtime, if the declining growth phase persist, the bacteria growth levels tend to remain constant resulting in a stationary phase in which growth rate and death rate are equal (as indicated in figure 5).

In the stationary phase, there are high metabolic activities during floc formation and this result in the production of high quantity of toxic substances in the enclosed system of the stationary phase (Junior *et al.*, 2021; Dong *et al.*, 2022). Moreso, during this phase, bacteria form a thick slime layer on the surface of their cell wall which they use to stick and attach to waste products and as well as use it to clump together with other microorganisms thereby resulting in floc formation (figure 6 and 7) in the wastewater (Sharma *et al.*, 2021; Qian *et al.*, 2023). Research reports have suggested the stationary phase bacteria could produce antibiotics (Zafar *et al.*, 2021) and spores (Ndao *et al.*, 2021) capable of affecting the estimation of viable bacteria in the STP aeration tank depicted in figure 5 (Li *et al.*, 2020).

Finally, the climax of the stationary phase tends to initiate the death phase or the endogenous phase - denoted as G in figure 5 (Gao *et al.*, 2022). During the death phase, the number of bacteria begin to decrease due to the combining factors of the lack of nutrients and space (overpopulation) and the death rate increases exponentially almost mirroring the lag phase.

In the WWTPs, the distribution of nutrients in the bioreactors vary depending on the design, operation, and conditions of the bioreactors. The bioreactors experience high nutrient contents mostly at the inflow or feeding inlet region, the mixing zone of the bioreactor and at the substrate addition points of the bioreactor. The regions of the bioreactor mostly experiencing low nutrients content are the effluent or outlet region of the bioreactor and as well as the settling zone of the bioreactors because the bacteria and microorganism biomass have consumed the nutrients during growth phase as show in figure 5 (Hayder *et al.*, 2022; Thomas *et al.*, 2022; Diaz *et al.*, 2022).

1.4. Tertiary Treatment Strategy.

In recent decades, scientist tends to terminate WWTPs at the secondary treatment phase. However, the tertiary treatment strategies (chemical treatment) are initiated to further enhance the final quality of the effluent water being discharged into certain sensitive ecosystem and in

some cases, water used for human activities. To achieve this, certain techniques such as filtration with sand beds and disinfections using chlorine (sodium hypochlorite) or UV light to reduce the indices of possible microscopic living organisms generated from STP (Alfonso *et al.*, 2021; Campana *et al.*, 2021).

1.5. Wastewater Activated Sludge morphology and microorganism communities.

The conglomerations of bacteria, protozoa, metazoan, algae, fungi, and other microorganisms, tends to constitute activated wastewater sludge and several primary and review research studies often described wastewater sludge as a mixture of microorganisms that make contact while feeding on organic materials in wastewater while digesting the biodegradable materials (Sonczyk *et al.*, 2021; Fan *et al.*, 2022). The removal of the biodegradable materials from the wastewater causes the microorganisms to grow in conglomerations, and because of their acquired weight (in mass), they settle-out as sludge (Hermosillo *et al.*, 2021; Lambert *et al.*, 2021). The activated sludge process tends to provide favourable conditions for certain microorganism resident within to grow in the system and the group of microorganisms within the system (biomass of activated sludge) is adjudged to be best suited to the environment (Corsino *et al.*, 2019; Arumugam *et al.*, 2021; Dottorini *et al.*, 2021).

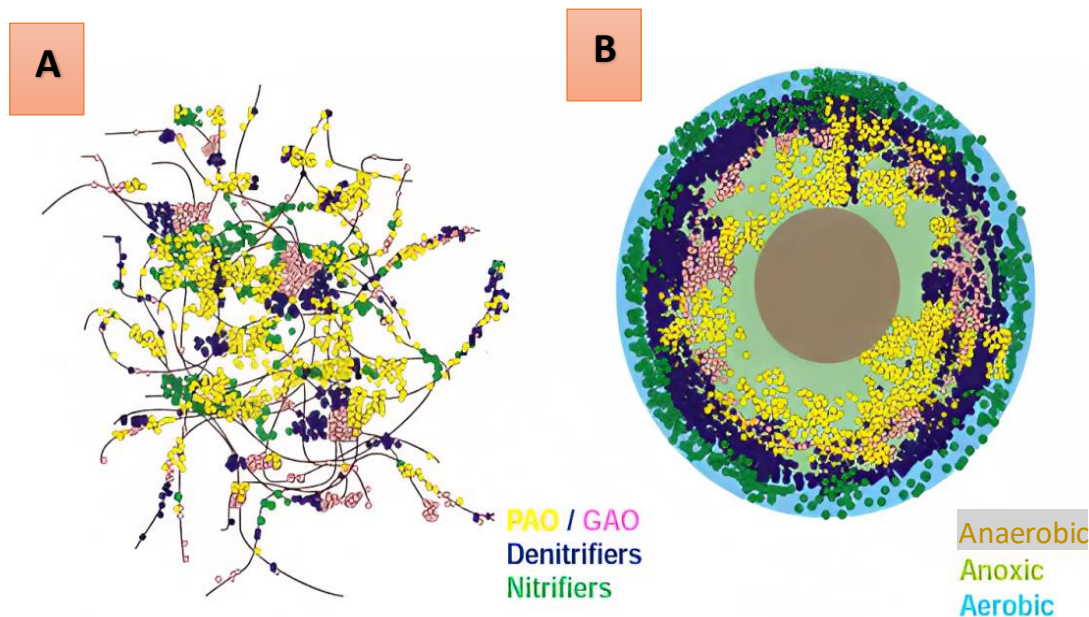
Over the decades, the emergence to prominence the concept of exploring the potentials of waste activated sludge and harnessing their valuable resources for wastewater treatment date back to the discovering of Flocculent Activated Sludge in about 1914 while a group of scientists were using batch reactors (Arden *et al.*, 1914; Bhathena *et al.*, 2006). Since then, several advances have been recorded from the development of activated wastewater sludge process (figure 4) with scientists now able to harness the potentials of the waste activated sludge by selection of desirable organisms. Some notable improvements over time include: 1970s – the anaerobic granular sludge, 1980s – secondary process selectors, 1990s – aerobic granular sludge, and between 2011 to 2020 – aerobic granular sludge and integrated fixed-film activation sludge in full scale application (Purba *et al.*, 2020; Trego *et al.*, 2021; Regmi *et al.*, 2021).

Processes with aerobic granular sludge have some advantages compared to processes with floccular aerobic sludge, such as enhanced settling properties, higher biomass concentration, improved biomass retention, increased tolerance to toxic compounds, enhanced nutrient removal and reduced sludge production amongst others (Kosar *et al.*, 2022). Table 3 summarizes important characteristics of both these types of aerobic sludge and figure 6 displays a morphological representation of a floc and a granule.

Table 3: The physical characteristics of floc and granular activated sludge.

Parameter	Floc	Granule
Morphology	Loose and irregular	Regular, compact, and smooth
Particle Size	Small (<400 μm)	Large (about 0.5 – 3 mm)
Sludge Volume Index ($\text{SVI}_{30 \text{ mins}}$)	$\sim 120 \text{ mL / g}$	20 -50 mL / g
Settling Velocity	Slow ($\sim 1 \text{ m/ h}$)	Fast ($> 5 \text{ min / h}$)
Settling Behaviour	Hindered	Discrete
$\text{SVI}_{5 \text{ mins}} / \text{SVI}_{30 \text{ mins}}$	~ 2.0 (slow thickening)	1.0 – 1.1 (rapid thickening)

(Pechaud *et al.*, 2021; Wei *et al.*, 2021).



Picture Courtesy Delft Technical University

Figure 6: Representation showing (A) conventional Floc and (B) Granular Sludge. PAO: Polyphosphate-Accumulating Organisms and GAO: Glycogen-Accumulating Organisms. In the blue layer (oxic zone) are where molecular or free oxygen is present and where nitrification occurs. In the green layer (anoxic zone) is where molecular or free oxygen are absent, but “chemically bound” oxygen (including nitrites and nitrates) is typically present, and the process of denitrification also occur in this region. In the brown nucleus (anaerobic zone) where both free and bound oxygen forms are absent and it’s the region where anaerobic bacteria perform anaerobic digestion (Liang *et al.*, 2022; Shameen *et al.*, 2023).

1.5.1. Flocculent Activated Sludge.

The physical-chemical structure of Activated Sludge Flocs (ASFs) or Flocculent Activated Sludge (FAS) – the flocculated conglomerates comprising microorganisms, Extracellular

Polymeric Substances (EPS) and adsorbed organic and inorganic material (as shown in figure 7) - influences the sludge settleability (Shrestha *et al.*, 2019; Liwarska *et al.*, 2020; Asensi *et al.*, 2022).

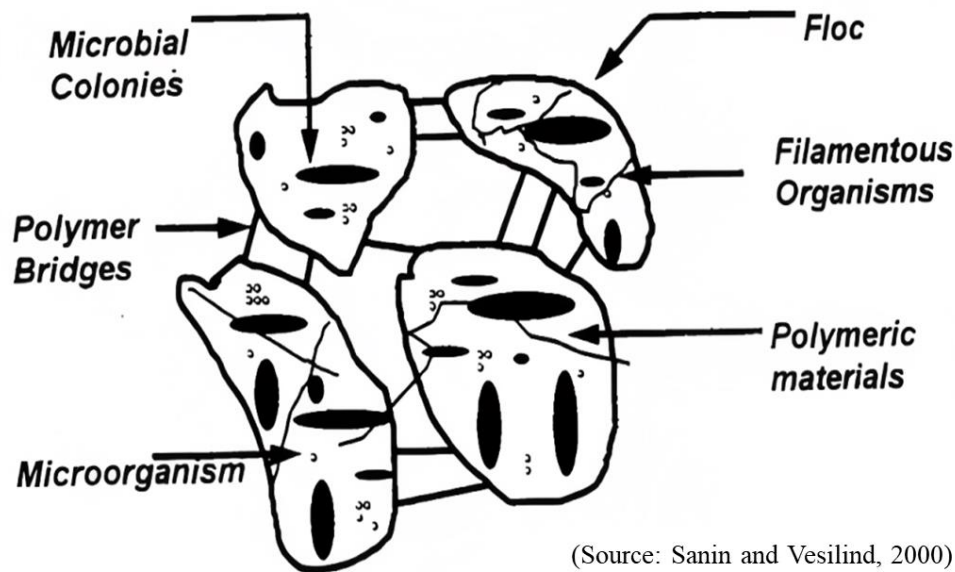
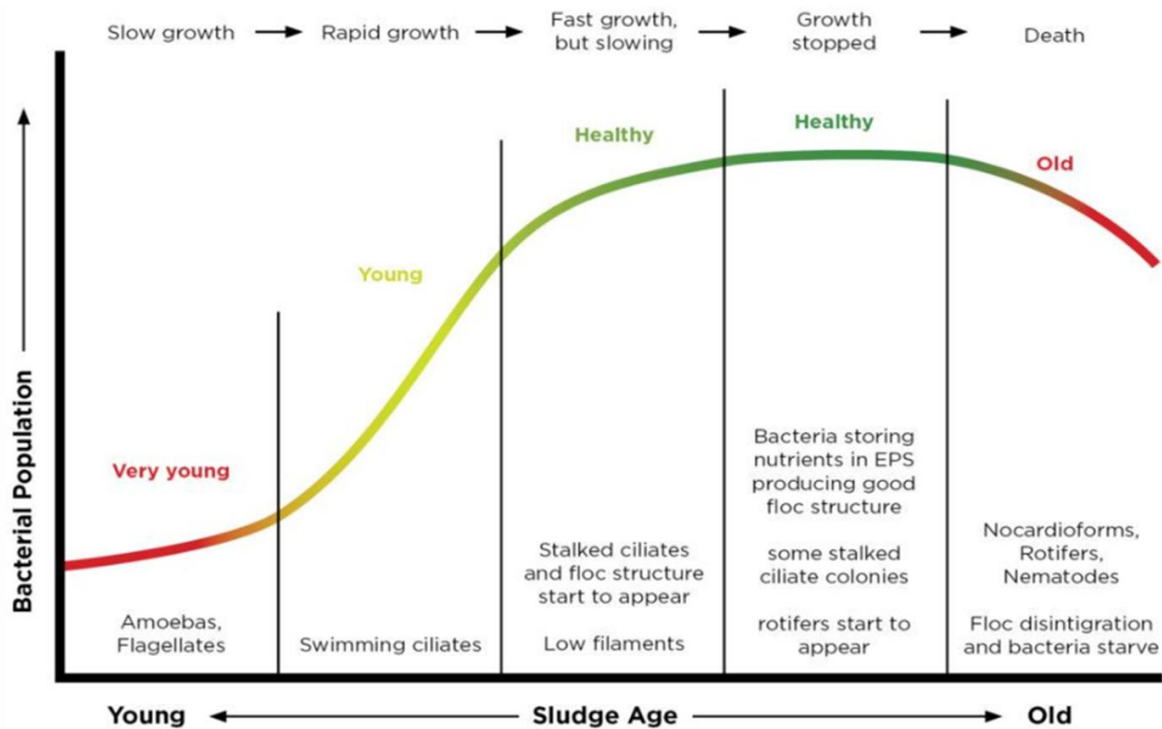


Figure 7: Schematics depicting the typical activated sludge flocs structure

The microbial EPS have been posited to dominate the key component for the aggregation of microorganism in flocs – an active stochastic (chemotaxis, swimming mobility and quorum sensing) and hydrolytic process (biofilm degradation) as microbial cells are dispersed in the direction of the fluid motion in WWTPs (Salehiziri *et al.*, 2020; Jia *et al.*, 2021). The microbial surface and the EPS of the flocs actualise bio-flocculation via polymer bridging and intrinsically these biopolymers tend to comprise functional groups such as hydroxyl, carboxyl and phosphate which contributes the physical-chemical negatively charged phenomenon ensuing from the interactions between microorganisms (predominantly bacteria), inorganic particles (such as silicates, calcium phosphate and iron oxides), exocellular polymers and multivalent cations (Ajao *et al.*, 2021; D Costa *et al.*, 2022). Moreover, hydrogen bonding, hydrophobic interactions (lipids and proteins from microbial cell wall) and polymer gel formation also form an important component of the mechanism leading to bio-flocculation (Bauaouine *et al.*, 2019; Bisht *et al.*, 2019).

Modern practices have seen a surge in the use of sludge age model (shown in figure 8) to monitor and analysis good floc formation as well as the food (incoming BOD) and microorganism ratio during wastewater treatments (Castellanos *et al.*, 2021; Preisner *et al.*, 2021). Furthermore, the sludge age model has become crucial in suggesting the biological

constituents of the ASFs and in turn determine the successes of bioflocculation in the aeration tank (Tirkey *et al.*, 2022).



Source: <https://teamaquafix.com/activated-sludge-fm-calculator/>

Figure 8: The illustration depicting sludge age process.

1.5.2. Aerobic Granular Sludge

The formation of Aerobic Granular Sludge (AGS) tends to evolve from series of complex processes (floc-to-microbial granule) and formations (Dockx *et al.*, 2021). Hence, the successful bioflocculation of flocs in WWTPs tanks and sequencing batch reactors has been reported to be pivotal to the formation of a microbial granule and as well as challenging (Da Costa *et al.*, 2022). The floc-to-microbial granules process under normal conditions undergo the triggering force process (Kong *et al.*, 2022), selection pressure process (Barros *et al.*, 2021), and growth process (as illustrated in figure- 9) to achieve the formation of a matured microbial granule.

In wastewater treatment sequencing batch reactor, the triggering force process comprise mainly of hydrodynamic shear force and feast-famine feeding regimes (Abouhend *et al.*, 2023). The hydrodynamic shear force influence the formation and certain characteristics of the AGS via its up-flow superficial air velocity (Miyake *et al.*, 2022). The hydrodynamic shear force also acts as a compaction force on the surface of the microbial aggregation as shown in figure 9 as

they assist in shaping the granular structure by detaching the loosely attached microbes (figure-6A and figure -9) from the outer surface of the aggregation (Uma *et al.*, 2023).

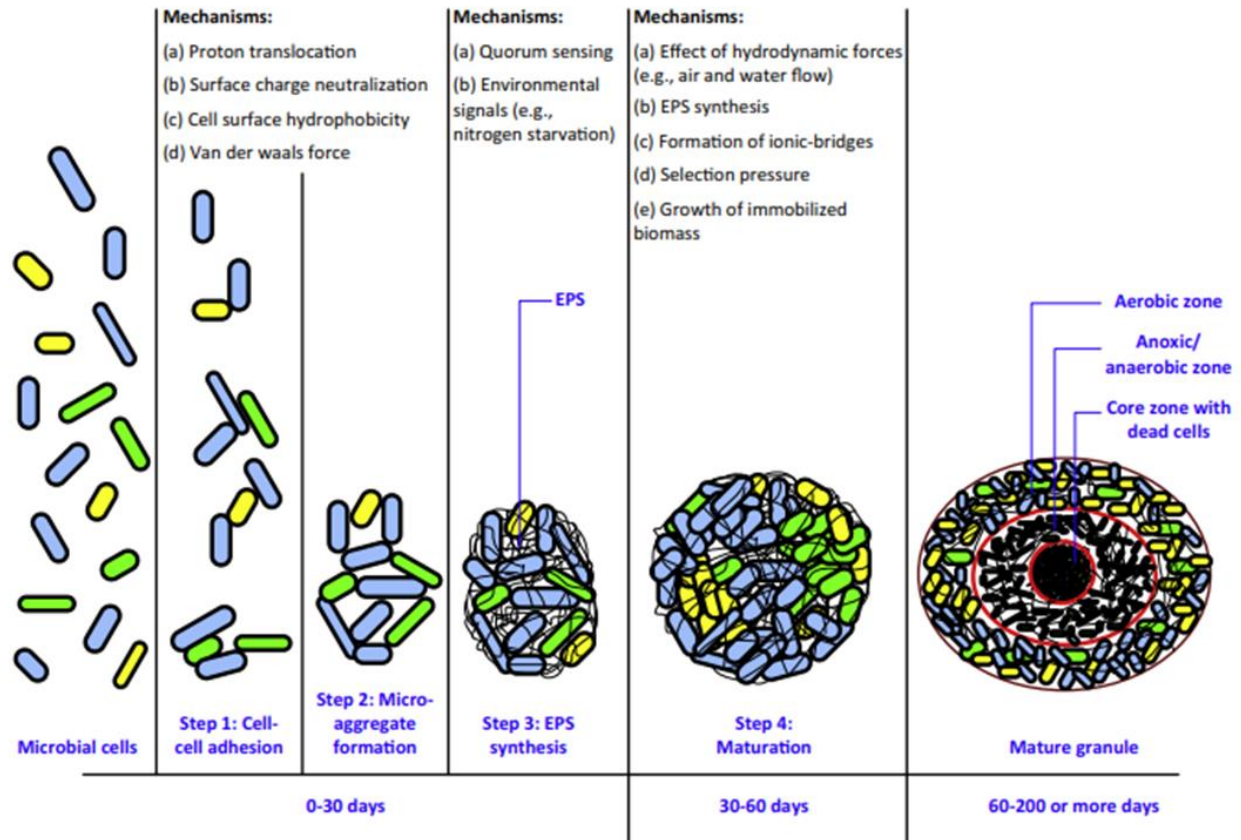


Figure 9: Schematics showing aerobic granule formation mechanism and process (Serma *et al.*, 2017).

The superficial air velocity (≥ 1.2 cm/s) enhances the production of exopolysaccharides, cell surface hydrophobicity, the gravity of AGS, and the cell-cell interactions resulting in the initiation of granular formation (De Pra *et al.*, 2021). Conversely, although up-flow superficial air velocity ≤ 0.8 cm/s could result in the formation of AGS, the granule microbial structure would be loose and unstable (De Sousa Rollemberg *et al.*, 2019). However, several reports have asserted that the formation of AGS depends on more than one parameter (Zaghloul *et al.*, 2020; Strubbe *et al.*, 2022).

Several morphological studies have shown aerobic granules to consist of different zones or layers – aerobic zone (Quoc *et al.*, 2021), anoxic zone (Du *et al.*, 2019), and anaerobic zone as illustrated in figure 10 (Pelivano *et al.*, 2021) and these zones have been postulated to perform

series of biological conversions (nitrification and denitrification) within the granule during the operations of wastewater treatment reactors (Bassin *et al.*, 2019; Roche *et al.*, 2021).

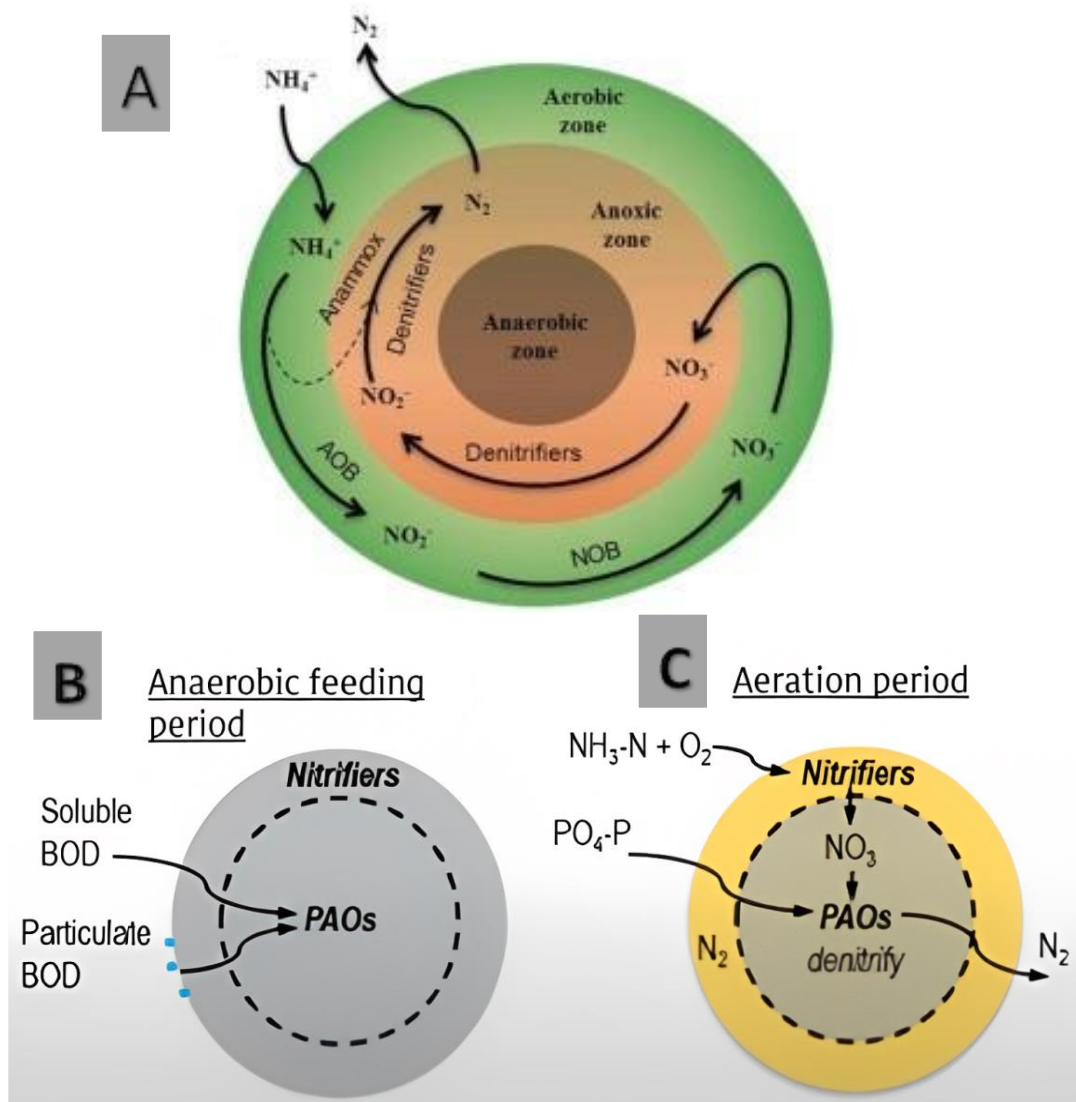


Figure 10: Graphical illustrations of aerobic granular sludge with (A) Inherent zones and nitrogen removal pathways, (B) Anaerobic feeding period, and (C) Aeration period (Lens and Reddy, 2018). The Polyphosphate-Accumulating Organisms (PAOs) able to perform denitrification can be called Denitrifying phosphorus-accumulating bacteria (DPAB).

Research works have reported alternating between aerobic and anaerobic operational periods in sequencing batch reactors contribute to the segregation of microorganisms (nitrifiers, denitrifiers, PAOs, and GAOs) within the granules due to dissolved oxygen gradient across depth (Pathiraya *et al.*, 2019; Papini *et al.*, 2022). The microscopical studies of wastewaters' aerobic granular sludge have shown nitrifying microorganisms to predominantly located in the

aerobic zone outer layer of the aerobic granular sludge as shown in figures 6 and 10. Similarly, the denitrifying microorganisms, PAOs, and GAOs have been posited to occupy the inner regions of the anoxic/anaerobic microenvironments of the aerobic granular sludge as depicted in figure 6 (Awad *et al.*, 2022; Gao *et al.*, 2022). GAOs cannot take up polyphosphate, thus when competing with PAOs for anaerobic Volatile Fatty Acid (VFA) can cause the failure of Enhanced Biological Phosphorus Removal (EBPR) processes; nevertheless, GAOs are usually also found in the granules and can have denitrifying capability (Bin *et al.*, 2015).

The wastewater nutrients nitrogen and phosphorus have been reported to be mainly eradicated via a combination of aerobic (with plenty of oxygen), anoxic (without molecular oxygen) and anaerobic (devoid of molecular oxygen and chemically bound oxygen including nitrites and nitrates) processes in aerobic granular sludge as shown in figure 10 (Falahati *et al.*, 2020; Lopes *et al.*, 2021). The process of Alternating Nitrification and Denitrification (AND) as well as Simultaneous Nitrification and Denitrification (SND) has been reported to dominate the redox conditions in a single granule as shown in figure 10b and 10c (Bucci *et al.*, 2021; Lagum 2022). The aerobic and anoxic/anaerobic zones in the granules are maintained by microbial respiration (high and low dissolved oxygen) in the outer region alongside diffusion limitation (Layer *et al.*, 2019). Furthermore, parameters such as high dissolved oxygen in the bulk liquid, size of granules (micro or macro-scale granules), electron donor capability and microbial activities ensure SND occurrence (Chen *et al.*, 2023; Insel *et al.*, 2023). The release of phosphorus in the anoxic zone as shown in figure 10c and the decrease of COD tends to confer certain challenges on denitrification during AND-strategies (Mbamba *et al.*, 2019; Aziz *et al.*, 2022). Thus, the success in the completion of the floc-to-microbial granule (Flocculent to aerobic granular sludge) formation ensures the occurrence of the biological conversion activities needed in the WWTPs sequencing batch reactors for domestic wastewater treatment.

1.6. The emerging Concept of Bioaugmentation Strategies of Batch Reactors.

Whilst evolving the biological wastewater treatment strategies especially during STPs, the need for an environmentally friendly, cost effective, and the reduction of toxic by-products from WWTPs remain sacrosanct. The deployment of bioaugmentation strategies has shown promising potential as it allows for the scientific manipulation of granular sludge microenvironments to increase populations of several bacteria with similar capacity (Figdore *et al.*, 2018) as well as the addition of isolated microorganisms (Duque *et al.*, 2011) to wastewater treatment bioreactors in a bid to biodegrade recalcitrant molecules in wastewater

samples. Moreover, several research works have studied the inoculation of bacteria species into wastewater treatment bioreactors to enhance the biodegradation of pharmaceuticals (Bessa *et al.*, 2021; Ely *et al.*, 2022). These studies have been heightening the possible prospects of bioaugmentations of AGS with several choices of microorganisms to complement the *in-situ* microorganism communities of the sludge (Duque *et al.* 2021).

1.7. Paracetamol removal in WWTPs

Wastewater treatment plants (WWTPs) for urban sewage are important sources of persistent pollutants to the environment and concern on harmful environmental impact is growing due to chronic trace concentration exposure caused by WWTPs inability to completely degrade such type of pollutants. Consequently, studies with activated sludge have revealed percentages of Paracetamol removal from 80% to 99.9%, revealing hydroquinone and 4-aminophenol as its intermediate metabolites, and allowed to isolate several Paracetamol degrading *Pseudomonas* strains by supplying synthetic WWTP with Paracetamol as the sole carbon source (De Gussemme *et al.*, 2011; Zhang *et al.*, 2013). Yet, its detection in receptor ecosystems suggests that the disposal in sewage overwhelms its removal in WWTPs (Peake *et al.*, 2015; Parolini *et al.*, 2020).

1.8. Objective

Recently, the team of the laboratory of Environmental Technologies of the Centre of Marine Sciences of the Algarve has isolated a bacterial strain from *Mycolicibacterium* genus able to proliferate in solid mineral medium having Hydroquinone as the sole carbon source and able to remove both Paracetamol and Hydroquinone from liquid mineral medium having these compounds as sole carbon sources. The aim of the study was to test standard methods for the analysis of Chemical Oxygen Demand (COD), total nitrogen, ammonia-nitrogen, nitrate-nitrogen, nitrite-nitrogen, and phosphate-phosphorus, and afterward to implement the methods to evaluate the wastewater treatment performance of laboratory-scale sequencing batch reactor with aerobic granular sludge during a bioaugmentation experiment (with a *Mycolicibacterium* spp strain).

2. Materials and Methods

2.1. Evaluation of methods for wastewater analysis

The parameters of interest (chemical oxygen demand, total nitrogen, ammonia nitrogen, nitrate nitrogen, and phosphate phosphorus) were analytically quantified via colorimetric methods of spectroscopy using kit reagents from HACH company GmbH, European headquarters, Dusseldorf, Germany, and the strategy adopted to test their application in this work was (first) to build standard calibration curves within the reported linearity concentration ranges; (second) calculate the respective Limits of Detection (LOD) and of Quantification (LOQ) and (third) use the calibration curves to measure standard reference materials and estimate parameters of precision (Standard Deviation and the Random Error of Mean), accuracy (Relative Bias) and trueness (which accounts with precision and accuracy).

2.1.2. Ammonia nitrogen method and calibration Standards

Two methods based on the indophenol (or Bertthelot) reaction (Searle 1984) were tested: the salicylate ammonia nitrogen powder-pillow method 8155 (HACH); tenth edition with specified concentration range (0.01 to 0.50 mg / L $\text{NH}_3\text{-N}$) and the indophenol blue ammonium nitrogen LCK – 304 methods (HACH); first edition with specified concentration range 0.015 to 2.0 mg / L $\text{NH}_4\text{-N}$.

To prepare the calibration standards a fresh stock solution was prepared in accordance with ISO 7150/1-1984 ammonia standard preparation procedure section E. The stock solution of 1000 mg / L was prepared by dissolving 1.9095 ± 0.0001 g of dried analysis grade ammonium chloride – NH_4Cl , $M = 53.49$ g / mol (Index number: 01014008, Merck KGaA Darmstadt, Germany) in about 400 mL of distilled water using a 500 mL volumetric flask and finally diluting with distilled water to the volumetric mark. The ammonium chloride stock solution (1000 mg / L) was used to obtain a series of final concentrations of: 2.0, 1.0, 0.5, 0.4, 0.3, 0.2, 0.1, and 0.01 mg / L. The last six were used for the method 8155 and the first 7 were used for the LCK – 304 methods.

The salicylate method entails the ammonia reacting with chlorine to produce monochloramine which later reacts with salicylate to form 5-aminosalicylate. The 5-aminosalicylate becomes oxidized in the presence of sodium nitroprusside catalyst to yield a blue colored indophenol-like compound which was measured by absorbance at wavelength 655 nm using a spectrophotometer. Usually, the reaction yields a final green colored solution due to the yellow color caused by excess reagents.

The indophenol blue method involves the ammonium ions reacting at pH 12.6 with hypochlorite ions and salicylate ions in the presence of a catalyst to yield indophenol blue, which was measured at wavelength 694 nm.

2.1.3. Total nitrogen method and calibration standards

For total nitrogen, the persulfate digestion method 10072 (HACH), tenth edition with concentration range (2 – 150 mg / L), was adopted as highlighted by the manufacturer in line with ISO 29441:2010.

The stock solution of 1000 mg / L ammonium chloride prepared as described above in the ammonia nitrogen section was used to prepare the following final concentration calibration standards: 2, 15, 30, 60, 90, 120, and 150 mg / L, within the limit of specified linearity range.

The alkaline persulfate digestion converts all forms of nitrogen to nitrate, and the nitrate reacts with chromotropic acid under a highly acidic conditions to yield a yellowish complex, which was measured by absorbance at wavelength 410 nm using a spectrophotometer.

2.1.4. Nitrate nitrogen method and calibration standards

The cadmium reduction powder-pillows method 8039 (HACH); ninth edition with specified concentration range of 0.3 – 30.0 mg / L $\text{NO}_3^- \text{ - N}$, was adopted as illustrated by the manufacturer and in line with the reference guidelines for nitrate determination from the American Public Health Association (APHA), American Water Works Association (AWWA), and Water Environment Federation (WEF) (Standard Method (SM) 4500 – $\text{NO}_3^- \text{ - B}$).

To prepare the calibration standards, a stock of nitrate solutions was prepared as described in the reference guidelines referred above. An amount of 0.7218 g of dry potassium nitrate (KNO_3) was dissolved in distilled water and 2 mL of chloroform (CHCl_3) was added for preservation before dilution to the mark in a 1000 mL volumetric flask, so that the solution had 100 mg / L $\text{NO}_3^- \text{ - N}$. Then, a series of calibration standards was prepared with final concentrations of 0.02, 0.2, 0.5, 1.0, 1.5, 2 and 2.5 mg / L.

The cadmium metal reduces nitrate to nitrite, and the nitrite ions react with sulfamic acid in an acidic medium to produce an intermediate diazonium salt which later binds with gentisic acid to yield an amber colored solution. The absorbance was measured at wavelength 500 nm with a spectrophotometer.

2.1.5. Phosphate-phosphorus method and calibration standards

The ascorbic acid method 8048 in powder pillows (HACH); tenth edition with specified concentration range (0.02 to 2.50 mg / L PO_4^{3-}) was adopted as indicated by the manufacturer

in line with the guidelines for phosphorous determination from the APHA, the AWWA and the WEF (SM 4500 – P -E).

The stock solution of 1000 mg/L ammonium chloride prepared as described above in the ammonia nitrogen section was used to prepare the following final concentration calibration standards: 2, 15, 30, 60, 90, 120, and 150 mg/L, within the limit of specified linearity range.

The alkaline persulfate digestion converts all forms of nitrogen to nitrate, and the nitrate reacts with chromotropic acid under highly acidic conditions to yield a yellowish complex, which was measured by absorbance at wavelength 410 nm using a spectrophotometer.

2.1.6. Chemical Oxygen Demand Standard

The chemical oxygen demand (COD) method LCI – 400 (HACH), first edition with specified concentration range (0 to 1000 mg / L) for water, wastewater and process analysis was adopted as indicated by the manufacturer and in accordance with ISO – 15705:2002 (E).

The stock solution was prepared by dissolving dried $0.4251 \text{ g} \pm 0.0001 \text{ g}$ of potassium hydrogen phthalate (KHP) [$\text{C}_6\text{H}_4(\text{COOH})(\text{COOK})$] in about 350 mL of distilled water and diluting to the 500 mL volumetric mark, making a COD stock solution of 1000 mg / L O_2 . Then, several calibration standards with the following concentrations were prepared: 20, 200, 400, 600, 800 and 1000 mg/L.

In this method, the oxidizable substances are oxidized by digestion with sulfuric acid and potassium dichromate in the presence of silver sulphate (a catalyst to oxidize the more refractory compounds) and mercury sulfate (to masks the interference of chloride). The amount of dichromate used in the oxidation of the sample is determined by measuring the green coloration of Cr^{3+} . The absorbances were obtained at wavelength 605 nm.

2.2. Calibration Curves construction

The calibration curves were developed using the aforementioned standard concentrations prepared by diluting stock solutions prepared in the same day as described above. For each analytical method six to seven replicates of absorbance reads were obtained for each standard concentration and data sets were treated as follows.

The first version of calibration linear function was plotted using all standard concentrations and the coefficient of correlation R^2 was used to evaluate linearity: if R^2 was below 0.98, the standard concentrations with reads far from the linear function (probably with dilution errors) evaluated by visual observation of plots, were removed until the set criteria ($R^2 > 0.98$) was

met. Then, a second calibration curve was plotted from which the concentrations and relative errors were calculated using equations 1 and 2, respectively. Finally, the three best reads, with the lowest relative errors, from each concentration were selected for plotting the Final Standard Calibration Curve (FSCC).

$$\text{Found Concentration} = \frac{\text{Absorbance} - \text{Intercept}}{\text{Slope}} \quad (1)$$

Where: absorbance = values obtained from the spectrophotometer, intercept = intercept of the regression line, and slope = slope of regression line.

$$\text{Relative error} = \left| \frac{\text{found concentration} - \text{expected concentration}}{\text{expected concentration}} \right| \times 100 \quad (2)$$

Where: found concentration = value from equation 1 and expected concentration = final concentration of the sample.

Afterward, the Limit of Detection (LOD) and the Limit of Quantification (LOQ) were calculated based on the standard error of the intercept and the slope of the regression line using the lowest three standard concentrations from each FSCC.

$$\text{LOD} = 3.3 \times \frac{\text{Standard error of intercept}}{\text{Slope of the regression line}} \quad (3A)$$

$$\text{LOQ} = 10 \times \frac{\text{Standard error of intercept}}{\text{Slope of regression line}} \quad (3B)$$

The correctness of the determined LOD was evaluated by comparing the calculated LOD value (obtained using equation 3A) with the lowest standard concentration (c_{\min}) of the FSCC and $10 \times \text{LOD}$, with the criteria stated as thus: when $\text{LOD} < c_{\min}$, and $10 \times \text{LOD} > c_{\min}$, the calculated LOD (equation 3A) was deemed correct.

2.3. Precision, accuracy, and trueness

To evaluate precision, accuracy, and trueness each method was applied with respective FSCC to analyze mixed standard reference materials with known concentrations (table 4). The reference solutions were commercially obtained from Hach company, Germany, and they are traceable to Standard Reference Materials (SRM) of NIST (except for ammonia).

Table 4: Standard reference materials concentrations

Parameters Standard	LCA -721 Low Range Reference Solution (mg/L)	LCA –720 High Range Reference Solution (mg/L)
Chemical Oxygen Demand	50 mg / L	500 mg / L
Phosphate-phosphorus	1 mg / L	10 mg / L
Ammonia Nitrogen and Ammonium Nitrogen	1 mg / L	25 mg / L
Nitrate Nitrogen	6 mg / L	25 mg / L
Total Nitrogen	20 mg / L	50 mg / L

Six to seven absorbance reads were obtained for each individual analytical method and the found concentrations were calculated using formula –1 from the FSCC for all absorbance reads in MS-excel software and then used to ascertain precision, accuracy, and trueness. The standard deviation of the observed values (obtained using equation 4A) and the random error of the mean (obtained using equation 4B) were used to evaluate the precision, while the relative bias in percentage in comparison with the known concentration (obtained using equation 5) was used to evaluate the accuracy. Finally, the precision and accuracy were used to evaluate the trueness (obtained using equation 6).

$$\text{Standard Deviation (SD)} = \sqrt{\frac{\sum(X_i - \bar{x})^2}{n - 1}} \quad (4A)$$

$$\text{Random error of the mean} = \frac{\text{SD of observed sample}}{\sqrt{n}} \quad (4B)$$

$$\text{Relative bias (\%)} = \left(\frac{X_{(\text{Lab value mean})} - X_{(\text{Ref. value})}}{X_{(\text{Ref. value})}} \right) \times 100 \quad (5)$$

Trueness = (Ref. value – lab. value mean) + (Random error of mean). (Konieczka and Namiesnik 2018) (6)

2.4. Bioreactor setup and operational conditions

Four sequencing batch reactors (SBRs) were setup with working capacities of about 1.3 L in volume each. The dimension of each individual reactor was 6.2 cm internal diameter and 44 cm in height while the discharge point was at mid height for an exchange rate of 50 % in each cycle. The SBRs started with automatic operations using sequential time switches in cycles of 6 hours with four different phases: anaerobic feed from bottom, aeration, settling and effluent removal; however, due to failures in the automatic discharges (after discharge the outlet pumps became unprime) the operation was adapted to manual discharges first with cycles of 12 hours and then with cycles of 24 hours (see details on table 5).

The oxygen was supplied using two Vultron 4000 air pumps (each with two air supplies) for the four reactors. Each reactor had an independent air supply connected to a hard PVC tube with two exits (< 1mm) to supply air at the bottom of reactors, resulting in a superficial air velocity of 0.8 cm / s.

The operation started with a volume of 150 mL mature granular sludge per reactor. Thus, aiming to have high selectivity for the fast-settling mature granules, a high minimal imposed settling velocity of 13.2 m/h (calculated using the following equation (Liu *et al.*, 2005)) was used.

$$\text{Minimal imposed settling velocity} = \frac{L}{t_s}$$

Where L is the distance to the discharge port (m) and t_s is the settling time (hour).

Table 5a: Time of each phase during the SBR cycles, throughout the operation, and minimal imposed settling velocity in the different operation stages.

		Stage I (Day 1 – 4)	Stage II (Day 5 – 7)	Stage III (Day 8 – 57)
Phase	Units	4 cycles / day	2 cycles / day	1 cycle / day

			day	night	
Anaerobic feed	Min	120	150	150	150
Aerobic incubation		237	387	747	1287
Settling		1	1	1	1
Effluent removal		2	2	2	2
Minimal imposed settling velocity	m h ⁻¹	13.2	13.2	13.2	13.2

To make the final composition of synthetic sewage, the reactors were fed from four separated solutions (Table 5b) that became mixed after a system of peristaltic pumps (Figure 11), so there was always a mix of nutrients in the four feed solutions to avoid the proliferation of contaminant microorganisms in the supply bottles.

Table 5b: Synthetic sewage preparation and composition.

Compounds	Stock at 4°C (g/L)	Dil. Factor to prepare solutions in the feed bottles	Dil. factor by mixing the four solutions - according to pump flows	Total dil. Factor	Influent (g/L)
<i>Carbon sources solution</i>					
Sodium acetate	90	31.9	4.7	150	0.6
D-glucose	55.5				0.37
Glycerol	24				0.16
MgSO₄·7H₂O	135				0.9
<i>Macronutrients solution 1</i>					
NH₄Cl	80	140.9	2.8	400	0.2
CaCl₂·2H₂O	12				0.03
<i>Macronutrients solution 2</i>					
K₂HPO₄	256	174.0	2.3	400	0.64
KH₂PO₄	60				0.15
KCl	16				0.04
<i>Trace elements solution</i>					
FeCl₃·6H₂O	9	220.5	4.5	1000	0.009
H₃BO₃	0.9				0.0009
CuSO₄·5H₂O	0.18				0.00018
KI	1				0.001
MnCl₂·4H₂O	0.72				0.00072
Na₂MoO₄·2H₂O	0.36				0.00036
ZnSO₄·7H₂O	0.72				0.00072
CoCl₂·6H₂O	0.9				0.0009
EDTA	60				0.06

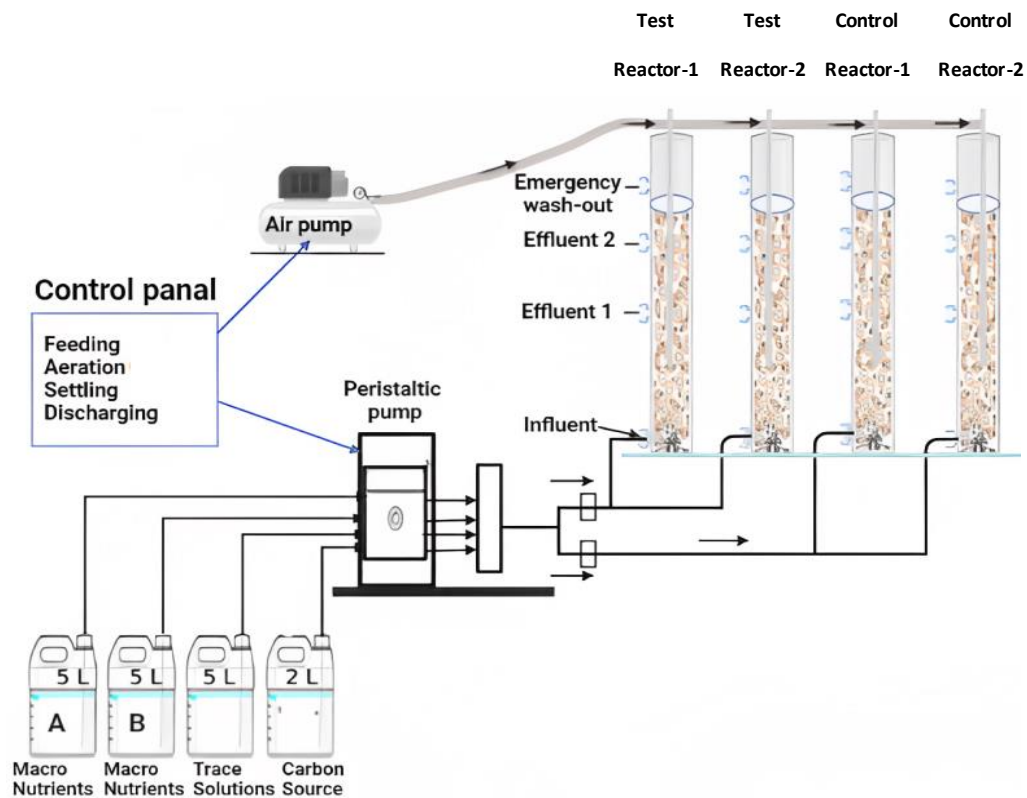


Figure 11: Schematics showing the bioreactor setup (Original diagram).

2.5. Characterization of Granular Sludge used in the experiment.

The granular sludge was kindly provided by the company Águas do Algarve and was obtained from the WWTP of municipal wastewater located between Faro and Olhão, Portugal.

2.5.1. Sludge Volume Index and Mixed Liquor Suspended Solids

The Sludge Volume (SV) of the obtained sample was measured by pouring 1 L of mixed liquor into a graduated cylinder and leave the sludge to settle for 5 and 10 minutes and the volumes recorded respectively for each time interval (SV_5 and SV_{10}). Then, the Sludge Volume Index (volume occupied by 1 gram of activated sludge after settling for a certain time) was calculated for 5 and 10 minutes (SVI_5 and SVI_{10}) using formula- 7, where settled sludge is the SV and suspended solids is the Mixed Liquor Suspended Solids (MLSS) calculated as described below and using equation- 8.

$$\text{SVI (mL/g)} = \frac{\text{(mL Settled Sludge per L of Mixed Liquor)}}{\text{Suspended Solids } \left(\frac{\text{g}}{\text{L}}\right)}$$

The MLSS was measured according to Kasper *et al.*, 2018 with modifications. Since it was for granular sludge, a filter with retention size of 20 – 30 μm (Whatman Grade 8 Ruled Qualitative Filter Paper Circle – 75 mm diameter) was used instead of a filter with 1 μm retention. The filter was washed three successive times with 50 mL portions of Mili-Q water and dried in an oven for 24 hours at 70 ° C, and using an analytical balance the weight of the filter (W1) was recorded in mg. Then, 100 mL (V) of mixed liquor was filtered and the filter with wet suspended solids (after filtration) was placed in the oven at 70 ° C for 3 days, and the filter with dry material weight in mg (W2) was measured using the analytical scale, and the MLSS was calculated using equation 8:

$$\text{MLSS (g/L)} = \frac{\text{(W2(mg)-W1(mg))} \times 1000}{\text{Volume of Sample(L)}} \quad (8)$$

2.5.2. Morphological characteristics

A sample of granular sludge mixed liquor was poured to a petri-dish and placed over millimetric paper for observation using a magnifier. The criteria defined by Beun *et al.*, 2002 were evaluated on a simplified scale by visual observation: diameter size (mm), shape factor - capriciousness of particle surface (smooth, half hairy, hairy), aspect ratio – roundness of particle (round, elongated, irregular).

2.5.3. Bioaugmentation and Paracetamol removal

The bacterial strain *Mycolicibacterium aubagnense* HPB1.1 used in the bioaugmentation experiment was isolated from sediment collected close to the wall of a cave at the Poderosa mine in Spain (in the Iberian Pyrite Belt), during a previous work on the selection of Paracetamol degrading bacteria.

The two test bioreactors (R1 and R2) were inoculated at four operational days (day 4, 6, 8 and 14) with *M.aubagnense* HPB1.1 strain, while the two control bioreactors (R3 and R4) were not. Each inoculation was as follows: (1) a culture of the selected strain was grown in 400 mL LB medium supplemented with glycerol (5 mL /L) till reaching 1.0 to 1.5 OD_{600nm}, and (2)

the cells were collected by centrifugation (at 2500 g for 15 minutes at room temperature) in 8 falcon tubes of 50 mL, the medium discarded, the cells of each tube resuspended in 20 mL of synthetic sewage (the influent medium) and the suspensions distributed equally to reactors R1 and R2.

After the fourth inoculation (at day 14) paracetamol was added to the four reactors just before starting the anaerobic feed to make a concentration of 50 mg/L (on the filled volume). Then, samples were collected for Paracetamol analysis immediately when aeration started and along the aeration period (times 0, 2.5, 5, 7.5, 10 and 22 h) of that cycle (cycle 1) and along the aeration period (0, 3, 12 and 22 h) of the subsequent cycle (cycle 2).

The concentration of paracetamol and its intermediate degrading metabolite Hydroquinone were monitored by HPLC analysis using an isocratic method with a XBridge™ C18 5µm, 4.6 x 250 mm column (Waters, USA) and methanol/miliQ-H₂O - 10/90 (%) at pH ~3 (adjusted with orthophosphoric acid) as mobile phase at 1.3 ml/min for 10 minutes, on a Ultra High Performance Liquid Chromatography Nexera system (SHIMADZU) with a semi-preparative configuration allowing both analytical runs and preparative runs, with the following modules (SHIMADZU): system Controller SLC-40, one Solvent Delivery Module LC-20AP which enables high flow rates (up to 150 mL/min) for highly efficient large-scale preparative fractionation or Another Solvent Delivery Module LC-20AP combined with an FCV-200AL low-pressure gradient unit to perform gradient analysis using up to four mobile phases (used in this work),

- Degassing Unit DGU-405,
- Autosampler SIL-10AP,
- Column Oven CTO-40 C,
- Photodiode Array UV-Vis Detector SPD-M40,
- Preparative Flow Cell for SPD-M40 or Conventional Flow-Cell for SPD-M40 (used in this work),
- Fraction Collector FRC-10A.

Paracetamol at ≥99.0% purity (ref. A7085-100G, Sigma-Aldrich) and Hydroquinone also at ≥99.0% purity (ref. H9003-100G, Sigma-Aldrich) were used to prepare calibration standards in the range of 5 to 50 mg/L, and a certified reference material of Hydroquinone, TraceCERT®,

from Supelco (ref. 74347, Sigma-Aldrich) was used to confirm the retention time of this compound.

3. Results

3.1. Calibration curves and trueness of analytical methods for wastewater analysis

3.1.1. Ammonium Nitrogen method

Indophenol blue method

The standard calibration curve developed using the ammonium chloride standard solutions at different concentrations and respective residuals plot obtained with the indophenol blue method (method LCK304, HACH) are presented in figure 12. Table 6a represents the final data set of this calibration curve while table 6b represents the data set for the parameters of trueness as a validation process:

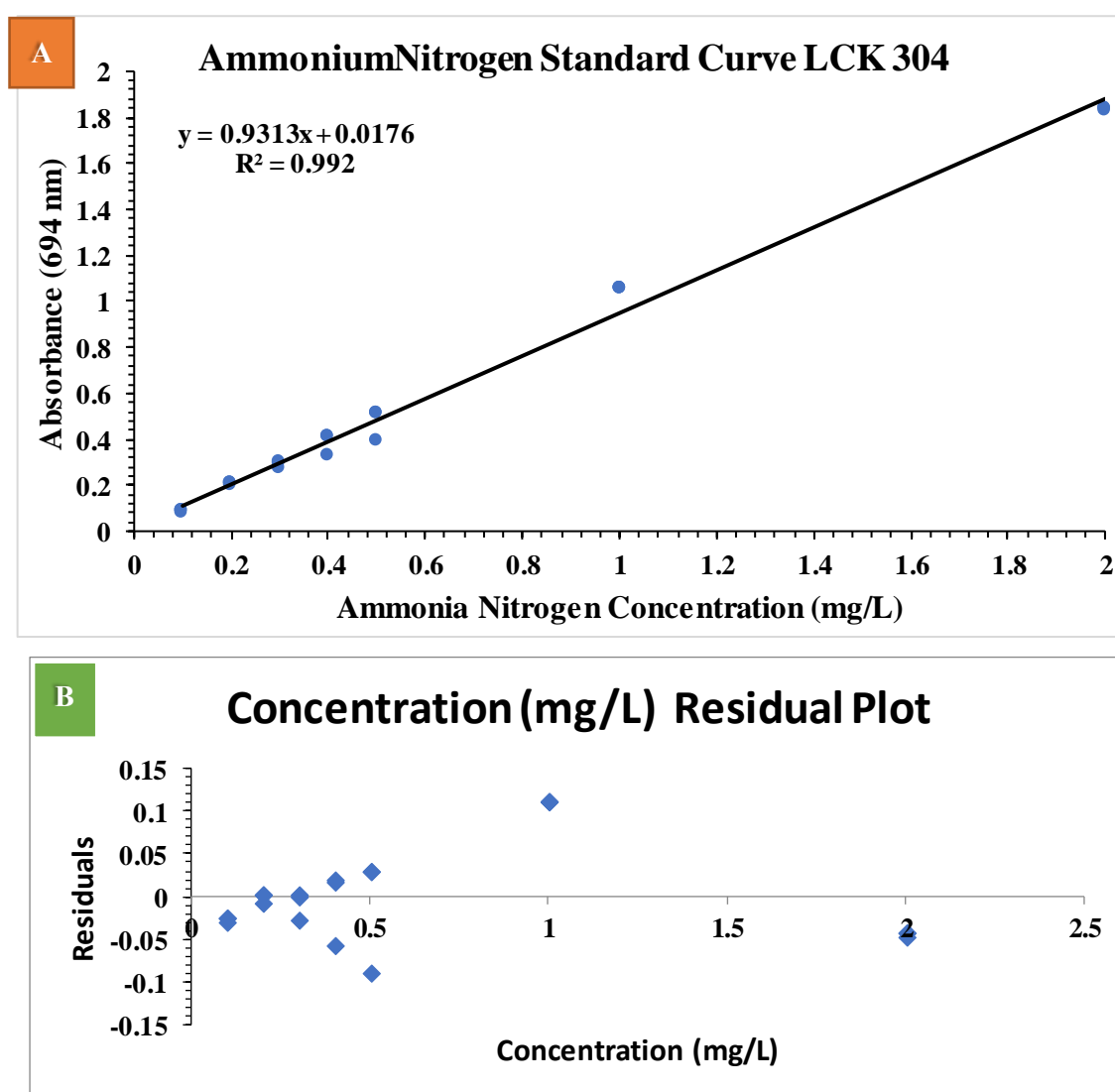


Figure 12: LCK 304 Ammonium Nitrogen calibration curve plot and residual plot.

Table 6a: The data set for the Ammonium Nitrogen indophenol blue method (LCK 304, HACH) standard calibration curve:

Expected Concentration (mg/L)	Absorbance (694 nm)	Found Concentration (mg/L)	Relative Error (%)
0.1	0.078	0.065	35.144
0.1	0.085	0.072	27.628
0.1	0.084	0.071	28.702
0.2	0.194	0.189	5.294
0.2	0.204	0.200	0.075
0.2	0.204	0.200	0.075
0.3	0.268	0.269	10.376
0.3	0.294	0.297	1.070
0.3	0.297	0.300	0.004
0.4	0.330	0.335	16.139
0.4	0.406	0.417	4.263
0.4	0.409	0.420	5.068
0.5	0.393	0.403	19.382
0.5	0.512	0.531	6.174
0.5	0.512	0.531	6.174
1	1.057	1.116	11.607
1	1.057	1.116	11.607
1	1.057	1.116	11.607
2	1.832	1.948	2.588
2	1.835	1.951	2.427
2	1.835	1.951	2.427
Regression Coefficient – r^2		0.992	
Slope		0.931	
Standard error of slope		0.020	
Intercept		0.018	
Standard error of intercept		0.020	
LOD (first three lowest concentration (n =9))		0.07 (mg/L)	
10*LOD		0.66 (mg/L)	
LOQ		0.20 (mg/L)	

Table 6b: The data sets for the Ammonium-Nitrogen indophenol blue method (LCK 304, HACH) parameters of trueness based on analysis of 1 mg/L ammonia nitrogen Reference Material:

Absorbance (694 nm)		Found Concentration (mg/L)
1.057		1.116
1.059		1.118
1.057		1.116
1.059		1.118
1.057		1.116
1.056		1.115
Mean of the obtained values		1.1166
Precision	Standard Deviation (mg/L)	0.0013
	Random error of mean (mg/L)	0.0005
Accuracy	Relative Bias (%)	11.66
	Accuracy (%)	100.12
Trueness		-0.1161

Salicylate method

The standard calibration curve and residuals plot generated using the ammonium chloride standards with the ammonia nitrogen salicylate method (method 8155, HACH) are presented in figure 13; while table 7a has the respective data set and table 7b has the parameters of trueness for the validation of the curve:

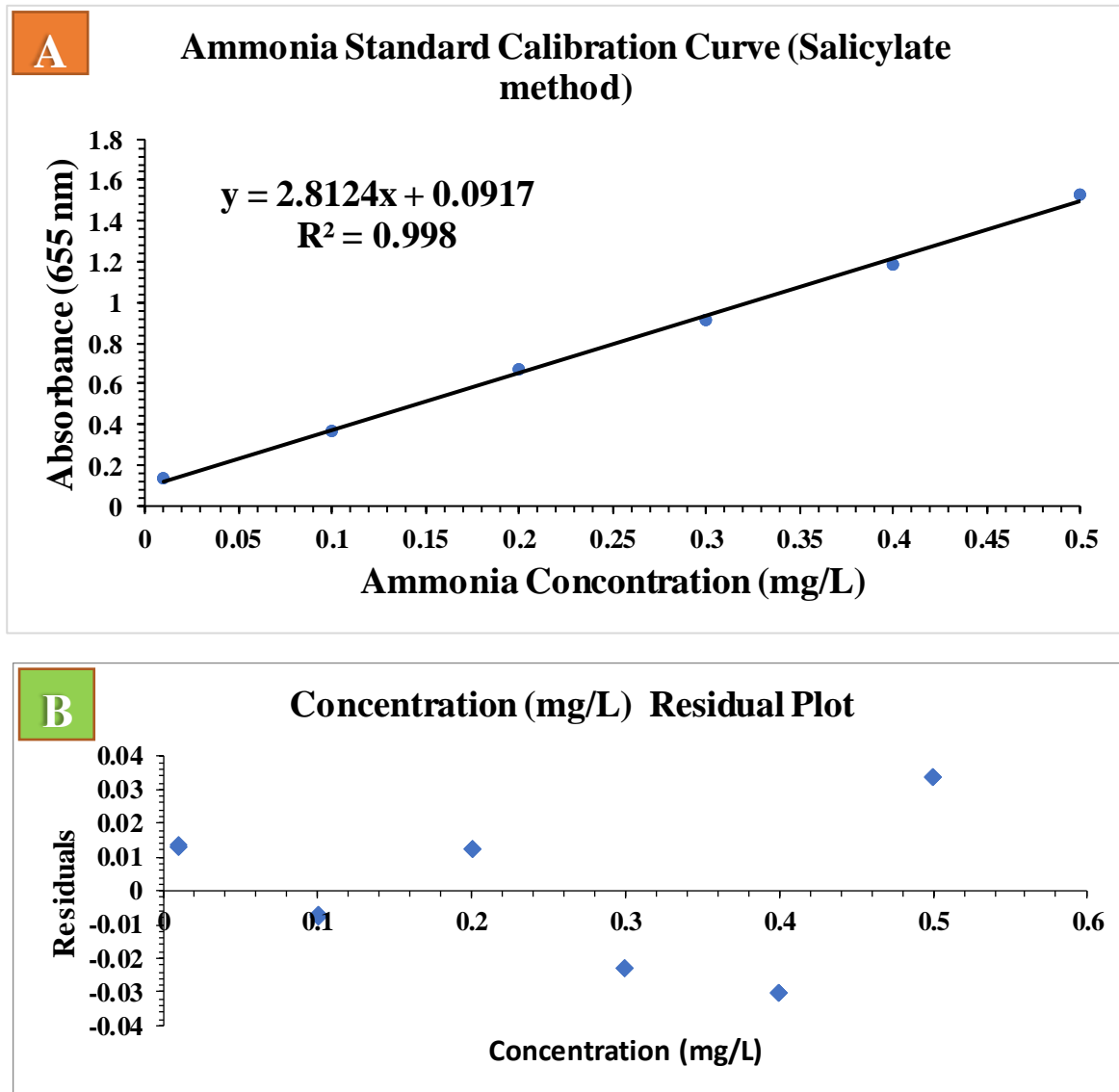


Figure 13: Ammonia nitrogen (Salicylate method) calibration curve and residual plot.

Table 7a: The data sets for the Ammonia- Nitrogen Salicylate method (method 8155, HACH) standard calibration curve:

Expected Concentration (mg/L)	Absorbance (655 nm)	Found Concentration (mg/L)	Relative Error (%)
0.01	0.133	0.015	47.432
0.01	0.133	0.015	47.432
0.01	0.134	0.015	49.398
0.1	0.366	0.097	2.523
0.1	0.366	0.097	2.523
0.1	0.365	0.097	2.720
0.2	0.667	0.205	2.289
0.2	0.667	0.205	2.289
0.2	0.667	0.205	2.289
0.3	0.913	0.292	2.657
0.3	0.913	0.292	2.657
0.3	0.913	0.292	2.657
0.4	1.187	0.390	2.625
0.4	1.187	0.390	2.625
0.4	1.187	0.390	2.625
0.5	1.531	0.512	2.425
0.5	1.531	0.512	2.425
0.5	1.531	0.512	2.425
Regression Coefficient – r²		0.998	
Slope		2.812	
Standard error of slope		0.033	
Intercept		0.092	
Standard error of intercept		0.010	
LOD (first three lowest concentration (n =9))		0.01 mg/L	
10*LOD		0.07 mg/L	
LOQ		0.02 mg/L	

Table 7b: The data sets for the Ammonia-Nitrogen Salicylate method (method 8155, HACH) parameters of trueness based on analysis of 0.25 mg/L ammonia nitrogen Reference Material:

Absorbance (655 nm)		Found Concentration (mg/L)
0.836		0.26465
0.838		0.26536
0.838		0.26536
0.839		0.26572
0.837		0.26500
0.837		0.26500
Mean of the obtained values		0.2652
Precision	Standard Deviation (mg/L)	0.0004
	Random error of mean (mg/L)	0.0002
Accuracy	Relative Bias (%)	6.07
	Accuracy (%)	93.9
Trueness		-0.0150

3.1.2. Total Nitrogen method

The calibration curve and residuals plot obtained with the total nitrogen persulfate digestion method (10072, HACH) using ammonium chloride standard solutions is presented in figure 14. Table 8a has the data set of the curve while table 8b has the parameters of trueness for validation.

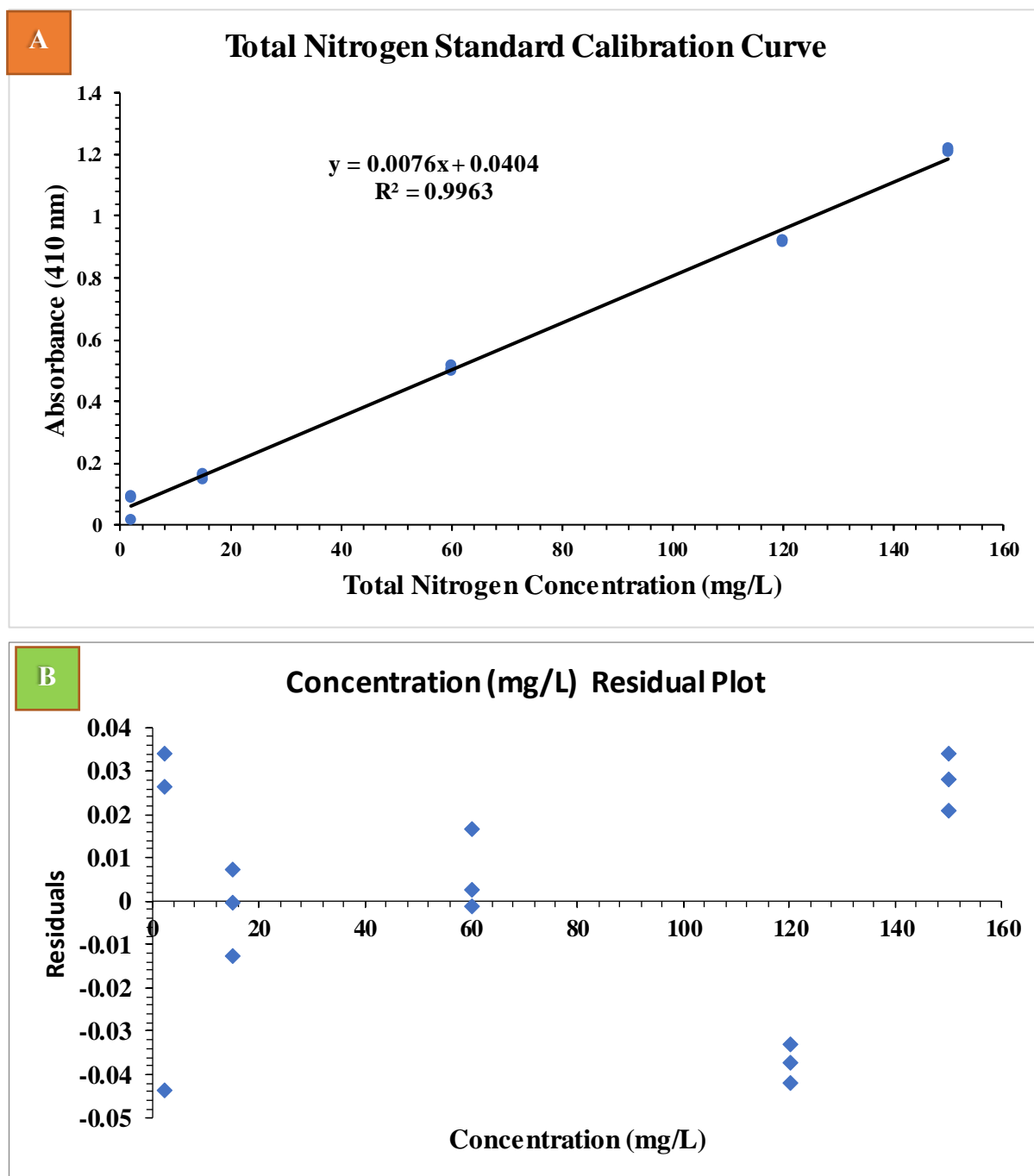


Figure 14: Total Nitrogen calibration curve plot and residual plot.

Table 8a: The data set for the Total Nitrogen method (10072, HACH) standard calibration curve:

Expected Concentration (mg/L)	Absorbance (410 nm)	Found Concentration (mg/L)	Relative Error (%)
2	0.095	7.184	259.211
2	0.087	6.132	206.579
2	0.017	-3.079	253.947
15	0.167	16.658	11.053
15	0.159	15.605	4.035
15	0.147	14.026	6.491
60	0.518	62.842	4.737
60	0.504	61.000	1.667
60	0.500	60.474	0.789
120	0.924	116.263	3.114
120	0.920	115.737	3.553
120	0.915	115.079	4.101
150	1.219	155.079	3.386
150	1.206	153.368	2.246
150	1.213	154.289	2.860
Regression Coefficient – r²		0.9963	
Slope		0.0080	
Standard error of slope		0.0003	
Intercept		0.0404	
Standard error of intercept		0.0117	
LOD (first three lowest concentration (n =9))		5.05 mg/L	
10*LOD		50.45 mg/L	
LOQ		15.29 mg/L	

Table 8b: The data sets for the total nitrogen method (10072, HACH) parameters of trueness based on the analysis of low range (7 mg / L nitrogen) and high range (50 mg / L nitrogen) standard reference materials:

LOW RANGE REFERENCE MATERIAL		HIGH RANGE REFERENCE MATERIAL	
Absorbance (410 nm)	Found Concentration (mg/L)	Absorbance (410 nm)	Foung Concentration (mg/L)
0.100	7.842	0.413	49.026
0.099	7.711	0.414	49.158
0.098	7.579	0.414	49.158
0.099	7.711	0.414	49.158
0.098	7.579	0.415	49.289
0.099	7.711	0.416	49.421
0.098	7.579	0.415	49.289
		Low Range (mg/L)	High Range (mg/L)
Expected Value		7	50
Mean of the obtained values		7.67	49.21
Precision	Standard Deviation	0.07	0.11
	Random error of mean	0.03	0.04
Accuracy	Relative Bias (%)	9.61	1.57
	Accuracy (%)	90.39	98.4
Trueness		-0.64	0.83

3.1.3. Nitrate Nitrogen method

The standard calibration curve and respective residuals plot generated with the nitrate nitrogen cadmium reduction method (8039, HACH) using concentration standards of potassium nitrate are presented in figure 15. Table 9a represents the corresponding data sets for the curve while 9b represents the curves' parameters of trueness for validation.

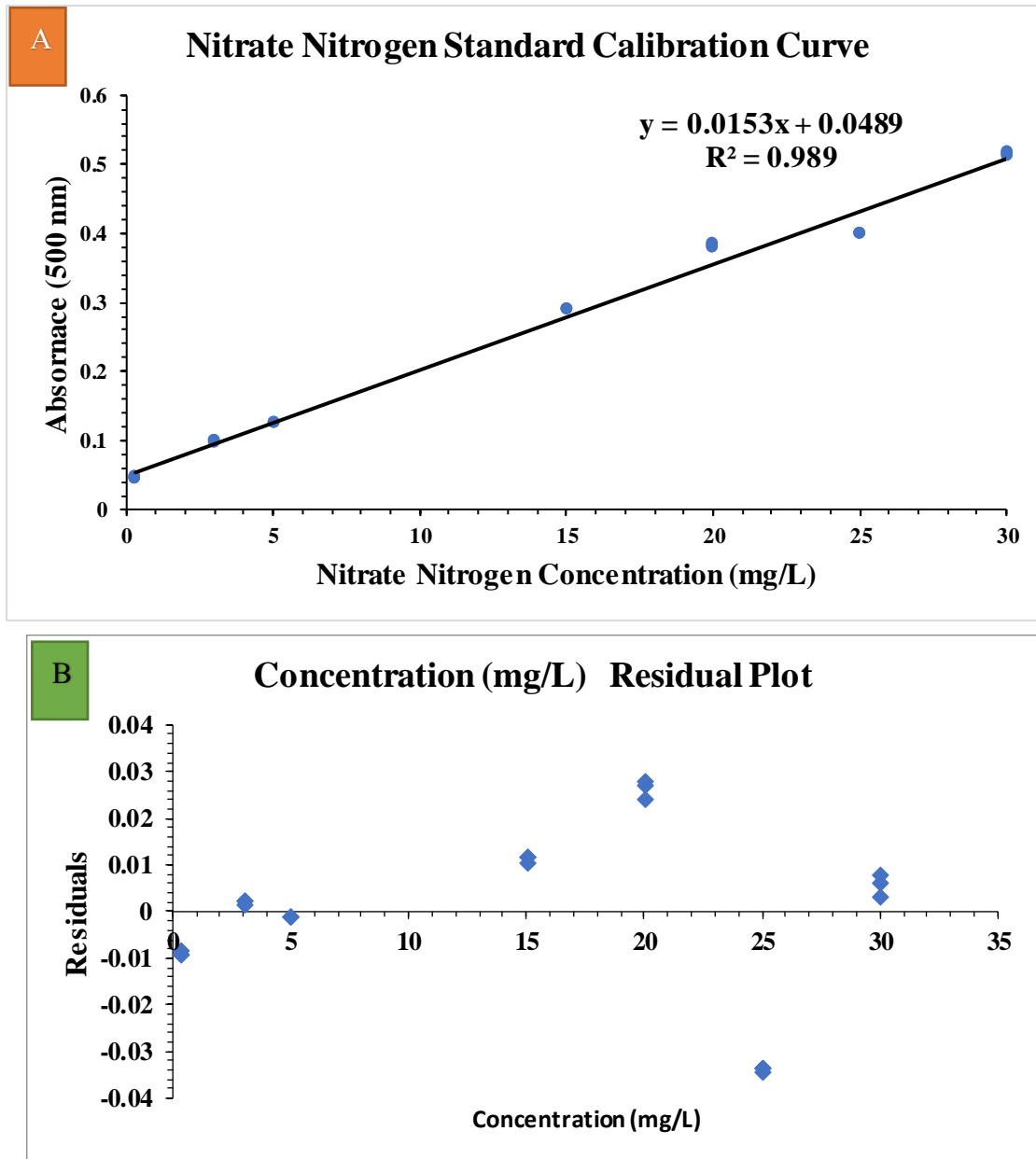


Figure 15: Nitrate Nitrogen calibration curve plot and residual plot.

Table 9a: The data sets for the Nitrate Nitrogen cadmium reduction method (8039, HACH) standard calibration curve:

Expected Concentration (mg/L)	Absorbance (500 nm)	Found Concentration (mg/L)	Relative Error (%)
0.3	0.045	-0.255	184.967
0.3	0.044	-0.320	206.754
0.3	0.044	-0.320	206.754
3	0.097	3.144	4.793
3	0.096	3.078	2.614
3	0.097	3.144	4.793
5	0.124	4.908	1.830
5	0.124	4.908	1.830
5	0.124	4.908	1.830
15	0.289	15.693	4.619
15	0.290	15.758	5.054
15	0.290	15.758	5.054
20	0.379	21.575	7.876
20	0.382	21.771	8.856
20	0.383	21.837	9.183
25	0.397	22.752	8.993
25	0.398	22.817	8.732
25	0.398	22.817	8.732
30	0.511	30.203	0.675
30	0.514	30.399	1.329
30	0.516	30.529	1.765
Regression Coefficient – r²		0.9890	
Slope		0.0150	
Standard error of slope		0.0005	
Intercept		0.0489	
Standard error of intercept		0.0087	
LOD (first three lowest concentration (n =9))		1.92 mg/L	
10*LOD		19.15 mg/L	
LOQ		5.80 mg/L	

Table 9b: The data sets for the nitrate nitrogen cadmium reduction method (8039, HACH) parameters of trueness based on the analysis of low range (6 mg / L nitrate nitrogen) and high range (25 mg / L nitrate nitrogen) standard reference materials:

LOW RANGE REFERENCE MATERIAL		HIGH RANGE REFERENCE MATERIAL	
Absorbance (500 nm)	Found Concentration (mg/L)	Absorbance (500 nm)	Found Concentration (mg/L)
0.161	7.327	0.421	24.320
0.161	7.327	0.412	23.732
0.161	7.327	0.421	24.320
0.163	7.458	0.423	24.451
0.161	7.327	0.424	24.516
0.163	7.458	0.423	24.451
0.162	7.392	0.425	24.582
		Low Range (mg/L)	High Range (mg/L)
Expected Value		6	25
Mean of the obtained values		7.38	24.34
Precision	Standard Deviation	0.06	0.31
	Random error of mean	0.03	0.13
Accuracy	Relative Bias (%)	23.02	2.63
	Accuracy (%)	76.98	97.37
Trueness		-1.36	0.78

3.1.4. Phosphate-phosphorus method

The standard calibration curve generated with the phosphate phosphorus ascorbic acid method (8048, HACH) using potassium dihydrogen phosphate standard solutions is presented in figure 16. Table 10a has the corresponding data sets of the curve while table 10b has the parameters of trueness obtained with a reference standard material for validating the method.

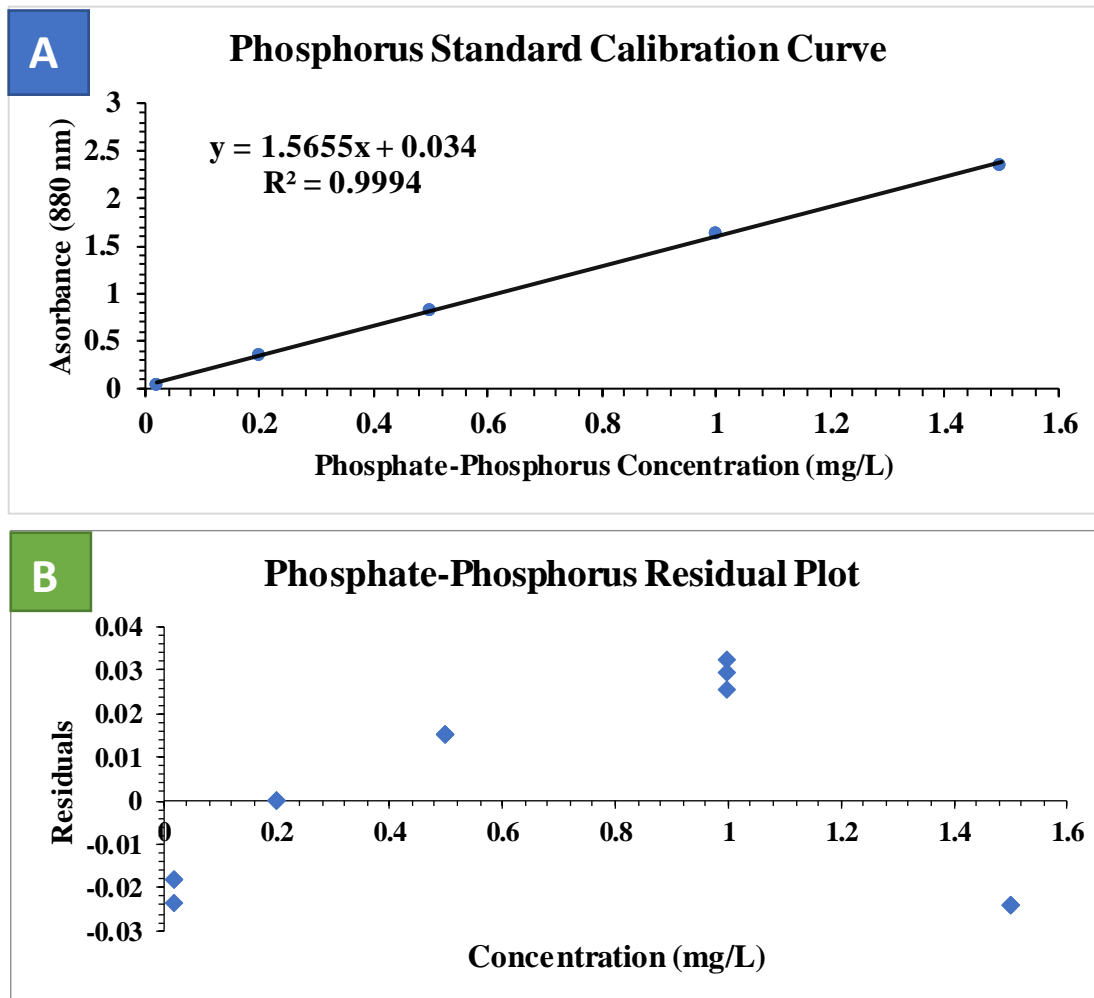


Figure 16: Phosphate-Phosphorus calibration curve plot and residual plot.

Table 10a: The data sets for the Phosphate-phosphorus ascorbic acid method (8048, HACH) standard calibration curve:

Expected Concentration (mg/L)	Absorbance (880 nm)	Found Concentration (mg/L)	Relative Error (%)
0.02	0.047	0.008	58.480
0.02	0.047	0.008	58.480
0.02	0.042	0.005	74.449
0.2	0.347	0.200	0.032
0.2	0.347	0.200	0.032
0.2	0.347	0.200	0.032
0.5	0.832	0.510	1.948
0.5	0.832	0.510	1.948
0.5	0.832	0.510	1.948
1	1.632	1.021	2.076
1	1.629	1.019	1.884
1	1.625	1.016	1.629
1.5	2.358	1.485	1.033
1.5	2.358	1.485	1.033
1.5	2.358	1.485	1.033
Regression Coefficient – r²		0.9994	
Slope		1.5655	
Standard error of slope		0.0065	
Intercept		0.0340	
Standard error of intercept		0.0020	
LOD (first three lowest concentration (n =9))		0.004 mg/L	
10*LOD		0.04 mg/L	
LOQ		0.01 mg/L	

Table 10b: The data sets for the phosphate-phosphorus ascorbic acid method (8048, HACH) parameters of trueness based on analysis of 1 mg /L phosphate phosphorus standard reference material.

Absorbance (880 nm)		Concentration (mg/L)
1.720		1.077
1.715		1.074
1.711		1.071
1.706		1.068
1.701		1.065
1.697		1.062
Mean of the obtained values		1.067
Precision	Standard Deviation	0.006
	Random error of mean	0.002
Accuracy	Relative Bias (%)	6.654
	Accuracy (%)	93.346
Trueness		-0.064

3.1.5. Chemical Oxygen Demand method

The calibration curve and its residuals plot obtained with the COD dichromate method (LCI – 400, HACH) using concentration potassium hydrogen phthalate standard solutions is presented in figure 17. Table 11a contains data sets of the standard curve while 11b portrays the parameters of trueness for validation.

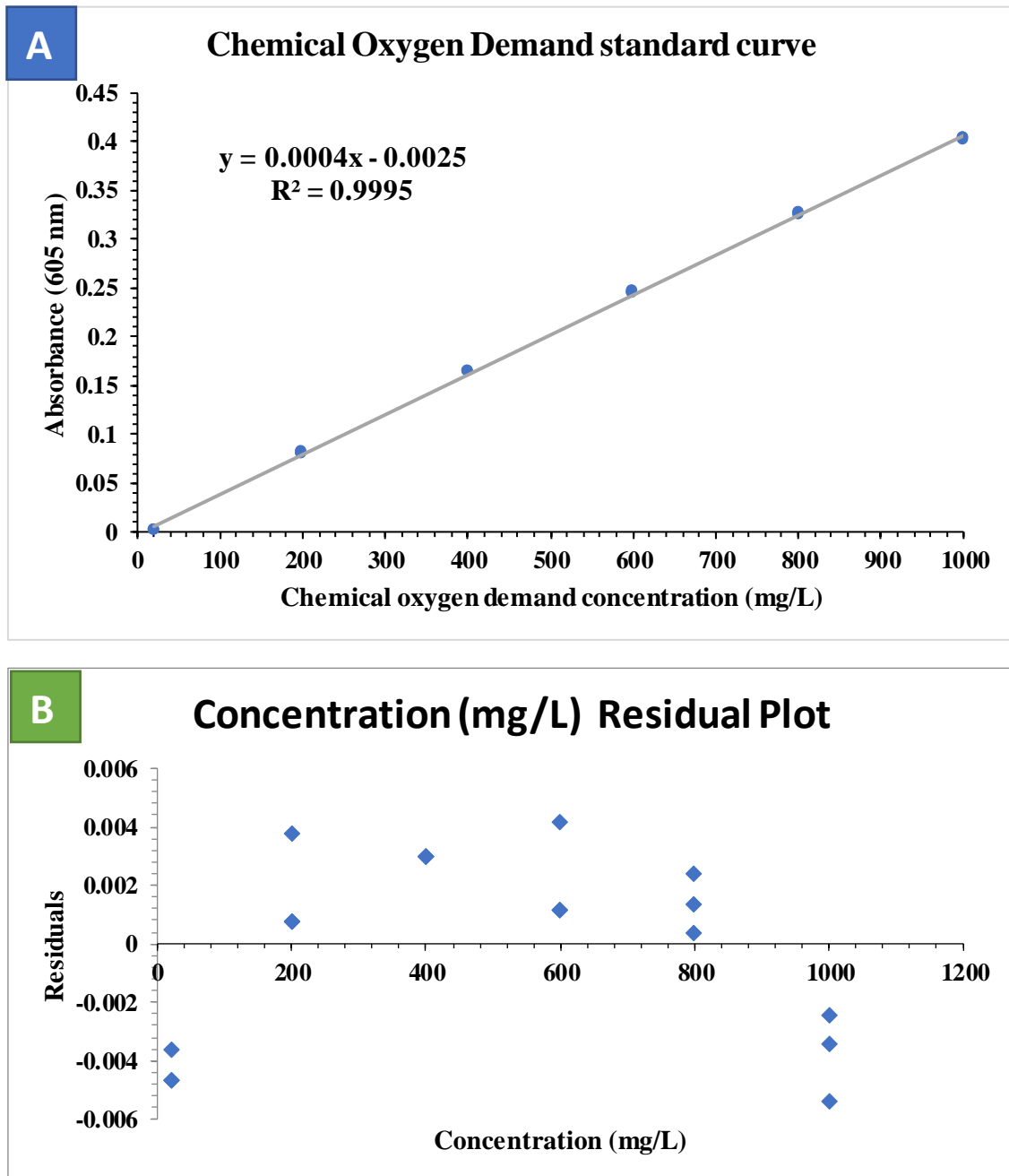


Figure 17: Chemical oxygen demand calibration curve plot and residual plot.

Table 11a: The data sets for the chemical oxygen demand dichromate method (LCI – 400, HACH) standard calibration curve:

Expected Concentration (mg/L)	Absorbance (605 nm)	Found Concentration (mg/L)	Relative Error (%)
20	0.001	3.750	81.250
20	0.002	1.250	93.750
20	0.001	3.750	81.250
200	0.080	193.750	3.125
200	0.080	193.750	3.125
200	0.083	201.250	0.625
400	0.164	403.750	0.938
400	0.164	403.750	0.938
400	0.164	403.750	0.938
600	0.244	603.750	0.625
600	0.244	603.750	0.625
600	0.247	611.250	1.875
800	0.325	806.250	0.781
800	0.326	808.750	1.094
800	0.327	811.250	1.406
1000	0.401	996.250	0.375
1000	0.404	1003.750	0.375
1000	0.403	1001.250	0.125
Regression Coefficient – r²		0.9995	
Slope		0.000400	
Standard error of slope		0.000002	
Intercept		-0.0025	
Standard error of intercept		0.0010	
LOD (first three lowest concentration (n =9))		7.29 mg/L	
10*LOD		72.95 mg/L	
LOQ		22.11 mg/L	

Table 11b: The data sets for the chemical oxygen demand dichromate method (LCI – 400, HACH) parameters of trueness based on analysis of 500 mg / L O₂ reference standard material.

LOW RANGE REFERENCE MATERIAL		HIGH RANGE REFERENCE MATERIAL	
Absorbance (605 nm)	Found Concentration (mg/L O ₂)	Absorbance (605 nm)	Found Concentration (mg/L O ₂)
0.050	118.750	0.185	456.250
0.055	131.250	0.195	481.250
0.060	143.750	0.202	498.750
0.059	141.250	0.202	498.750
0.065	156.250	0.188	463.750
0.060	143.750	0.200	493.750
0.055	131.250	0.202	498.750
		Low Range (mg/L O ₂)	High Range (mg/L O ₂)
Expected Value		50	500
Mean of the obtained values		138.04	484.46
Precision	Standard Deviation	12.05	17.95
	Random error of mean	4.56	6.79
Accuracy	Relative Bias (%)	176.07	3.11
	Accuracy (%)	-76.1	96.9
Trueness		-83.48	22.32

3.2.0. The performance of the bioreactor on wastewater treatment.

To evaluate the organic load and nutrients removals, the influent and the effluents discharged from each of the four sequencing batch reactors were sampled once a week along the experiment and the following parameters were determined using the tested methods with respective constructed standard calibration curves: chemical oxygen demand, total nitrogen, ammonia nitrogen, nitrate nitrogen, and phosphate phosphorus. The Nitrites were estimated by mass balance using the measured concentrations of total nitrogen, ammonia nitrogen and nitrate nitrogen.

3.2.1. Total Nitrogen in Bioreactors

The concentrations of total nitrogen obtained in the SBRs using the persulfate digestion method (10072, HACH) with the calibration curve equation in figure 14 ($y = 0.0076x + 0.0404$) were displayed in figure 18:

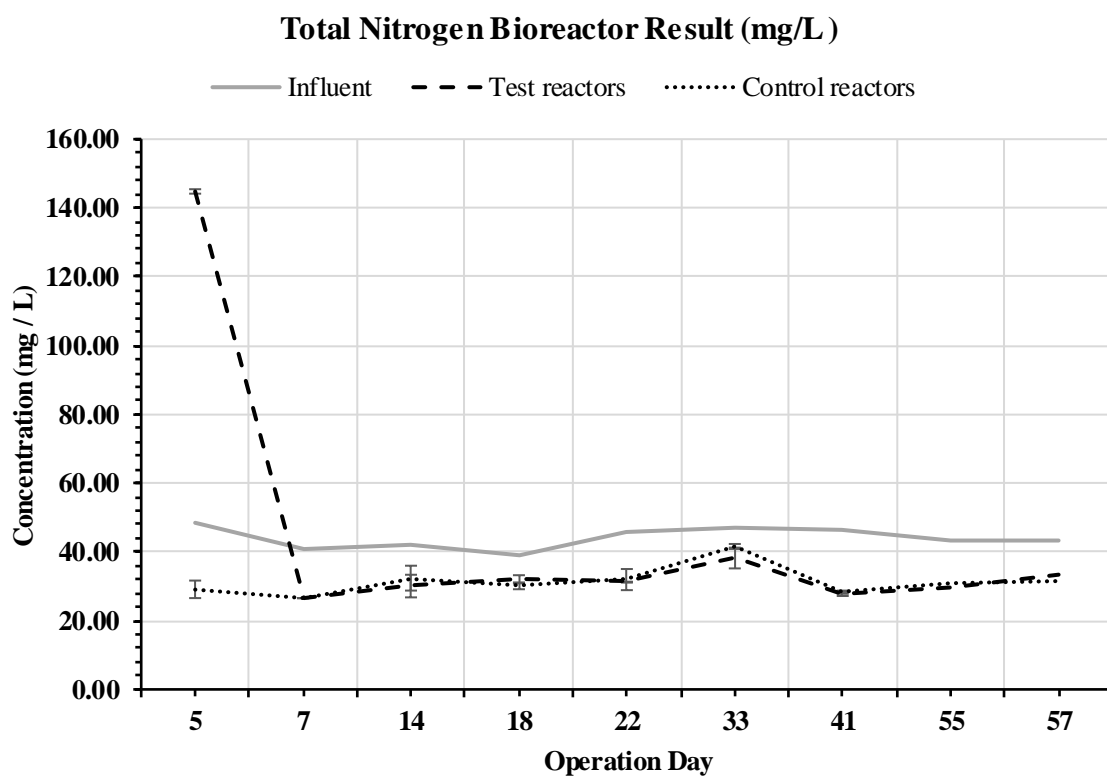


Figure 18: Graph showing total nitrogen results from test reactors and control reactors.

3.2.2. Ammonia Nitrogen in Bioreactors

The concentration of ammonia nitrogen in the SBRs was obtained using the ammonia nitrogen salicylate method (8155, HACH) with the calibration curve equation in figure 13 ($y = 2.8124x + 0.0917$) and is displayed in figure 19:

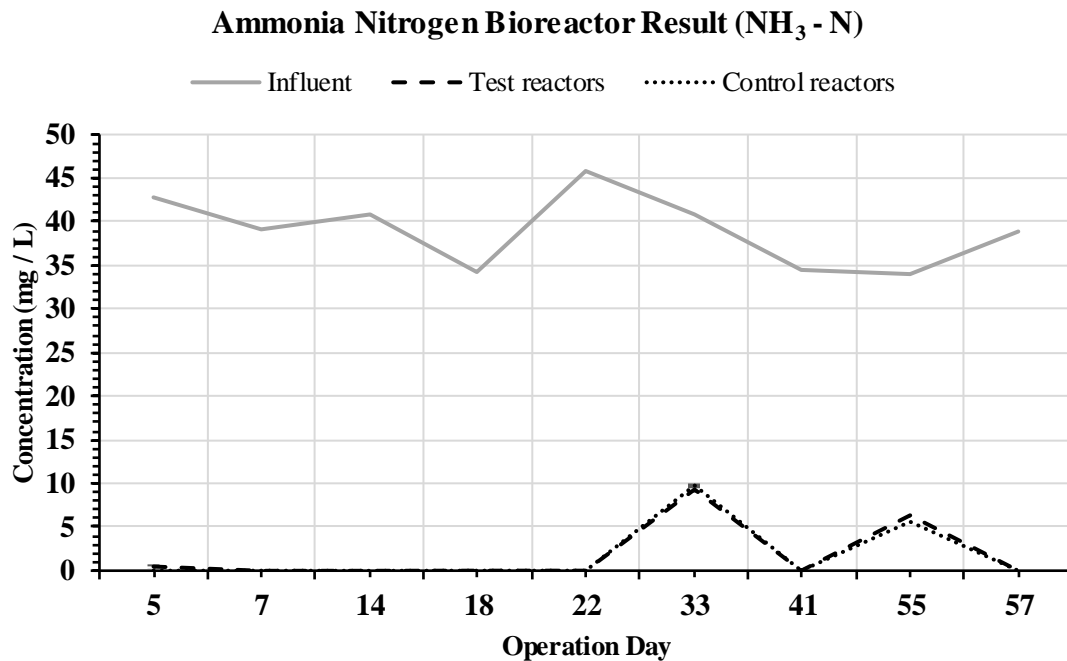


Figure 19: Graph showing ammonia nitrogen results from test reactors and control reactors.

3.2.3. Nitrite Nitrogen in Bioreactors

The concentrations of nitrite nitrogen obtained in the SBRs were calculated by mass balance using the measured concentrations of total nitrogen, ammonia nitrogen and nitrates nitrogen, and are represented in figure 20:

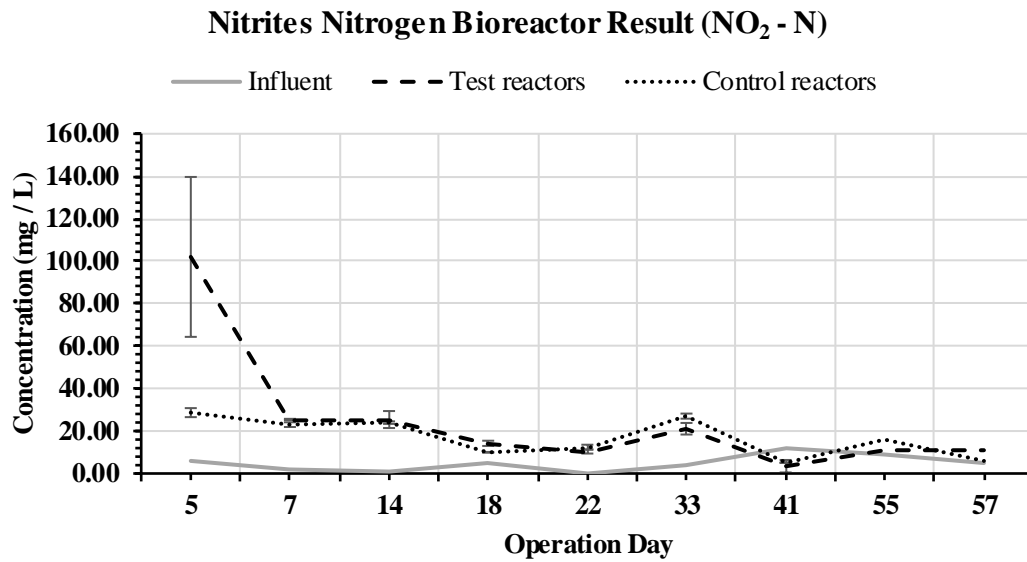


Figure 20: Graph showing nitrite nitrogen results from test reactors and control reactors.

3.2.4. Nitrate Nitrogen in Bioreactors

The concentrations of nitrate-nitrogen in the SBRs were obtained using the nitrate nitrogen cadmium reduction method (8039, HACH) with the calibration curve equation in figure 15 ($y = 0.0153x + 0.0489$) and are presented in figure 21 :

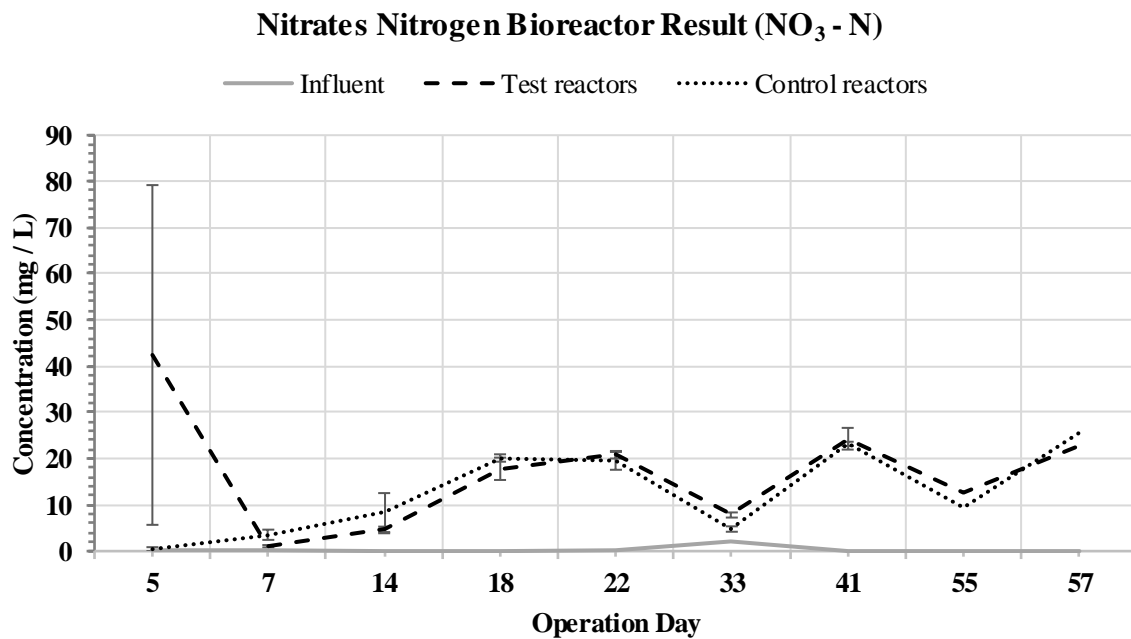


Figure 21: Graph showing nitrate nitrogen results from test reactors and control reactors.

3.2.5. Chemical Oxygen Demand (COD) in Bioreactors

The values of COD in the SBRs were obtained using the dichromate method (LCI – 400, HACH) with the calibration curve equation in figure 17 ($y = 0.0004x + 0.0025$) and are presented in figure 22:

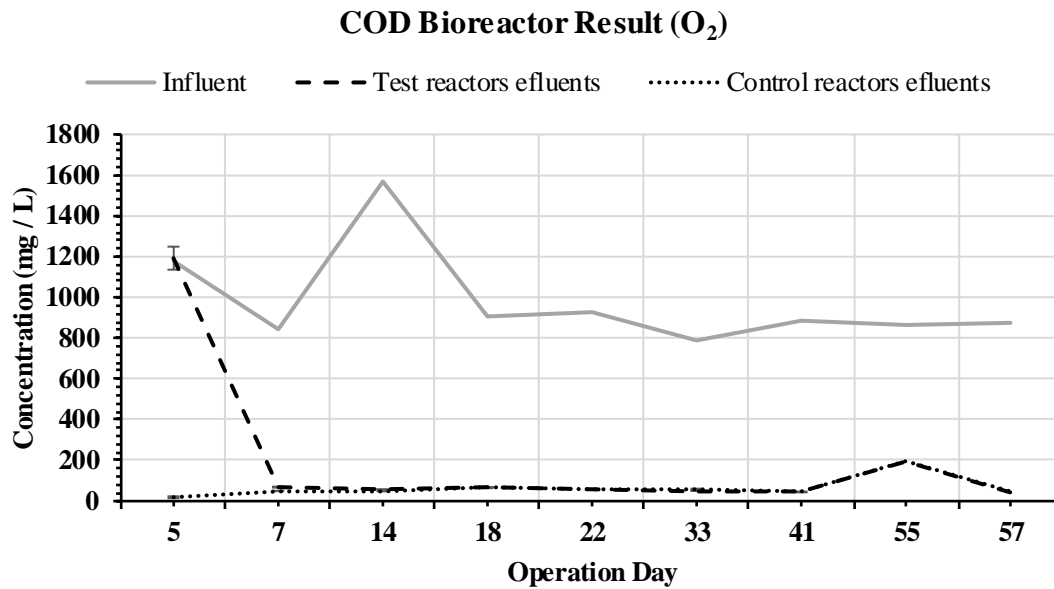


Figure 22: Graph showing COD results from test reactors and control reactors.

3.2.5. Phosphate-Phosphorus in Bioreactors

The concentrations of phosphate-phosphorus in the SBRs were obtained using the ascorbic acid method (8048, HACH) with the calibration curve equation in figure 16 ($y = 1.5655x + 0.034$) and are displayed in figure 23:

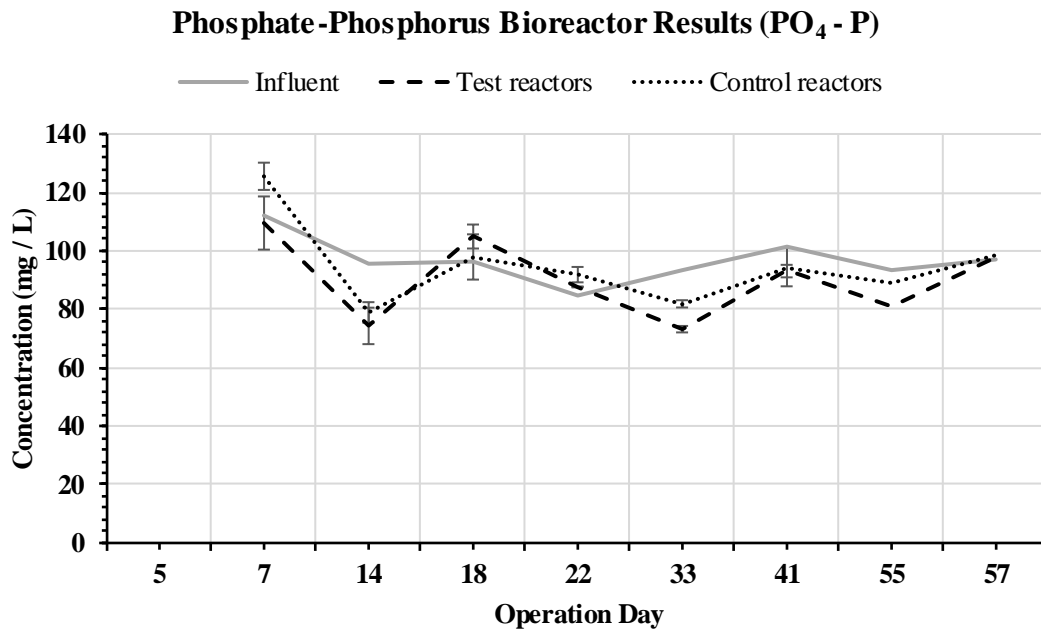


Figure 23: Graph showing phosphate-phosphorus results from test reactors and control reactors.

3.2.6. pH conditions in the bioreactors

The pH conditions measured in the influent and in the samples discharged from bioreactors are presented in figure 24:

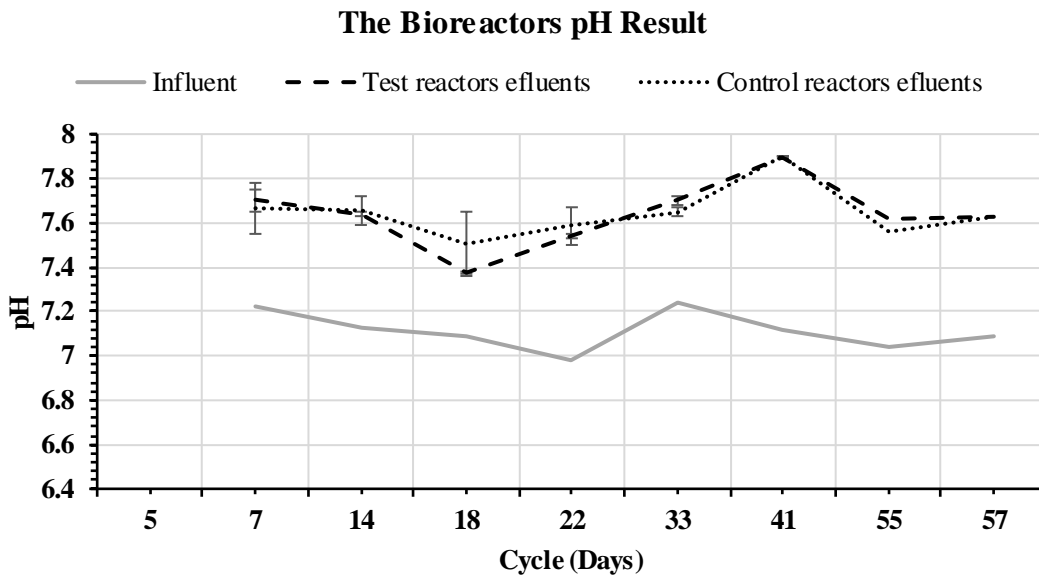


Figure 24: Graph showing the bioreactors pH results for test reactors and control reactors.

3.3. Characterization of granular sludge used in the experiment.

The morphological observations of the collected wastewater granular sludge sample used in this work with the aid of magnifier in a bid to obtain a characterization of diameter size (mm), shape factor - capriciousness of particle surface (smooth, half hairy, hairy) and aspect ratio – roundness of particle (round, elongated, irregular), as exemplified in figure 25, yielded the relative abundancies and average diameter size displayed in figure 26:

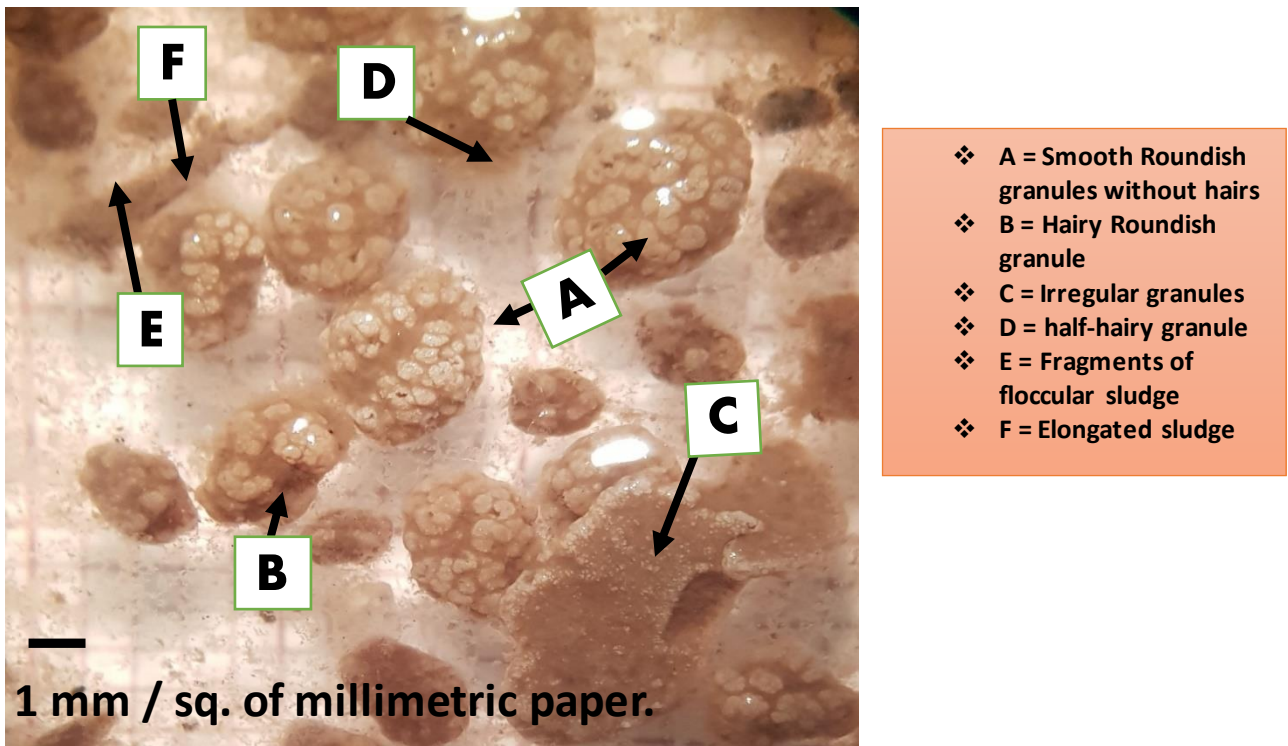
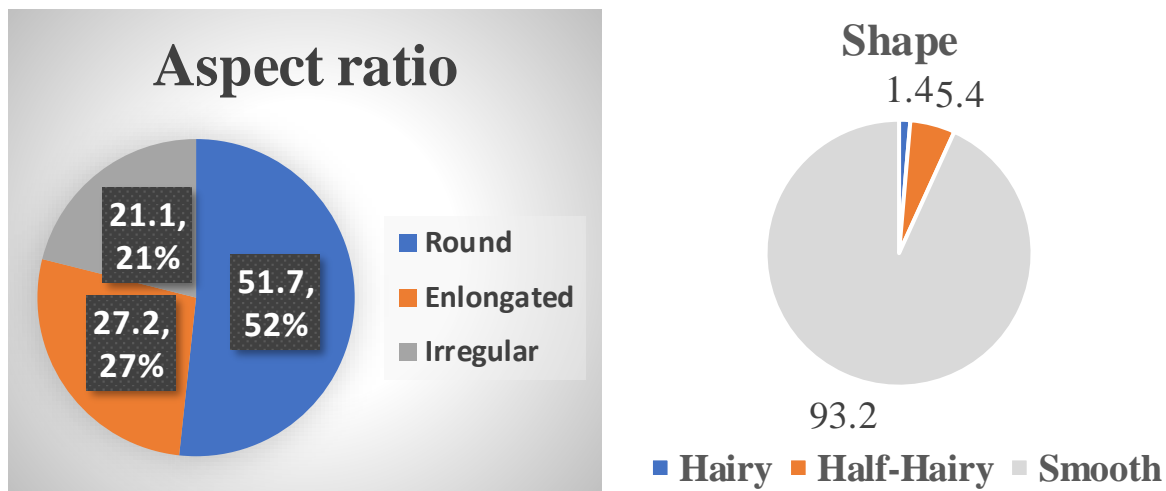


Figure 25: The morphological observation of granular sludge under a Leica Zoom 2000 Magnifier (x 7)



Average size of the granules in diameter = 3.3 ± 0.9

Figure 26: Pie chart statistical representation aspects and shape of the observed granules.

3.4.0. The results of paracetamol removal after bioaugmentation.

To evaluate the removal of Paracetamol and its intermediate degradation product Hydroquinone after the bioaugmentation with *M. aubagnense* HPB1.1, samples collected from the test and control bioreactors along two aerated stages after Paracetamol spiking were filtered with Polyethersulfone (PES) sterile syringe filters (pore size $0.22 \mu\text{m}$) to 2 mL glass vials and analyzed by HPLC as described in materials and methods.

The calibration curves obtained to determine the concentrations of Paracetamol and its metabolite Hydroquinone with their respective peak areas on HPLC chromatograms are displayed in figures 27 and 28:

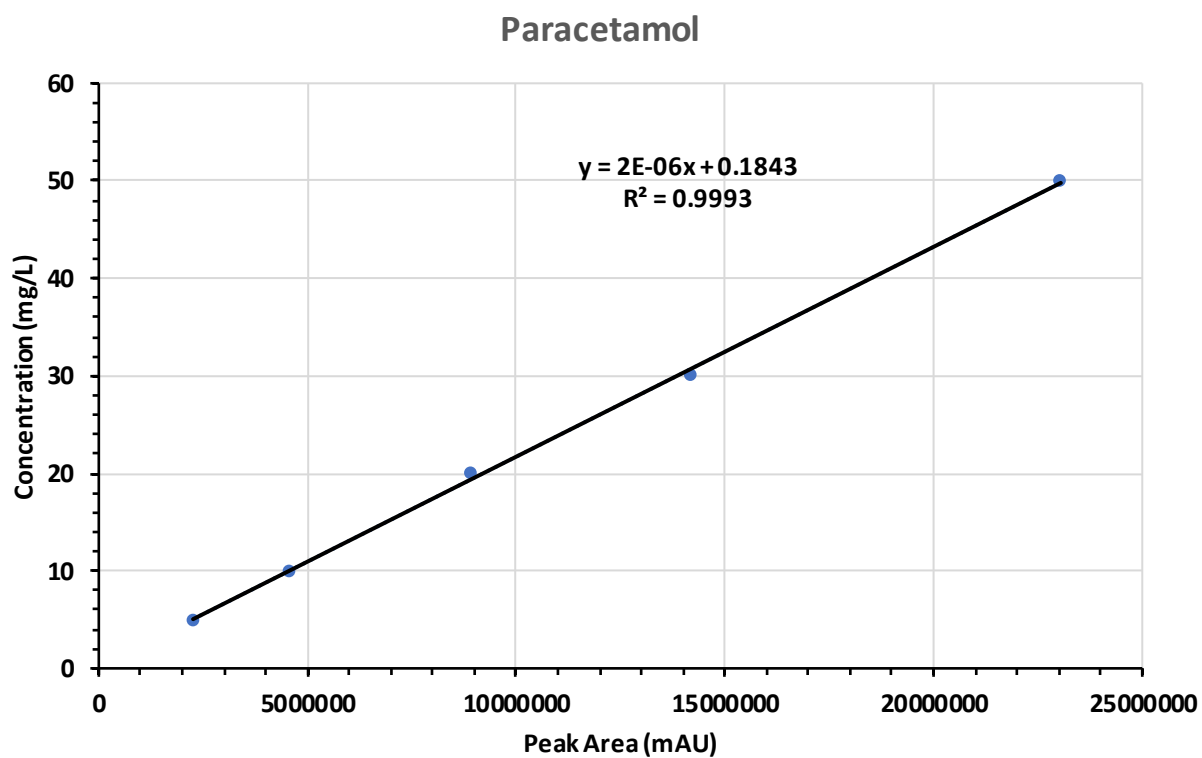


Figure 27: Calibration curve obtained for Paracetamol by HPLC analysis with 200 μ L injections of each standard concentration using the method described in materials and methods with absorbance measured at a wavelength of 190 nm (peak retention time = ~6.2 minutes).

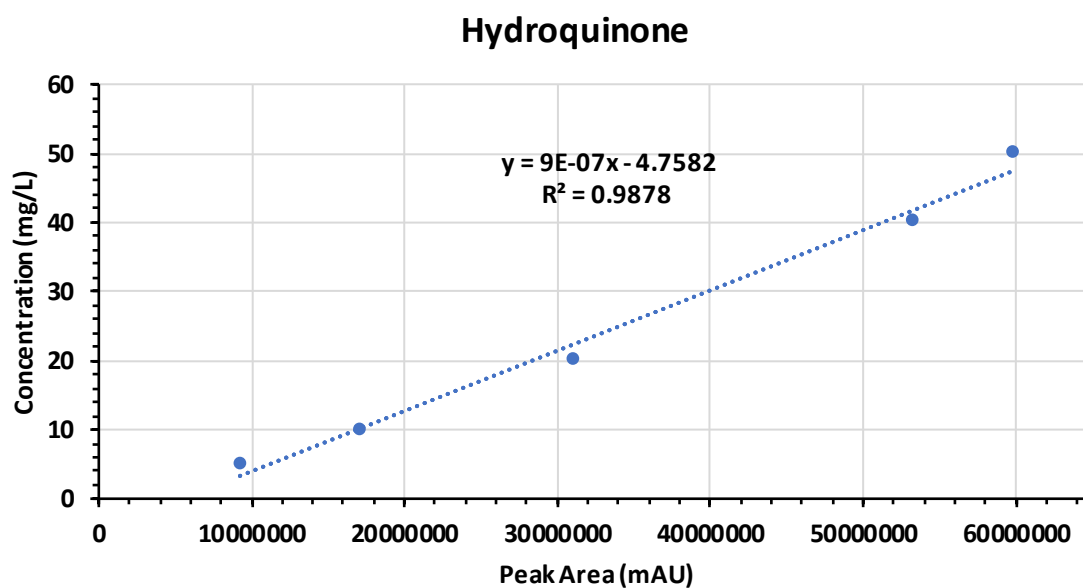


Figure 28: Calibration curve obtained for Hydroquinone by HPLC analysis with 200 μ L injections of each standard concentration using the method described in materials and methods with absorbance measured at a wavelength of 190 nm (peak retention time = \sim 4.3 minutes). LOD = 2.51; LOQ = 17.27.

The evolution of Paracetamol in the test and control bioreactors along the two aerated stages after Paracetamol spiking is displayed in figures 29 and 30 below as values of concentration calculated using the respective calibration curve:

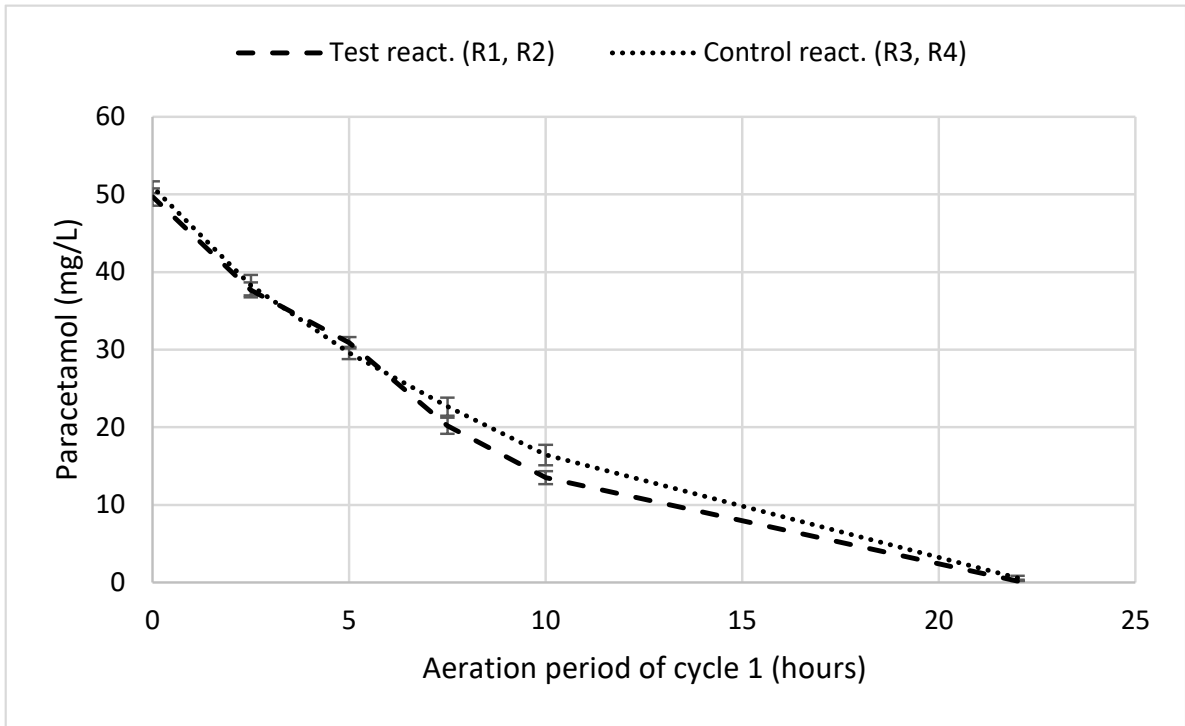


Figure 29: Graph showing the evolution of paracetamol during the first cycle aeration period.

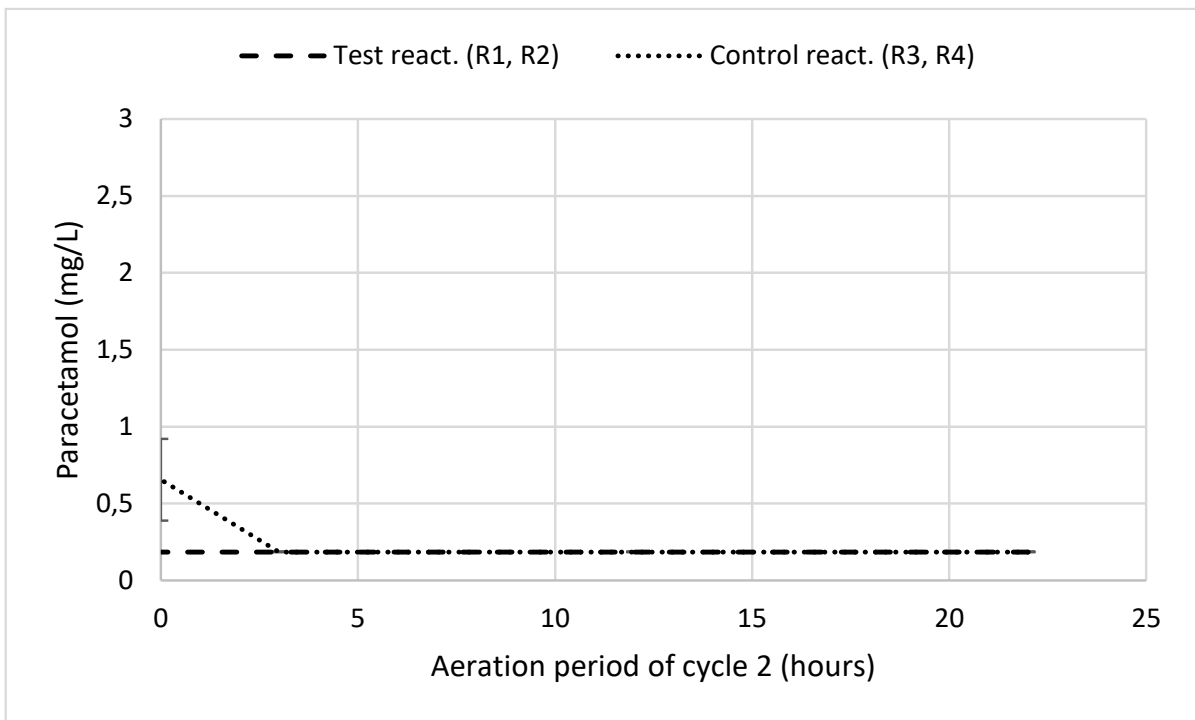


Figure 30: Graph showing the evolution of paracetamol during the second cycle aeration period.

The figures 31 and 32 below show the peak value area for the evolution of hydroquinone. The use of calibration curve showed the paracetamols' transformation products returned with a negative value.

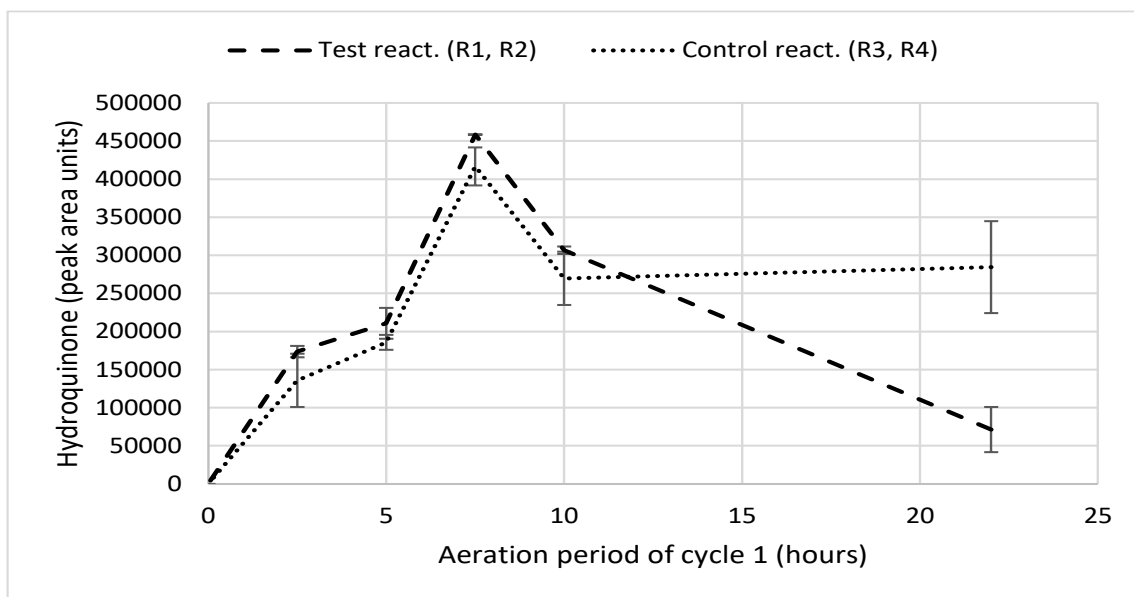


Figure 31: Graph showing the evolution of hydroquinone during the first cycle aeration period.

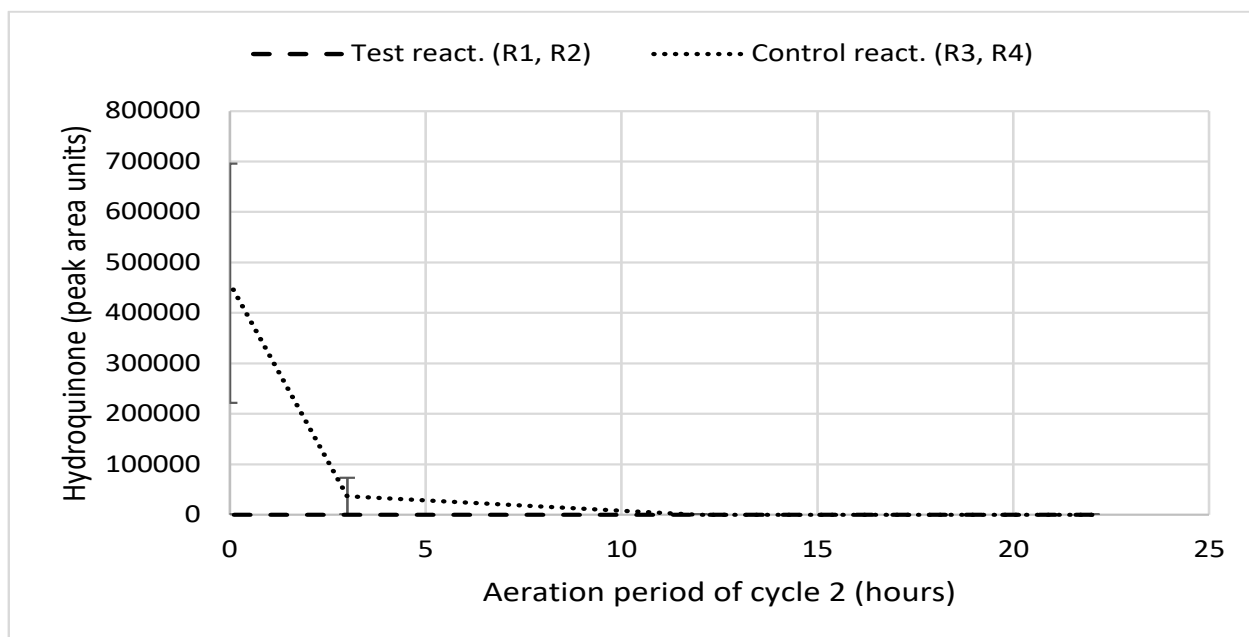


Figure 32: Graph showing the evolution of hydroquinone during the second cycle aeration period.

4. Discussion

4.1. Calibration curves and trueness of analytical methods for wastewater analysis

4.1.1. Total nitrogen standard calibration curve

The total nitrogen standard calibration curve results as shown in table 8a and figure 14 indicated 0.997 as the regression coefficients which suggests the degree of correlation between the absorbance values and the concentration values obtained were closely related such that the total nitrogen predictions (concentrations) yielded significantly low uncertainty of 0.01 from the standard error of regression.

Moreso, the residuals plot results (figure 14b) which typically illustrates how well the regression line fits into the data sets, indicates a sparsely distribution of the residuals about zero with the Sum of squares (SS) regression terms 0.32 ± 0.01 and the SS residuals terms 0.0042 ± 0.0003 . The SS regression terms of 0.32 ± 0.01 illustrated the extent to which the relationship between the total nitrogen concentration variables on the x-axis were with the corresponding absorbances on the y-axis. And by implication, since the SS regression terms 0.32 ± 0.01 was greater than the SS residual terms of 0.0042 ± 0.0003 , the regression line was adjudged to fit perfectly to the data sets depicted in figure 14a.

Similarly, the t-stat value 4.06 ± 0.01 result from the ANOVA output was greater than the p-value $6.67 \times 10^{-08} \pm 3.0 \times 10^{-4}$ which was less than 0.05 significance level (at the 95 % confidence interval). Consequently, the significance of coefficients output further suggests that the point of interception between x-axis and y-axis is significantly different from zero but with a lower margin of 4.06 ± 0.01 .

The calculated LOD $5.0454 \text{ mg/L} \pm 0.0003$ of the calibration curve (figure 14a) indicates the minimum concentration of total nitrogen that can be detected in water samples with a repeatability precision. The calculated LOQ which was $15.2891 \text{ mg / L} \pm 0.0003$ represented the lowest concentration of total nitrogen that can be quantified in water samples within an acceptable precision and accuracy.

Finally, the results from the validation process (figure 8b) showed the calibration curve was 98.4 % accurate in the instance of using a high range reference material (50 mg /L of total nitrogen standard). Hence, the trueness of the curve was 0.83 mg / L, which represents the amount in deficit (to be added) in the obtained concentrations. In instance of using the low range reference material (7 mg / L of total nitrogen standard), the calibration curve was 90.4 %

accurate with its trueness value as -0.64 mg/L , the excess amount of the obtained concentration using the calibration curve.

4.1.2. Ammonium Standard Calibration Curve Indophenol blue method

The ammonium standard calibration curve build for the indophenol blue method (as shown in figure 12) yielded a regression coefficient of 0.9916 which suggested the degree of correlation between the absorbance and standard concentration values were strong. Since the regression coefficient value (0.9916) is close to one, the predictions (ammonium standard concentrations) derived from the calibration curve had smaller uncertainties (0.02) from the standard error regression. Moreover, the analysis of variance (ANOVA) of the calibration curve significance of the coefficients t-stat value (-0.83 ± 0.02) and p-value ($1.66 \times 10^{-6} \pm 7 \times 10^{-2}$) at the 95 % confidence interval suggests the regression line intercept is not statistically significantly different from zero because the t-stat value is smaller than zero even when the p-value is less than 0.05 significance level (at the 95 % confidence level).

The ANOVA output of the SS regression term which was 0.14 ± 0.02 suggested the presence of a minimal source of variability in the calibration data sets because of the regression line. Similarly, the SS residual terms (which was 0.005 ± 0.068) was smaller than the SS regression terms thereby suggesting the regression line fits perfectly to the data sets. The residual plot in figure 12b implied the ammonium standard absorbance residuals were somewhat scattered randomly around zero due to the standard deviation of the instrument, while the absorbance responses are less scattered with the higher ammonium standard concentrations.

The LOD of the standard calibration curve $0.07 \text{ mg/L} \pm 0.02$ obtained value (as shown in table 6a) represents the lowest concentration of ammonium that can be detected in the influent and effluent wastewater samples with a repeatability precision. Similarly, the LOQ of the standard calibration curve $0.20 \text{ mg/L} \pm 0.02$ value depicts the lowest standard concentration of ammonium that can be quantified in the influent and effluent wastewater samples with acceptable precision and accuracy. Thanh-Nho *et al.*, 2022 reported a lower LOD and LOQ (0.044 and 0.147 mg/L, respectively) for indophenol methods while comparing the outcome of the analysis of dissolved ammonia nitrogen using both salicylate and indophenol methods and concluded the salicylate method could be more favorable for the analysis of dissolved ammonia nitrogen.

Overall, the attempts to validate the standard calibration curve (figure 12a) in a bid to ascertain its conformity with the expected concentration of 1 mg / L using the reference material (table 4 and 6b) yielded a Standard deviation of 0.0013 mg/L and a random error of mean of 0.00054 mg/L as measures of precision and a relative bias of 11.66 % - or accuracy of 88.34%. These (precision and accuracy) were then used in characterizing a trueness of -0.12 mg / L (the excess value in the concentration obtained using the standard calibration curve).

Salicylate Method

The ammonia calibration curve regression coefficient recorded as 0.998 (figure 13a) was closer to one and indicates the absorbance values and those of the concentration values were closely related, and as such, the predictions (ammonia standard concentrations) derived from the calibration curve yielded significantly lower uncertainty from of 0.01 from the standard error of the regression. Moreover, the residuals ammonia standard concentration plot portrayed in figure 13b suggests the residuals were randomly distributed and the standard deviation of the spectrophotometer responses (the absorbances) increased proportionately with the respective ammonia standard concentrations.

The ANOVA data outputs showed t-stat value (16.128 ± 0.006) was greater than the p-value ($9.62 \times 10^{-11} \pm 5 \times 10^{-2}$) and the p-value is less the 0.05 significance level (at the 95 % confidence interval). These values represent the significance of the coefficients at the 95 % confidence interval as they suggest the intercept is significantly different from zero. Furthermore, the sum of squares (SS) regression terms was recorded as 0.43 ± 0.006 and was significantly larger than the SS residual term (which was 0.0008 ± 0.0470). This implies the regression line fits perfectly to the data sets as shown in the calibration curve figure 13a. However, the SS regression term value (0.429 ± 0.006) indicates the extent of the source of variability in the calibration data probably due to the position of the regression line.

The calculated LOD $0.007 \text{ mg / L} \pm 0.006$ as shown in table 7a indicates the minimum concentration of ammonia that can be detected in water samples using this calibration curve with a repeatability precision. Similarly, the calculated LOQ of $0.022 \text{ mg / L} \pm 0.006$ suggests the lowest concentration of ammonia samples that can be quantified in water samples with certain acceptable precision and accuracy. The obtained LOD and LOQ was similar to the report of Huang *et al.*, 2019, who reported an LOD of 0.014 mg / L and LOQ of 0.045 mg / L of their calibration curve while attempting to determine the concentration of free ammonia via conductance using micro-distillation and micro-conductance instrument and they concluded

that micro-DCMI method was simple, robust and monitoring systems for the detecting low concentrations of ammonia in the quest to manage chloramination.

The validation results confirmed the conformity of the curve concentration when using the reference material with 0.25 mg / L as highlighted in table 7b and this suggests that the results obtained using the standard calibration curve were 94 % accurate and thus aided in permeating the trueness of -0.02 mg / L (the excess value in the obtained concentration using the standard calibration curve) along the concentrations of ammonia samples.

Salicylate method *versus* Indophenol blue method for sample analysis

The calibration curve of the salicylate method (figure 13) in comparison with the curve of the indophenol blue method (figure 12) was considered more suitable for the determination of ammonia concentration from the influents and effluents samples from sequencing batch reactors in this study. Although they both had good coefficient correlations, the salicylate method had better precision and accuracy indicators and therefore the obtained results were associated with higher trueness.

4.1.3. The Nitrate Nitrogen Standard Curve

The standard calibration curve of nitrate nitrogen (figure 15) had a regression coefficient of 0.989 which was relatively closer to 1 and thus suggesting the extent of the degree of correlation between the absorbance values on the y-axis and those of the concentration values on the x-axis of the nitrate nitrogen standards and this degree of correlation influenced the nitrate nitrogen predictions (concentrations) thereby resulting in a relatively significantly low uncertainty of 0.01 derived from the standard error of regression line. The points of influence at 15 mg / L, 20 mg / L, and 25 mg / L might have conferred certain levels of leverage along the x-axis causing the calibration line to tilt upwards or downwards in a bid to fit perfectly to the data sets hence the resultant regression coefficient 0.989.

Furthermore, the residuals plot (figure 15b) disclosed how well the regression line were suited to the data sets as well as expressing the random distribution of the residuals about zero while the standard deviation due to the spectrophotometer response (absorbances) increased with the nitrate nitrogen concentrations along the x-axis bearing SS regression terms of 0.40 ± 0.01 and SS residuals terms $0.0040 \text{ mg / L} \pm 0.0003$. Consequently, since the SS regression terms 0.40 ± 0.01 (which often illustrate the extent of interactions between the nitrate nitrogen concentration variables with the absorbances) were greater than the SS residuals terms 0.0040

mg / L \pm 0.0003, it further proves the regression line fits suitably to the data sets portrayed in figure 15a.

In the same manner, the ANOVA data output showed the t-stat value of 6.24 ± 0.01 to be greater than p-value of $4.06 \times 10^{-16} \pm 5 \times 10^{-4}$ (less than 0.05 significance level) at the 95 % confidence interval. These significance of coefficients results further buttress the fact that the intercept of x ,y-axis were significantly different from zero.

The calibration curve LOD of $1.9154 \text{ mg / L} \pm 0.0005$ as shown in table 9a indicates the minimum concentration of nitrate nitrogen that could be detected in water samples with a repeatability precision. While the LOQ of the calibration curve which was $5.8041 \text{ mg / L} \pm 0.0005$ connotes the lowest concentration of nitrate nitrogen that can be quantified in water within an acceptable precision and accuracy.

Overall, the validation of the nitrate nitrogen calibration curve experimentation as shown in table 9b presented the curve to have had 97.4 % accuracy (in the instance of using the high range reference material: $25 \text{ mg / L NO}_3^- \text{-N}$) and its trueness at 0.78 mg / L which represents the value in deficit in the obtained concentration values using the nitrate nitrogen standard calibration curve. This coincides with the routine validation processes employed during an analytical method development as shown in the report by Jiwarungrueangkul *et al.*, 2023 who modified and validated the method for determination of nitrate concentration spectrophotometrically (at wavelength 543 nm) in seawater sample by the reduction of nitrite with zinc powder and concluded the modified method yielded high-efficiency reduction with excellent accuracy of 95 % using CRM. In the instance of using the low range reference material ($7 \text{ mg/L NO}_3^- \text{-N}$), the nitrate nitrogen standard curve was adjudged to be 77 % accuracy and its trueness was $-1.38 \text{ mg / L} \pm 0.06$, suggesting 1.38 mg/L as the excess value in the obtained concentration using standard calibration curve. However, the 77 % accuracy in this instance did not downgrade the sensitivity of the curve (as regards to low range concentration) such that the expected concentration of the reference material 7 mg/L was exceeded with the obtained concentration as $7.38 \text{ mg/L} \pm 0.06$, hence the bias of -1.38 mg/L .

4.1.4. Phosphate-Phosphorus Standard Curve and Validation Results.

The phosphate-phosphorus standard curve (figure 16a) yielded a regression coefficient of 0.9994 which suggests the extent to which the degree of correlation between the absorbances on the y-axis were in relation with the known concentrations on the x-axis and thus exert certain influence on the phosphate-phosphorus predictions (concentrations) with significantly low uncertainty of 0.002 derived from the standard error of regression line. This is complementary to the data reported by Da Costa *et al.*, 2019 who postulated a coefficient of determination (R^2) for phosphorus as 0.990 and 0.998 while demonstrating the use of colorimetric analysis tool photometrix® (using spectrophotometric reagents) for the determination of phosphorus ion concentration in treated and natural waters.

Furthermore, insights into the residuals plot result of the curve (as shown in figure 16b) showcased there was random distribution of the residuals with concentration about zero and the standard deviation of the instrument responses were increasing with the phosphate-phosphorus concentrations along the x-axis thereby causing the regression line to fit perfectly into the sets of data with an SS regression terms of 0.945 ± 0.002 and the SS residuals terms $0.0001 \text{ mg / L} \pm 0.0065$. The regression line was adjudged to fit the data sets because the SS regression terms 0.945 ± 0.002 value indicated the quality of the interactions between the phosphate-phosphorus concentrations on the axis and those of the corresponding absorbances which portrayed the SS regression terms to be greater than the SS residuals terms $0.0001 \text{ mg / L} \pm 0.0065$.

The ANOVA t-stat value of 7.598 ± 0.002 was greater than the p-value $4.03 \times 10^{-15} \pm 6 \times 10^{-3}$ (less than 0.05 significance level) at the 92 % confidence interval and thus suggesting the intercept between x and y axis were significantly different from zero with a margin lower than 7.598 ± 0.002 . These data outputs were comparable with the results reported by Scott *et al.*, 2021 who experimented the removal of phosphorus from eighteen steel slag polluted freshwater samples coated with aluminum and reported in their summary of multiple linear regression prediction of the cumulative phosphorus removal results, higher t-stats values in comparison to the p-values in all the variables considered except the bulk density variable.

The curves' calculated LOD $0.004 \text{ mg / L} \pm 0.006$ (table 10a) represented the minimum concentration of phosphate-phosphorus that can be detected in the water samples with repeatability precision. Similarly, the calculated LOQ $0.012 \text{ mg / L} \pm 0.006$ represents the lowest concentration of phosphate-phosphorus that can be quantified in the water samples within an acceptable precision and accuracy.

Conclusively, the validation process of the phosphate-phosphorus calibration curve suggested the curve was 93.4 % accurate (using a reference standard of 1 mg / L PO₄ - P) with a trueness value of -0.06 mg / L as a result of the obtained concentration of 1.07 mg / L and this thus implied the true value of -0.06 mg / L was the value needed to be subtracted from the obtained concentration (1.07 mg / L) using the calibration curve in an effort to ensure the trueness at the respective concentrations of the phosphate-phosphorus derived from the wastewater influents and effluents sample. This is in accordance with the global scientific norm and comparable with the report by Cheong *et al.*, 2021 who used seawater certified reference material for nutrients from national research council of Canada CRM to validate the analytical method for phosphate determination in seawater sample using spectrophotometry and ion-exclusion chromatography and concluded method was able had acceptable high accuracy and sensitivity for phosphate-phosphorus.

4.1.5. COD Calibration Curve and validation result.

The COD standard curve (figure 17a) recorded a regression coefficient of 0.9995 (value closer to one) which illustrates the degree of correlation existing between the absorbance values in relation to the concentration values on the x-axis which in turn influenced the COD predictions (concentrations) with significantly low uncertainty of 0.001. These results were similar to those reported by Rohyami *et al.*, 2022 while experimenting method determination of COD for hospital wastewater using UV-Vis spectrophotometry and they outlined the determined coefficient as 0.9975 and affirmed the method to have had high precision and 85 – 110 % accuracy.

Further insights from the residuals plot (figure 17b) indicates there was no trend in the spread of the residuals with concentration standards: 400 mg / L, 600 mg / L, and 1000 mg / L as they were randomly distributed with the SS regression terms of 0.34 ± 0.001 and SS residuals terms of $0.0002 \text{ mg / L} \pm 2.30 \times 10^{-06}$. The SS regression terms being greater than the residuals terms further buttresses the regression line aligned perfectly to the data sets as shown in figure 17a because these obtained values highlight the correlation between the COD standard concentration variables on the x-axis versus the absorbances on y-axis. Similarly, Pouretedal *et al.*, 2021 employed the use of residual plots in examining the goodness-of-fit in regression and ANOVA results of Box-Benhken experimental design while investigation the removal efficiency of nitrocellulose by calculation of the reduction of COD in wastewater samples using electrocoagulation method.

The ANOVA data summary highlighted the significance of the coefficients t-stat value as -1.80 ± 0.001 was less than the p-value $8.24 \pm 2.30 \times 10^{-06}$ (value less than 0.05 significance level) at the 95 % confidence interval and thus emphasized the regression line intercept was not statistically significantly different from zero.

The calibration curve LOD value $7.29 \text{ mg / L} \pm 2.30 \times 10^{-06}$ obtained (table 11a) represents the minimum concentration of COD that can be detected in wastewater samples with a repeatability precision. Similarly, the LOQ value obtained as $22.11 \text{ mg / L} \pm 2.30 \times 10^{-06}$ epitomizes the lowest concentration of COD that can be quantified in the wastewater samples from the SBRs within a possible precision and accuracy.

Lastly, the validation process (table 11b) results of the COD standard calibration curve as shown in figure 17a (in instance of using 500 mg / L – COD high reference material), had a 97 % accuracy with trueness of $22.32 \text{ mg / L} \pm 17.95$. Instructively, the trueness value in this instance typifies the precision value necessary to be added to the subsequent obtained values using the calibration curve to ascertain the trueness of COD concentration for the wastewater influent and effluent samples. Observably, on using the low reference material (50 mg / L - COD) as illustrated in table 11b, the COD standard calibration curve was deemed not suitable for concentrations less than or equal to 50 mg / L .

4.2. SBR bioreactors

4.2.1. Total Nitrogen, Ammonia and Nitrates

The total nitrogen concentration of $\sim 145 \text{ mg / L}$ in the effluents of test reactors at the beginning of the experiments (obtained using the calibration curve equation in figure 14) was remarkably high in comparison to the control reactors (which was $\sim 28 \text{ mg / L}$) as illustrated in figure 18 and this was as a result of the SBRs' first stage bioaugmentation inoculum at day 4 involving the direct addition of *M. aubagnense* HPB1.1 bacterial cells to test reactors with the LB medium (instead of first collecting cells by centrifugation, removing the growth medium and resuspending the cells in the reactors influent as described in the methods). However, the results data from operation day 5 and onward maintained lower levels of total nitrogen concentration, with $31 \pm 4 \text{ mg / L N}$ in test reactors and $32 \pm 5 \text{ mg / L N}$ in control reactors (ranging between $28 - 40 \text{ mg / L}$), while in the influent it was $44 \pm 4 \text{ mg / L N}$ (ranging between $36.5 - 48.5 \text{ mg / L}$), as shown in figure 18. These slightly reduced total nitrogen concentrations in reactors effluents were primarily induced by a combination of nitrification and denitrification processes in the *in situ* granular sludge layers (figure 10a) and its' environs (figures b and c) ending by some N release to the atmosphere. Similarly, Cao *et al.*, 2019 reported 4.0 mg N / L of total

nitrogen in the effluent samples while experimenting an innovative partial denitrification anammox process in SBR wastewater treatment process.

These results are complemented by the data (obtained using calibration curve equation $y = 2.8124x + 0.0917$) of the ammonia-nitrogen concentrations (figure 19), in that, majority of the total nitrogen derivatives considered in this study were in the form of ammonia in the influents ($\text{NH}_4 - \text{N}$ ranging between 34 – 46 mg / L) but were consumed mainly by a combination of Ammonia-Oxidizing Bacteria (AOB) and Nitrite-Oxidizing Bacteria (NOB) *in situ* in the granular sludge depicted in figure 10, thus reaching values mainly below 1 mg / L $\text{NH}_4 - \text{N}$ in the SBRs effluents. These results were lower than the report by De Freitas Bueno *et al.*, 2020, who postulated 2.7 mg / L ammonia concentration in the effluent sample of wastewater while investigating the treatment of landfill leachate using aerobic granular sludge process and concluded the aerobic granular sludge process to be suitable for domestic wastewater treatment under tropical climate conditions.

Furthermore, the concentration deviations observed in operational day 33 and 55 in figure 19 was caused by operational problems that lead to a short aeration period of just around 90 minutes before discharge. Thus, the shorter aeration time led to incomplete oxidation of ammonia in the nitrification processes and peaks of $\text{NH}_4 - \text{N}$ concentration in the effluents on those days.

Overall, the SBRs successfully removed ammonia from the influent. Indeed, this happened even after the addition of Paracetamol to the four reactors at day 14 (after the fourth bioaugmentation inoculum) to make a concentration of 50 mg / L on the filled volume. Although Park and Seungdae 2020 reported inhibitory effects of 100 mg / L of this drug on activated sludge under nitrifying aerobic conditions, resulting in lower ammonia oxidation and the reduction (> 80 %) in the population of *Nitrosomonas oligotropha* in the activated sludge bioreactor.

The nitrate-nitrogen concentrations (derived using calibration curve equation figure 15) were ranging between 1 – 24 mg / L, while nitrite-nitrogen concentrations (estimated by mass balance using concentrations of total N, ammonia N and nitrates N) in the SBR effluents ranged between 4 and 28 mg / L for the test reactors and control reactors, as evident in figures 20 and 21. Similarly, Maia *et al.*, 2022 reported nitrate concentration of 5.5 mg / L in the effluent sample of SBR with AGS while investigating the efficacy of wastewater treatment. The trends along the experiment reveal that nitrite oxidation by NOB (facilitated by nitrite oxidoreductase)

was successful in converting nitrite to nitrate mainly after day 14 probably due to an initial adaptation of the microbial populations in the granules to the medium used as influent and to the reactors' operating conditions. Furthermore, the presence of trace amounts of nitrite concentrations (about 2 mg / L) in the influent (as shown in figure 20) might be as a result of some active AOB in the tubes transporting the influent to reactors (where the influent was sampled) whom might have begun the conversion of ammonia-nitrogen to nitrite-nitrogen even before the influent reached the bioreactors with the granular sludge. Also, the observable data-trend deviations in the test and control reactors at the operational days 33 and 55 were uniform across the figures 19, 20, and 21 and the reasons were the same as earlier stated in the paragraphs above.

In the SBRs, the nitrate-nitrogen concentration residues were higher than ammonia-nitrogen because, on the completion of the nitrification process in the SBRs (by AOB and NOB) the denitrification process (usually favoured by prolonged anaerobic conditions) was ineffective due to the inactiveness of denitrifying bacteria whose primary duties were to utilize the available nitrate-nitrogen in the wastewater and as well as functioning as an electron acceptor in the absence of oxygen, converting it to nitrogen gas. Zhou *et al.*, 2020 reported 96.92 % and 82.49 % of ammonia-nitrogen and nitrite removal efficiency respectively while investigating the relative abundance of NOB and AOB during nitrification and intermittent aeration using SBR – AGS.

One possible justification for such incomplete denitrification could have been that the anaerobic feeding period was not long enough and/or the small sized bioreactors used did not allow to create enough anaerobic conditions in the sludge, because oxygen could be diffused from the atmosphere through the small water column till the bottom of reactors without being consumed.

4.2.2. COD

The COD concentrations in the influent and effluents samples were ascertained using the COD standard calibration curve equation portrayed in figure 17a. The results data showed COD concentration in the range of 20 – 40 mg / L O₂ in the test and control reactors except for the ~1200 mg / L O₂ in the effluents of test reactors at day 5 due to the bioaugmentation inoculum of *M. aubagnense* HPB1.1 bacteria in LB medium (as previously explained) and the 200 mg / L COD concentration recorded on the operational day 55 (due to lower aeration period caused by operational problems). The concentration of COD in the influent was ranging from 800 to 900 mg / L O₂, except for two times: 1181 mg/L O₂ at day 5 in which the analyzed influent was

manually prepared by mixing the four feeding solutions instead of being collected from the reactors' inlet pipe coming from the pumping system, and 1580 mg / L O₂ at day 14 probably due to a mistake in the preparation of the carbon sources feeding solution. Thus, apart from day 5, the COD removal was always above 90% except on day 55 in which it was ~77 %. This study effluent COD results were lower than those reported by Jiang *et al.*, 2021 who stated their COD concentration of the effluent sample as 650 ± 50 mg / L during their investigation of the efficiency and effects of advance nitrogen removal using SBR.

During the anaerobic conditions in the SBRs, the anaerobic microbial activities promoted the fermentation and denitrification breaking down of some organic compounds and thus contributing to reduce the COD concentration. Moreover, the routine aeration and mixing conditions in the SBRs favor the reduction of COD in the effluent by providing oxygen for AOB, NOB and other microorganisms, thus enhancing the metabolic activities and aerobic degradation of organic compounds eventually to complete mineralization into CO₂ resulting in reduced COD concentration. Furthermore, the transformation of some organic compounds into volatile organic compounds in the reactors could have also contributed to reducing COD because during aeration and mixing, the volatile organic compounds could have given off into the atmosphere. Mourao *et al.*, 2021 emphasized the influence of aeration and mixing conditions on the removal of COD from swine wastewater effluent samples using SBRs with AGS during their experiment evaluating the applicability of AGS technology for treating swine wastewater.

The structural architecture of the granular sludge also contributed to the reduction of COD concentrations in the SBRs. These structural capabilities include biofilm formation, high concentration biomass of bacteria and other organisms (figures 25 and 26), and the porosity of the granular sludge. For instance, the matrix of the EPS (figure 7) enhances the formation of biofilms which allows the attachment of and growth of bacteria and microorganisms which are involved in degradations of organic compounds, fermentation and denitrification processes and thus reduce the COD concentration in the SBRs. This assertion was comparable to the report by Araujo *et al.*, 2022 who studied the influence of temperature (20 – 30 ° C) on the formation of AGS in SBR and reported the relationship of the AGS sizes with the removal of nitrate-nitrogen, COD, and ammonia-nitrogen and postulated the key roles of EPS in nutrients removal and proffered strategies to remove poorly sedimentable biomass.

Overall, some of the prominent oxidizing bacteria often engaging in reduction of COD concentration include: *Pseudomonas* species (often consume organic compounds as energy source) (Sarvajith *et al.*, 2022), *Acinetobacter* species (they oxidize the carbon sources and contribute to the degradation of organic matter) (Gao *et al.*, 2020), *Aeromonas* species (often consume organic compounds under aerobic conditions and contribute to the oxidation of organic matter), *Bacillus* species (they utilize organic compounds and contribute to oxidation of organic matter), and *Enterobacter* species (they contribute to the degradation of organic matter). The study by Buhari *et al.*, 2022 experimented with a certain array of AOB consortium isolated from AGS of coffee wastewater for the polishing of low ammonia-contaminant and COD removal and concluded the optimized consortium had 85 % and 78 % of ammonia and COD removal efficiency respectively.

4.2.3. Phosphate-phosphorus

The concentrations of phosphate-phosphorus in the SBRs (figure 23) were obtained using the calibration equation shown in figure 18a. The obtained results data revealed the influent sample phosphate-phosphorus concentrations to range between 84.5 – 112 mg / L while the effluent sample of the test reactors had concentration range between 76 – 108.5 mg / L and the control reactors had concentrations ranging between 80 – 128 mg / L of phosphate-phosphorus. These results imply the SBRs conditions deployed in the study was insufficient in reducing the phosphorus concentrations. The inability of the SBRs to effectively treat the synthetic wastewater for phosphorus might have been due to lack of enough anaerobic conditions during the feeding periods in the granular sludge reactors adequate for the PAOs communities (figure 10b and 10c) to have selective advantage over other bacterial populations present under the ‘feast-famine’ conditions and thus serve as the internal phosphorus reservoir. PAO have an advantage under the cycling anaerobic feeding : aerobic fasting conditions because: (i) under anaerobic conditions, they can consume simple organic compounds - like acetate for example - to synthesize and accumulate poly- β -hydroxyalkanoates (PHA) while using stored polyP as energy source and releasing orthophosphate, and then (ii) in the absence of organic compounds and under aerobic or anoxic conditions they are able to use oxygen or nitrogen oxides, respectively, to metabolize the accumulated PHA as a source carbon and energy to grow and to assimilate phosphate to synthesize polyP and recover its levels (Seviour *et al.*, 2003). Removal of P from water is achieved when the conditions encourage an excessive accumulation of P in bacterial cells in the form of polyphosphate (polyP) comparing with the levels required in the metabolic demand for growth. Thus, if during the feeding period the conditions are not

anaerobic, the PAO will not accumulate PHA by and therefore they will not have a source of carbon and energy to use for proliferation and phosphate assimilation during the aerobic fasting period.

The study by Maslon *et al.*, 2022 investigated the effects of the unevenness in wastewater flow on SBRs treatment efficiency while monitoring the routine parameters in WWTPs and reported the phosphorus removal percentage for different locations as 24.9 – 95.1 % and 70.4 – 95.3 % in a wastewater quality of 0.25 – 3.4 g P/m³ and 0.21 – 4.8 g P/m³ respectively and concluded the use of SBRs as an independent element of biological wastewater treatment does not always guarantee a high degree of nutrients removal in the event of varying uneven wastewater inflow.

Moreover, there were possibilities of PAOs versus other microorganisms to have been competing for volatile fatty acids and nutrients in the SBRs especially during the anaerobic phase, thereby affecting the phosphorus removal efficiency. The study of Andreiadakis *et al.*, 2022 investigated the effect of free nitrous acid and free ammonia on the anoxic phosphorus uptake rate of PAOs via the utilization of nitrite and inoculation of the SBRs with strong PAO culture and reported the effects of free nitrous acid to have had an optimum effect on phosphorus uptake to about 1.6 µg N / L and 37 mg N / L using a non-competitive inhibitory model and Levenspiel model respectively.

4.3. pH

The pH values obtained from the bioreactor, as shown in figure 24, were for the influent between the range 6.9 – 7.2, while the test reactors pH value was between range 7.3 – 7.8, and the control reactors had pH values between range 7.5 – 7.8 over the experimental period. The pH conditions in the bioreactors were sensitive to other occurring interfering factors chiefly because of bioaugmentation and Paracetamol bio-removal activities. For instance, after the addition of Paracetamol to reactors on day 14 the pH conditions changed with a slight decay until day 18. Then, the pH gradually raised until the addition of p-Benzoquinone (a Paracetamol metabolite) to reactors (in a study out of the scope of this thesis) at day 42, as shown in figure 24. The study by Zajac *et al.*, 2023 characterized the pH conditions of their experiment while investigating the possibility of improving the efficiency of diclofenac removal from AGS using SBRs reactor and concluded that pH conditions had influenced the outcome of their results.

4.3.1 Role of pH in Total nitrogen removal

The conversion of ammonia (NH₃) to ammonium ions (NH₄⁺) in wastewater is tightly regulated by pH conditions and an increase in the pH prompts the conversion of NH₄⁺ to NH₃. Ammonia

(the un-ionized NH_3 form) is more toxic than ammonium (the ionized NH_4^+ form) and can be toxic to a variety of bacteria but especially to Nitrobacter (Kim *et al.*, 2008; Folino *et al.*, 2020; Meng *et al.*, 2022). This implies higher pH values in bioreactors can result in increased concentrations of toxic NH_3 and imper the nitrification process leading to high total nitrogen concentrations in the bioreactors. Nevertheless, the pH values obtained (as shown in figure 24) in the influent (pH values 6.9 – 7.2) and the effluents (pH value 7.3 – 7.8 and 7.5 – 7.8 for test and control reactors respectively) indicated a pH range with low toxicity, therefore high microbial activities of the bacteria during SBRs treatment process. The study by Soroosh *et al.*, 2022 recorded extreme pH conditions values greater than 9.5 and adjusted pH-conditions less than 8.0 while experimenting the influence of hydraulic retention time on microalgae-bacteria floc in SBRs for municipal wastewater treatments and concluded that the extreme pH condition was less desirable because the $\text{pH} > 9.5$ led to culture collapse and biomass washout while the $\text{pH} < 8.0$ led to efficient treatments of the wastewater.

Furthermore, the crucial role of AOB and NOB are essential for achieving nitrification as mentioned in the above paragraphs and the activities and growth of these nitrifying bacterial are influenced by optimal pH range (between 7.5 – 8.5). The optimal pH value range recorded in this study (pH value 7.3 – 7.8 and 7.5 – 7.8 for test and control reactors respectively) favored the activities of AOB and NOB, hence, the successful removal of total nitrogen from the SBRs (figures 18,19,20, and 21). Indeed, these values are within acceptable/optimal values for nitrification for example according to the “Nitrification (Ammonia Oxidation) In Wastewater Treatment Plants” White Paper from Bioscience, Inc. (<http://www.bioscienceinc.com>).

Similarly, the denitrifying bacteria during denitrification are sensitive to pH conditions in the SBRs and tend to favor slight basic to neutral pH conditions in a bid to successfully remove total nitrogen from the bioreactors. Pan *et al.*, 2012 for instance reported an optimal pH range for nitrate and nitrite reduction between 7.5 to 8.0. The present study influent pH value range 6.9 – 7.2 (figure 24) was neutral and thus suitable to kick-start the denitrification process (during anaerobic periods) and as the influent entered the bioreactors the pH value range became slightly basic (pH value 7.3 – 7.8 and 7.5 – 7.8 for test and control reactors respectively), within acceptable/optimal values. Therefore, it is difficult to ascertain if pH is the cause of the observed weak denitrifications and nitrogen removals.

4.3.2. Role of pH in Phosphorus removal

Apart from the biological removal by the PAO described above, the amount of phosphorus in the effluent can be controlled by addition of chemicals to change the solubility, speciation, and precipitation of phosphorus compounds, which is generally influenced by pH conditions. The ideal pH range of phosphorus precipitation depends on the wastewater composition and the chosen chemicals added for precipitation. Generally, an iron or aluminum salt is used, but magnesium can also be used with the added benefit of forming struvite ($\text{NH}_4\text{MgPO}_4 \cdot 6\text{H}_2\text{O}$), an effective source of nitrogen, magnesium, and phosphorus that can be used in agriculture. Mavhungu *et al.*, 2021 studied four process parameters, magnesite dosage, contact time, pH conditions and temperature of municipal wastewater while investigating the influence of these operational parameters in struvite precipitation and concluded that at low dosage, contact time and optimal pH conditions of about 7.5, there were effective removal of phosphorus and total nitrogen from the wastewater.

Indeed, even in the biological systems chemical precipitation of phosphorus can occur without the addition of chemicals for that purpose. When concentrations of orthophosphate-phosphorus ($\text{PO}_4\text{-P}$), ammonia-nitrogen ($\text{NH}_4\text{-N}$) and magnesium (Mg^{2+}) are high enough with solution pH of specific values (e.g. > 8.5) in high turbulent areas, the formation of struvite can take place (Leng and Soares 2021). Yet, the pH range (pH value 7.3 – 7.8 and 7.5 – 7.8 for test and control reactors respectively) in our reactors did not favor this phenomenon.

Similarly, the biological uptake of phosphorus via the microbial activities of PAOs and their intracellular storage as polyphosphates in the anaerobic or anoxic layers of the granular sludge are influenced by optimal pH conditions (between 6.5 – 7.5), because the PAOs growth and microbial activities are more effective in said pH conditions. Thus, the pH range in this study (pH value 7.3 – 7.8 and 7.5 – 7.8 for test and control reactors respectively) was adequate to ensure and promote the removal of phosphorus in the SBRs, and therefore it cannot be indicated as the cause of the observed inefficiency in this regard. This was in consonance with the report by Nguyen *et al.*, 2023 who stated that *Tetrasphaera* PAOs displayed kinetic advantages at high pH range between 6.0 – 8.0 while they were investigating phosphorus removal in WWTPs and concluded that *Tetrasphaera spp* activities at high pH had synergistic potentials of impacting phosphorus removal.

4.3.3. Role of pH in COD removal

The effects of pH conditions in COD removal in SBRs are primarily direct such that pH conditions influence microbial activity (membrane transport mechanisms, enzymatic activities, metabolic pathways, etc.), and thus biomass growth in the granules (bacteria indices and other microorganisms in the granules) and also indirect effects since it has influence in nutrients availability (nitrogen, phosphorus, and micronutrients) which also affects the organism's activity. The obtained pH values close to neutral (pH value 7.3 – 7.8 and 7.5 – 7.8 for test and control reactors respectively) as shown in figure 24, is adequate to promote the effective intracellular breakdown of organic compounds as well as extracellular hydrolysis by enzymes such as proteases, lipases, and carbohydrase present in the bioreactors. In fact, other works studying wastewater treatment with granular sludge report successful treatment at pH values close to neutral, as for example the report by Verma *et al.*, 2023 who examined municipal wastewater with pH 7.1 ± 0.3 conditions while using granular activated carbon-SBRs in a bid to treat the wastewater and remove COD, ammonia, nitrate, and phosphorus.

4.4.0. The removal of Paracetamol after bioaugmentation

The HPLC results on the evolution of paracetamol suggest the removal of this drug was successful during the aeration period as shown in figures 29 and 30 for cycle 1 and 2 after the drug spiking, respectively. Although in the first aeration cycle the differences between the bioaugmented and control reactors were not so evident, when the second aeration cycle started paracetamol was no longer detected in the first ones, while in the second ones it still was. In fact, other works had already shown successful Paracetamol removal in bioreactors with bioaugmented sludge. For example, Marchlewicz *et al.*, 2023 reported the successful degradation of paracetamol during a degradation test in the presence of *Bacillus thuringiensis* B1(2015b) and *Pseudomonas moorei* KB4 strains. However, although it is known that one of the products of Paracetamol transformation is hydroquinone, to our knowledge the few works focused on improving its biodegradation are based on acclimation strategies (Zhao, 2017; Zhang *et al.*, 2022), and usually this compound is not a target in works monitoring WWTP or receiving waters. In our work, the HPLC results of the evolution of hydroquinone in the SBRs during the first and second cycles of aeration after Paracetamol spiking (as shown in figures 31 and 33) clearly indicate there was a faster removal of hydroquinone in the bioreactors bioaugmented with the bacterial strain *Mycolicibacterium aubagnense* HPB1.1. On the other hand, independently of bioaugmentation, the removal of this type of recalcitrant pollutants with potential toxicity in the aeration phase of SBR reactors indicates that aerobic organisms play a

fundamental role. Similarly, Struck-Sokolowska *et al.*, 2022 reported an 80 % quantitative degradation of 1H-benzotriazole during aeration phase after SBR process.

4.5. Conclusions

Overall, the validation of the calibration curves using reference materials was successful as the curves were adjudged to have over 90 % accuracy and were suitably fit to be implemented in the present research study.

Maintaining the stability of granules in the bioreactors was successful over the course of the experiment. However, there was not phosphate removal and the total nitrogen removal was not efficient and nitrates-nitrogen content in the effluent was high, indicating the dephosphatation in the granules did not occur and denitrification was very weak. The possible cause pointed is the inadequate anaerobic conditions in the sludge due to the small size of the bioreactors. The anaerobic conditions are crucial for the Denitrifying Poly-phosphate Accumulating Organisms to perform nitrate reduction into nitrogen gas (N₂) which is released into the atmosphere while using the stored poly-phosphates as energy source and transforming the consumed carbon sources into stored poly-β-hydroxyalkanoates, which is then used under aerobic or anoxic conditions as carbon and energy source while phosphate is assimilated to synthesize poly-phosphates. Nevertheless, the total nitrogen was slightly removed and ammonia and organic matter (indicated by COD) were considerable removed in the SBRs such that the effluent samples had total nitrogen concentrations of 31 ± 4 mg / L N (test reactor) and 32 ± 5 mg / L N (control reactor), ammonia-nitrogen concentrations below 1 mg / L (both test and control reactors), nitrate-nitrogen concentrations between 1 – 24 mg / L (test and control reactors), COD concentrations between 20 – 40 mg / L (test and control reactors), and phosphate-phosphorus concentrations had 76 – 108.5 mg / L (test reactor) and 80 – 128 mg / L (control reactor).

This work shows that aerobic organisms play a fundamental role in the biodegradation of paracetamol and that strategies of granular sludge bioaugmentation with the bacterial strain *Mycolicibacterium aubagnense* HPB1.1 have the potential to induce faster removals of this drug in WWTP and to improve the removal of its recalcitrant metabolite Hydroquinone. Moreover, in general, this outcome suggests the SBRs with AGS will be suitable for bacteria bioaugmentation and pharmaceutical drug inoculation experiments in a bid to evolve strategies to eradicate recalcitrant pollutants with potential toxicity tendencies.

4.6. Future prospects

To evaluate the impact of the bioaugmentation inoculum on the bacterial communities in the granular sludge, a taxonomic study based on 16S rRNA gene sequences will be performed on sludge samples from the bioaugmented SBRs as well as on samples from the control reactors, collected before and after the several inoculations.

With the aim of better understanding the incomplete removal of N and P nutrients from water, it is necessary to:

- 1) analyse the water quality parameters in study (COD, Total N, $\text{NH}_3 - \text{N}$, $\text{NO}_2^- - \text{N}$, $\text{NO}_3^- - \text{N}$, $\text{PO}_4^{3-} - \text{P}$ and pH) at the beginning, at mid-time and at the end of both the main SBR operational stages (anaerobic feeding and aeration starving);
- 2) monitor the dissolved oxygen (DO) at the bottom of the SBRs, where the granular sludge settles, in real time throughout all the operating cycle to assess whether anaerobic or anoxic conditions are achieved during the feeding stage.
- 3) monitor the water temperature in the SBRs to evaluate eventual deviations from the laboratory typical room temperature (23 ± 2 °C), caused by air conditioning failures.

5.0. Reference

- Abdel-Aal, M. *et al.* (2018) “Modelling the potential for multi-location in-sewer heat recovery at a city scale under different seasonal scenarios,” *Water Research*, 145, pp. 618–630. Available at: <https://doi.org/10.1016/j.watres.2018.08.073>.
- Abey Siriwardana-Arachchige, I.S.A. and Nirmalakhandan, N. (2019) “Predicting removal kinetics of biochemical oxygen demand (BOD) and nutrients in a pilot scale fed-batch algal wastewater treatment system,” *Algal Research*, 43, p. 101643. Available at: <https://doi.org/10.1016/j.algal.2019.101643>.
- Abouhend, A.S. *et al.* (2023) “Role of Hydrodynamic Shear in the Oxygenic Photogranule (OPG) Wastewater Treatment Process,” *ACS ES&T Water* [Preprint]. Available at: <https://doi.org/10.1021/acsestwater.2c00317>.
- Abu-Reesh, I.M., Kunju, A. and Sevda, S. (2022) “Performance of microbial fuel cells in treating petroleum refinery wastewater,” *Journal of Water Process Engineering*, 49, p. 103029. Available at: <https://doi.org/10.1016/j.jwpe.2022.103029>.
- Aghasadeghi, K. *et al.* (2021) “Pilot-scale comparison of sodium silicates, orthophosphate and pH adjustment to reduce lead release from lead service lines,” *Water Research*, 195, p. 116955. Available at: <https://doi.org/10.1016/j.watres.2021.116955>.
- Ahmed, S. *et al.* (2021) “Recent developments in physical, biological, chemical, and hybrid treatment techniques for removing emerging contaminants from wastewater,” *Journal of Hazardous Materials*, 416, p. 125912. Available at: <https://doi.org/10.1016/j.jhazmat.2021.125912>.
- Ajao, V. *et al.* (2021) “Biofloculants from wastewater: Insights into adsorption affinity, flocculation mechanisms and mixed particle flocculation based on biopolymer size-fractionation,” *Journal of Colloid and Interface Science*, 581, pp. 533–544. Available at: <https://doi.org/10.1016/j.jcis.2020.07.146>.
- Akhkha, A., Al-Radaddi, E.S. and Al-Shoaibi, A.K. (2019) “The impact of treated and untreated municipal sewage water on growth and physiology of the desert plant *Calotropis procera*,” *Journal of Taibah University for Science*, 13(1), pp. 746–754. Available at: <https://doi.org/10.1080/16583655.2019.1605650>.
- Akizuki, S., Cuevas-Rodríguez, G. and Toda, T. (2019) “Microalgal-nitrifying bacterial consortium for energy-saving ammonia removal from anaerobic digestate of slaughterhouse wastewater,” *Journal of Water Process Engineering*, 31, p. 100753. Available at: <https://doi.org/10.1016/j.jwpe.2019.01.014>.

- Alfonso-Muniozguren, P. *et al.* (2021) “The role of ozone combined with UVC/H₂O₂ process for the tertiary treatment of a real slaughterhouse wastewater,” *Journal of Environmental Management*, 289, p. 112480. Available at: <https://doi.org/10.1016/j.jenvman.2021.112480>.
- Alves, O.I.M. *et al.* (2022) “Formation and stability of aerobic granular sludge in a sequential batch reactor for the simultaneous removal of organic matter and nutrients from low-strength domestic wastewater,” *Science of the Total Environment*, 843, p. 156988. Available at: <https://doi.org/10.1016/j.scitotenv.2022.156988>.
- Andersen, I.M. *et al.* (2019) “Nitrate, ammonium, and phosphorus drive seasonal nutrient limitation of chlorophytes, cyanobacteria, and diatoms in a hyper-eutrophic reservoir,” *Limnology and Oceanography*, 65(5), pp. 962–978. Available at: <https://doi.org/10.1002/lno.11363>.
- Andreadakis, D. *et al.* (2021) “Inhibition of free nitrous acid and free ammonia on polyphosphate accumulating organisms: Evidence of insufficient phosphorus removal through nitrification-denitrification,” *Journal of Environmental Management*, 297, p. 113390. Available at: <https://doi.org/10.1016/j.jenvman.2021.113390>.
- Andreadakis, D. *et al.* (2022) “The Inhibitory Effect of Free Nitrous Acid and Free Ammonia on the Anoxic Phosphorus Uptake Rate of Polyphosphate-Accumulating Organisms,” *Energies*, 15(6), p. 2108. Available at: <https://doi.org/10.3390/en15062108>.
- Anh, H.T.H. *et al.* (2021) “Bioaugmentation of seafood processing wastewater enhances the removal of inorganic nitrogen and chemical oxygen demand,” *Aquaculture*, 542, p. 736818. Available at: <https://doi.org/10.1016/j.aquaculture.2021.736818>.
- Aragón-Briceño, C.I. *et al.* (2020) “Hydrothermal carbonization of sewage digestate at wastewater treatment works: Influence of solid loading on characteristics of hydrochar, process water and plant energetics,” *Renewable Energy*, 157, pp. 959–973. Available at: <https://doi.org/10.1016/j.renene.2020.05.021>.
- Araújo, J.M. *et al.* (2022) “Influence of temperature on aerobic granular sludge formation and stability treating municipal wastewater with high nitrogen loadings,” *Environmental Research*, 212, p. 113578. Available at: <https://doi.org/10.1016/j.envres.2022.113578>.
- Ardern M.SC, E. and Lockett, W. T (1914) “Experiments on the oxidation of sewage without the aid of filters,” *Journal of the Society of Chemical Industry*, 33 523–539(10), pp. 523–539. Available at: <https://doi.org/10.1002/jctb.5000331005>.
- Arumugam, K. *et al.* (2021) “Recovery of complete genomes and non-chromosomal replicons from activated sludge enrichment microbial communities with long read metagenome

- sequencing,” *Npj Biofilms and Microbiomes*, 7(1). Available at: <https://doi.org/10.1038/s41522-021-00196-6>.
- Asensi, E. and Alemany, E. (2022) “A hindered settling velocity model related to the fractal dimension and activated sludge flocs characteristics: Application to a sludge with a previous fragmentation and flocculation process,” *Separation and Purification Technology*, 300, p. 121812. Available at: <https://doi.org/10.1016/j.seppur.2022.121812>.
- Aswin Kumar, I. and Viswanathan, N. (2020) “Fabrication of zirconium(IV) cross-linked alginate/kaolin hybrid beads for nitrate and phosphate retention,” *Arabian Journal of Chemistry*, 13(2), pp. 4111–4125. Available at: <https://doi.org/10.1016/j.arabjc.2019.06.006>.
- Atif, K. *et al.* (2018) “Pathogens Evolution During the Composting of the Household Waste Mixture Enriched with Phosphate Residues and Olive Oil Mill Wastewater,” *Waste and Biomass Valorization*, 11(5), pp. 1789–1797. Available at: <https://doi.org/10.1007/s12649-018-0495-3>.
- Awad, H.E.A. *et al.* (2022) “A divided flow aerobic-anoxic baffled reactor for simultaneous nitrification-denitrification of domestic wastewater,” *Science of the Total Environment*, 833, p. 155247. Available at: <https://doi.org/10.1016/j.scitotenv.2022.155247>.
- Aziz, A. *et al.* (2022) “Biogas production and nutrients removal from slaughterhouse wastewater using integrated anaerobic and aerobic granular intermittent SBRs – Bioreactors stability and microbial dynamics,” *Science of the Total Environment*, 848, p. 157575. Available at: <https://doi.org/10.1016/j.scitotenv.2022.157575>.
- Bankston, E.M., Wang, P. and Higgins, B.T. (2020) “Algae support populations of heterotrophic, nitrifying, and phosphate-accumulating bacteria in the treatment of poultry litter anaerobic digestate,” *Chemical Engineering Journal*, 398, p. 125550. Available at: <https://doi.org/10.1016/j.cej.2020.125550>.
- Barros, A.R.M. *et al.* (2021) “Effect of calcium addition to aerobic granular sludge systems under high (conventional SBR) and low (simultaneous fill/draw SBR) selection pressure,” *Environmental Research*, 194, p. 110639. Available at: <https://doi.org/10.1016/j.envres.2020.110639>.
- Bashandy, S.R., Abd-Alla, M.H. and Dawood, M.F.A. (2020) “Alleviation of the toxicity of oily wastewater to canola plants by the N₂-fixing, aromatic hydrocarbon biodegrading bacterium *Stenotrophomonas maltophilia*-SR1,” *Applied Soil Ecology*, 154, p. 103654. Available at: <https://doi.org/10.1016/j.apsoil.2020.103654>.

- Bassin, J.P. *et al.* (2019) “Development of aerobic granular sludge under tropical climate conditions: The key role of inoculum adaptation under reduced sludge washout for stable granulation,” *Journal of Environmental Management*, 230, pp. 168–182. Available at: <https://doi.org/10.1016/j.jenvman.2018.09.072>.
- Bawiec, A. (2018) “Efficiency of nitrogen and phosphorus compounds removal in hydroponic wastewater treatment plant,” *Environmental Technology*, 40(16), pp. 2062–2072. Available at: <https://doi.org/10.1080/09593330.2018.1436595>.
- Bensaida, K. *et al.* (2021) “The impact of iron bimetallic nanoparticles on bulk microbial growth in wastewater,” *Journal of Water Process Engineering*, 40, p. 101825. Available at: <https://doi.org/10.1016/j.jwpe.2020.101825>.
- Bertanza, G. *et al.* (2020) “Promoting biological phosphorus removal in a full scale pre-denitrification wastewater treatment plant,” *Journal of Environmental Management*, 254, p. 109803. Available at: <https://doi.org/10.1016/j.jenvman.2019.109803>.
- Bessa, V.S. *et al.* (2021) “Biological removal processes in aerobic granular sludge exposed to diclofenac,” *Environmental Technology*, 43(21), pp. 3295–3308. Available at: <https://doi.org/10.1080/09593330.2021.1921048>.
- Beun, J.J., Van Loosdrecht, M.C.M. and Heijnen, J.J. (2002) “Aerobic granulation in a sequencing batch airlift reactor,” *Water Research*, 36(3), pp. 702–712. Available at: [https://doi.org/10.1016/s0043-1354\(01\)00250-0](https://doi.org/10.1016/s0043-1354(01)00250-0).
- Bhathena, J. *et al.* (2006) “Effects of Nitrogen and Phosphorus Limitation on the Activated Sludge Biomass in a Kraft Mill Biotreatment System,” *Water Environment Research*, 78(12), pp. 2303–2310. Available at: <https://doi.org/10.2175/106143006x95401>.
- Bin, Z. *et al.* (2015) “Denitrifying capability and community dynamics of glycogen accumulating organisms during sludge granulation in an anaerobic-aerobic sequencing batch reactor,” *Scientific Reports*, 5(1). Available at: <https://doi.org/10.1038/srep12904>.
- Bisht, V. and Lal, B. (2019) “Exploration of Performance Kinetics and Mechanism of Action of a Potential Novel Bioflocculant BF-VB2 on Clay and Dye Wastewater Flocculation,” *Frontiers in Microbiology*, 10. Available at: <https://doi.org/10.3389/fmicb.2019.01288>.
- Boom Cárcamo, E.A. and Peñabaena-Niebles, R. (2022) “Opportunities and challenges for the waste management in emerging and frontier countries through industrial symbiosis,” *Journal of Cleaner Production*, 363, p. 132607. Available at: <https://doi.org/10.1016/j.jclepro.2022.132607>.
- Boonnorat, J. *et al.* (2021) “Treatment efficiency and greenhouse gas emissions of non-floating and floating bed activated sludge system with acclimatized sludge treating landfill leachate,”

- Bioresource Technology*, 330, p. 124952. Available at: <https://doi.org/10.1016/j.biortech.2021.124952>.
- Bouaouine, O. *et al.* (2019) “Identification and role of *Opuntia ficus indica* constituents in the flocculation mechanism of colloidal solutions,” *Separation and Purification Technology*, 209, pp. 892–899. Available at: <https://doi.org/10.1016/j.seppur.2018.09.036>.
- Bracher, G.H. *et al.* (2020) “Optimization of an electrocoagulation-flotation system for domestic wastewater treatment and reuse,” *Environmental Technology*, 42(17), pp. 2669–2679. Available at: <https://doi.org/10.1080/09593330.2019.1709905>.
- Bucci, P. *et al.* (2021) “Heterotrophic nitrification-aerobic denitrification performance in a granular sequencing batch reactor supported by next generation sequencing,” *International Biodeterioration & Biodegradation*, 160, p. 105210. Available at: <https://doi.org/10.1016/j.ibiod.2021.105210>.
- Buhari, J. *et al.* (2022) “Unveiling the optimal ammonia-oxidising bacterial consortium for polishing low ammonia-contaminated wastewater,” *Journal of Water Process Engineering*, 47, p. 102753. Available at: <https://doi.org/10.1016/j.jwpe.2022.102753>.
- Burdon, F.J. *et al.* (2019) “Agriculture versus wastewater pollution as drivers of macroinvertebrate community structure in streams,” *Science of the Total Environment*, 659, pp. 1256–1265. Available at: <https://doi.org/10.1016/j.scitotenv.2018.12.372>.
- Bustos-Terrones, Y.A. *et al.* (2022) “Enhanced biological wastewater treatment using sodium alginate-immobilized microorganisms in a fluidized bed reactor,” *Water Science and Engineering*, 15(2), pp. 125–133. Available at: <https://doi.org/10.1016/j.wse.2022.02.002>.
- Campana, P.E. *et al.* (2021) “100% renewable wastewater treatment plants: Techno-economic assessment using a modelling and optimization approach,” *Energy Conversion and Management*, 239, p. 114214. Available at: <https://doi.org/10.1016/j.enconman.2021.114214>.
- Cao, S. *et al.* (2019) “Novel two stage partial denitrification (PD)-Anammox process for tertiary nitrogen removal from low carbon/nitrogen (C/N) municipal sewage,” *Chemical Engineering Journal*, 362, pp. 107–115. Available at: <https://doi.org/10.1016/j.cej.2018.12.160>.
- Cardoso, L.G. *et al.* (2020) “Spirulina sp. LEB 18 cultivation in outdoor pilot scale using aquaculture wastewater: High biomass, carotenoid, lipid and carbohydrate production,” *Aquaculture*, 525, p. 735272. Available at: <https://doi.org/10.1016/j.aquaculture.2020.735272>.

- Cardoso, L.G. *et al.* (2021) “Spirulina sp. as a Bioremediation Agent for Aquaculture Wastewater: Production of High Added Value Compounds and Estimation of Theoretical Biodiesel,” *Bioenergy Research*, 14(1), pp. 254–264. Available at: <https://doi.org/10.1007/s12155-020-10153-4>.
- Carmo, T.S.D. *et al.* (2019) “Phosphorus Recovery from Phosphate Rocks Using Phosphate-Solubilizing Bacteria,” *Geomicrobiology Journal*, 36(3), pp. 195–203. Available at: <https://doi.org/10.1080/01490451.2018.1534901>.
- Castellanos, R.M. *et al.* (2021) “Effect of sludge age on aerobic granular sludge: Addressing nutrient removal performance and biomass stability,” *Chemical Engineering Research & Design*, 149, pp. 212–222. Available at: <https://doi.org/10.1016/j.psep.2020.10.042>.
- Cetin, E. *et al.* (2018) “Effects of high-concentration influent suspended solids on aerobic granulation in pilot-scale sequencing batch reactors treating real domestic wastewater,” *Water Research*, 131, pp. 74–89. Available at: <https://doi.org/10.1016/j.watres.2017.12.014>.
- Chaturvedi, A. *et al.* (2021) “A Computational Approach to Incorporate Metabolite Inhibition in the Growth Kinetics of Indigenous Bacterial Strain *Bacillus subtilis* MN372379 in the Treatment of Wastewater Containing Congo Red Dye,” *Applied Biochemistry and Biotechnology*, 193(7), pp. 2128–2144. Available at: <https://doi.org/10.1007/s12010-021-03538-4>.
- Chauhan, R. and Srivastava, V.C. (2020) “Electrochemical denitrification of highly contaminated actual nitrate wastewater by Ti/RuO₂ anode and iron cathode,” *Chemical Engineering Journal*, 386, p. 122065. Available at: <https://doi.org/10.1016/j.cej.2019.122065>.
- Chen, F. *et al.* (2023) “Evaluation of nitrogen removal and nitrous oxide turnovers in granule-based simultaneous nitrification and denitrification system,” *Science of the Total Environment*, 873, p. 162446. Available at: <https://doi.org/10.1016/j.scitotenv.2023.162446>.
- Chen, H. *et al.* (2019) “Hydrothermal conversion of sewage sludge: Focusing on the characterization of liquid products and their methane yields,” *Chemical Engineering Journal*, 357, pp. 367–375. Available at: <https://doi.org/10.1016/j.cej.2018.09.180>.
- Chen, W.-H. *et al.* (2022) “Facultative-like anaerobic packed bed reactor treating low strength wastewater: microbial community and energy balance appraisements,” *Chemical Engineering Research & Design*, 157, pp. 420–428. Available at: <https://doi.org/10.1016/j.psep.2021.11.017>.

- Chen, Y. *et al.* (2021) “A novel strategy for improving volatile fatty acid purity, phosphorus removal efficiency, and fermented sludge dewaterability during waste activated sludge fermentation,” *Waste Management*, 119, pp. 195–201. Available at: <https://doi.org/10.1016/j.wasman.2020.09.044>.
- Cheong, C., Miura, T. and Nonose, N. (2021) “Determination of phosphate in seawater by ion chromatography inductively coupled plasma sector field mass spectrometry,” *Limnology and Oceanography-methods*, 19(10), pp. 682–691. Available at: <https://doi.org/10.1002/lom3.10453>.
- Choudhury, P. *et al.* (2021) “Process engineering for stable power recovery from dairy wastewater using microbial fuel cell,” *International Journal of Hydrogen Energy*, 46(4), pp. 3171–3182. Available at: <https://doi.org/10.1016/j.ijhydene.2020.06.152>.
- Contreras, J.D. *et al.* (2020) “Modeling Spatial Risk of Diarrheal Disease Associated with Household Proximity to Untreated Wastewater Used for Irrigation in the Mezquital Valley, Mexico,” *Environmental Health Perspectives*, 128(7), p. 077002. Available at: <https://doi.org/10.1289/ehp6443>.
- Corsino, S.F. *et al.* (2019) “Comparison between kinetics of autochthonous marine bacteria in activated sludge and granular sludge systems at different salinity and SRTs,” *Water Research*, 148, pp. 425–437. Available at: <https://doi.org/10.1016/j.watres.2018.10.086>.
- Crusberg, T.C. (2022) “Effects of Irrigation with Municipal Wastewater on the Microbiome of the Rhizosphere of Agricultural Lands,” *Re-visiting the Rhizosphere Eco-system for Agricultural Sustainability*, pp. 427–444. Available at: https://doi.org/10.1007/978-981-19-4101-6_21.
- Da Costa, A.B. *et al.* (2019) “Point-of-use determination of fluoride and phosphorus in water through a smartphone using the PhotoMetrix® app,” *BrJAC Brazilian Journal of Analytical Chemistry*, 6(25). Available at: <https://doi.org/10.30744/brjac.2179-3425.tn-25-2019>.
- Da Costa, N.P.A.V., Libardi, N. and Da Costa, R.H.R. (2022) “How can the addition of extracellular polymeric substances (EPS)-based biofloculant affect aerobic granular sludge (AGS)?,” *Journal of Environmental Management*, 310, p. 114807. Available at: <https://doi.org/10.1016/j.jenvman.2022.114807>.
- Dan, Q. *et al.* (2021) “Side-stream phosphorus famine selectively strengthens glycogen accumulating organisms (GAOs) for advanced nutrient removal in an anaerobic-aerobic-anoxic system,” *Chemical Engineering Journal*, 420, p. 129554. Available at: <https://doi.org/10.1016/j.cej.2021.129554>.

- Daneshvar, E. *et al.* (2018) “Versatile applications of freshwater and marine water microalgae in dairy wastewater treatment, lipid extraction and tetracycline biosorption,” *Bioresource Technology*, 268, pp. 523–530. Available at: <https://doi.org/10.1016/j.biortech.2018.08.032>.
- Dang, B.-T. *et al.* (2022) “Comparison of degradation kinetics of tannery wastewater treatment using a nonlinear model by salt-tolerant *Nitrosomonas* sp. and *Nitrobacter* sp.,” *Bioresource Technology*, 351, p. 127000. Available at: <https://doi.org/10.1016/j.biortech.2022.127000>.
- De Freitas Bueno, R. *et al.* (2020) “Simultaneous removal of organic matter and nitrogen compounds from landfill leachate by aerobic granular sludge,” *Environmental Technology*, 42(24), pp. 3756–3770. Available at: <https://doi.org/10.1080/09593330.2020.1740798>.
- De Graaff, D.R., Van Loosdrecht, M.C.M. and Pronk, M. (2020) “Biological phosphorus removal in seawater-adapted aerobic granular sludge,” *Water Research*, 172, p. 115531. Available at: <https://doi.org/10.1016/j.watres.2020.115531>.
- De Gusseme, B. *et al.* (2011) “Degradation of acetaminophen by *Delftia tsuruhatensis* and *Pseudomonas aeruginosa* in a membrane bioreactor,” *Water Research*, 45(4), pp. 1829–1837. Available at: <https://doi.org/10.1016/j.watres.2010.11.040>.
- De Prá, M.C. *et al.* (2021) “Novel one-stage reactor configuration for deammonification process: Hydrodynamic evaluation and fast start-up of NITRAMMOX® reactor,” *Biochemical Engineering Journal*, 171, p. 108005. Available at: <https://doi.org/10.1016/j.bej.2021.108005>.
- De Sousa Rollemberg, S.L. *et al.* (2019) “Influence of sequencing batch reactor configuration on aerobic granules growth: Engineering and microbiological aspects,” *Journal of Cleaner Production*, 238, p. 117906. Available at: <https://doi.org/10.1016/j.jclepro.2019.117906>.
- Dehghani, S. *et al.* (2021) “Exploring mechano-bactericidal nature of *Psalmocharias cicadas* wings: an analytical nanotopology investigation based on atomic force microscopy characterization,” *Surfaces and Interfaces*, 26, p. 101407. Available at: <https://doi.org/10.1016/j.surfin.2021.101407>.
- Del Angel-Acosta, Y.A. *et al.* (2021) “Co-digestion of corn (nejayote) and brewery wastewater at different ratios and pH conditions for biohydrogen production,” *International Journal of Hydrogen Energy*, 46(54), pp. 27422–27430. Available at: <https://doi.org/10.1016/j.ijhydene.2021.05.208>.
- Despot, D., Pacheco Fernández, M. and Barjenbruch, M. (2021) “Comparison of Online Sensors for Liquid Phase Hydrogen Sulphide Monitoring in Sewer Systems,” *Water*, 13(13), p. 1876. Available at: <https://doi.org/10.3390/w13131876>.

- Díaz, V.M. *et al.* (2022) “Microalgae bioreactor for nutrient removal and resource recovery from wastewater in the paradigm of circular economy,” *Bioresource Technology*, 363, p. 127968. Available at: <https://doi.org/10.1016/j.biortech.2022.127968>.
- Dockx, L. *et al.* (2021) “Impact of the substrate composition on enhanced biological phosphorus removal during formation of aerobic granular sludge,” *Bioresource Technology*, 337, p. 125482. Available at: <https://doi.org/10.1016/j.biortech.2021.125482>.
- Dong, G. *et al.* (2022) “Comparison of O₃, UV/O₃, and UV/O₃/PS processes for marine oily wastewater treatment: Degradation performance, toxicity evaluation, and flocs analysis,” *Water Research*, 226, p. 119234. Available at: <https://doi.org/10.1016/j.watres.2022.119234>.
- Dorji, U. *et al.* (2022) “On-site domestic wastewater treatment system using shredded waste plastic bottles as biofilter media: Pilot-scale study on effluent standards in Bhutan,” *Chemosphere*, 286, p. 131729. Available at: <https://doi.org/10.1016/j.chemosphere.2021.131729>.
- Dottorini, G. *et al.* (2021) “Mass-immigration determines the assembly of activated sludge microbial communities,” *Proceedings of the National Academy of Sciences of the United States of America*, 118(27). Available at: <https://doi.org/10.1073/pnas.2021589118>.
- Drozdova, J. *et al.* (2018) “Heavy metals in domestic wastewater with respect to urban population in Ostrava, Czech Republic,” *Water and Environment Journal*, 33(1), pp. 77–85. Available at: <https://doi.org/10.1111/wej.12371>.
- Du, B. *et al.* (2019) “Impacts of long-term exposure to tetracycline and sulfamethoxazole on the sludge granules in an anoxic-aerobic wastewater treatment system,” *Science of the Total Environment*, 684, pp. 67–77. Available at: <https://doi.org/10.1016/j.scitotenv.2019.05.313>.
- Duque, A.F. *et al.* (2011) “2-Fluorophenol degradation by aerobic granular sludge in a sequencing batch reactor,” *Water Research*, 45(20), pp. 6745–6752. Available at: <https://doi.org/10.1016/j.watres.2011.10.033>.
- Duque, A.F. *et al.* (2021) “Simultaneous nitrification and phosphate removal by bioaugmented aerobic granules treating a fluoroorganic compound,” *Water Science and Technology*, 83(10), pp. 2404–2413. Available at: <https://doi.org/10.2166/wst.2021.142>.
- Eladel, H. *et al.* (2019) “Evaluation of *Chlorella sorokiniana* isolated from local municipal wastewater for dual application in nutrient removal and biodiesel production,” *Bioprocess and Biosystems Engineering*, 42(3), pp. 425–433. Available at: <https://doi.org/10.1007/s00449-018-2046-5>.

- Ely, C. *et al.* (2022) “Treatment of saline wastewater amended with endocrine disruptors by aerobic granular sludge: Assessing performance and microbial community dynamics,” *Journal of Environmental Chemical Engineering*, 10(2), p. 107272. Available at: <https://doi.org/10.1016/j.jece.2022.107272>.
- Ezeonuegbu, B. *et al.* (2022) “Characterization and phylogeny of fungi isolated from industrial wastewater using multiple genes,” *Scientific Reports*, 12(1). Available at: <https://doi.org/10.1038/s41598-022-05820-9>.
- Falahati-Marvast, H. and Karimi-Jashni, A. (2020) “A new modified anoxic-anaerobic-membrane bioreactor for treatment of real wastewater with a low carbon/nutrient ratio and high nitrate,” *Journal of Water Process Engineering*, 33, p. 101054. Available at: <https://doi.org/10.1016/j.jwpe.2019.101054>.
- Fan, Y. *et al.* (2021) “Molecular characterization of the waterborne pathogens *Cryptosporidium* spp., *Giardia duodenalis*, *Enterocytozoon bienersi*, *Cyclospora cayentanensis* and *Eimeria* spp. in wastewater and sewage in Guangzhou, China,” *Parasites & Vectors*, 14(1). Available at: <https://doi.org/10.1186/s13071-020-04566-5>.
- Fan, Z. *et al.* (2022) “A novel partial denitrification, anammox-biological phosphorus removal, fermentation and partial nitrification (PDA-PFPN) process for real domestic wastewater and waste activated sludge treatment,” *Water Research*, 217, p. 118376. Available at: <https://doi.org/10.1016/j.watres.2022.118376>.
- Farahani, S.S., Asoodar, M.A. and Moghadam, B.K. (2019) “Short-term impacts of biochar, tillage practices, and irrigation systems on nitrate and phosphorus concentrations in subsurface drainage water,” *Environmental Science and Pollution Research*, 27(1), pp. 761–771. Available at: <https://doi.org/10.1007/s11356-019-06942-w>.
- Farahbakhsh, M.T. and Chahartaghi, M. (2020) “Performance analysis and economic assessment of a combined cooling heating and power (CCHP) system in wastewater treatment plants (WWTPs),” *Energy Conversion and Management*, 224, p. 113351. Available at: <https://doi.org/10.1016/j.enconman.2020.113351>.
- Feigin, A., Ravina, I. and Shalhevet, J. (1991) *Irrigation with Treated Sewage Effluent: Management for Environmental Protection (Advanced Series in Agricultural Sciences)*. 1st edn. Springer.
- Fernando, E.Y. *et al.* (2019) “Resolving the individual contribution of key microbial populations to enhanced biological phosphorus removal with Raman–FISH,” *The ISME Journal*, 13(8), pp. 1933–1946. Available at: <https://doi.org/10.1038/s41396-019-0399-7>.

- Figdore, B.A., Stensel, H.D. and Winkler, M.K.H. (2018) “Comparison of different aerobic granular sludge types for activated sludge nitrification bioaugmentation potential,” *Bioresource Technology*, 251, pp. 189–196. Available at: <https://doi.org/10.1016/j.biortech.2017.11.004>.
- Folino, A., Lucas-Borja, M.E. and Calabrò, P. (2020) “Organic matter removal and ammonia recovery by optimised treatments of swine wastewater,” *Journal of Environmental Management*, 270, p. 110692. Available at: <https://doi.org/10.1016/j.jenvman.2020.110692>.
- Forouzanmehr, F. *et al.* (2022) “Sulfur transformations during two-stage anaerobic digestion and intermediate thermal hydrolysis,” *Science of the Total Environment*, 810, p. 151247. Available at: <https://doi.org/10.1016/j.scitotenv.2021.151247>.
- Fouda-Mbanga, B.G., Prabakaran, E. and Pillay, K. (2021) “Carbohydrate biopolymers, lignin based adsorbents for removal of heavy metals (Cd²⁺, Pb²⁺, Zn²⁺) from wastewater, regeneration and reuse for spent adsorbents including latent fingerprint detection: A review,” *Biotechnology Reports*, 30, p. e00609. Available at: <https://doi.org/10.1016/j.btre.2021.e00609>.
- Gao, S., He, Q. and Wang, H. (2020) “Research on the aerobic granular sludge under alkalinity in sequencing batch reactors: Removal efficiency, metagenomic and key microbes,” *Bioresource Technology*, 296, p. 122280. Available at: <https://doi.org/10.1016/j.biortech.2019.122280>.
- Gao, X. *et al.* (2022) “Balance nitrogen and phosphorus efficient removal under carbon limitation in pilot-scale demonstration of a novel anaerobic/aerobic/anoxic process,” *Water Research*, 223, p. 118991. Available at: <https://doi.org/10.1016/j.watres.2022.118991>.
- Gao, Y. and Erdner, D.L. (2022) “Dynamics of cell death across growth stages and the diel cycle in the dinoflagellate *Karenia brevis*,” *Journal of Eukaryotic Microbiology*, 69(1). Available at: <https://doi.org/10.1111/jeu.12874>.
- García-Depraect, O. *et al.* (2019) “Enhanced biohydrogen production from the dark co-fermentation of tequila vinasse and nixtamalization wastewater: Novel insights into ecological regulation by pH,” *Fuel*, 253, pp. 159–166. Available at: <https://doi.org/10.1016/j.fuel.2019.04.147>.
- Garg, A. *et al.* (2021) “Effect of waste activated sludge pretreatment methods to mitigate Gordonia foaming potential in anaerobic digestion,” *Water and Environment Journal*, 35(1), pp. 381–389. Available at: <https://doi.org/10.1111/wej.12636>.
- Giraldo Mejía, H.F. *et al.* (2022) “Direct recycling of discarded reverse osmosis membranes for domestic wastewater treatment with a focus on water reuse,” *Chemical Engineering*

- Research and Design*, 184, pp. 473–487. Available at: <https://doi.org/10.1016/j.cherd.2022.06.031>.
- Golzar, F., Nilsson, D. and Martin, V. (2020) “Forecasting Wastewater Temperature Based on Artificial Neural Network (ANN) Technique and Monte Carlo Sensitivity Analysis,” *Sustainability*, 12(16), p. 6386. Available at: <https://doi.org/10.3390/su12166386>.
- González-Balderas, R.M. *et al.* (2020) “Intensified recovery of lipids, proteins, and carbohydrates from wastewater-grown microalgae *Desmodesmus* sp. by using ultrasound or ozone,” *Ultrasonics Sonochemistry*, 62, p. 104852. Available at: <https://doi.org/10.1016/j.ulsonch.2019.104852>.
- Guo, T. *et al.* (2020) “Coupling of Fe-C and aerobic granular sludge to treat refractory wastewater from a membrane manufacturer in a pilot-scale system,” *Water Research*, 186, p. 116331. Available at: <https://doi.org/10.1016/j.watres.2020.116331>.
- Gurung, K., Ncibi, M.C. and Sillanpää, M. (2019) “Removal and fate of emerging organic micropollutants (EOMs) in municipal wastewater by a pilot-scale membrane bioreactor (MBR) treatment under varying solid retention times,” *Science of the Total Environment*, 667, pp. 671–680. Available at: <https://doi.org/10.1016/j.scitotenv.2019.02.308>.
- Gutberlet, J., Bramryd, T. and Johansson, M. (2020) “Expansion of the Waste-Based Commodity Frontier: Insights from Sweden and Brazil,” *Sustainability*, 12(7), p. 2628. Available at: <https://doi.org/10.3390/su12072628>.
- Gutierrez, F., Kinney, K.A. and Katz, L.E. (2020) “Phosphorus Speciation in Municipal Wastewater Solids and Implications for Phosphorus Recovery,” *Environmental Engineering Science*, 37(5), pp. 316–327. Available at: <https://doi.org/10.1089/ees.2019.0360>.
- Hamill, P. *et al.* (2020) “Microbial lag phase can be indicative of, or independent from, cellular stress,” *Scientific Reports*, 10(1). Available at: <https://doi.org/10.1038/s41598-020-62552-4>.
- Hamoda, M.F. and Alshalhi, S.F. (2021) “Assessment of hydrogen sulfide emission in a wastewater pumping station,” *Environmental Monitoring and Assessment*, 193(6). Available at: <https://doi.org/10.1007/s10661-021-09116-9>.
- Haq, I. and Kalamdhad, A.S. (2021) “Phytotoxicity and cyto-genotoxicity evaluation of organic and inorganic pollutants containing petroleum refinery wastewater using plant bioassay,” *Environmental Technology & Innovation*, 23, p. 101651. Available at: <https://doi.org/10.1016/j.eti.2021.101651>.
- Hayder, G. *et al.* (2022) “Removal of nutrients from pulp and paper biorefinery effluent: Operation, kinetic modelling and optimization by response surface methodology,”

- Environmental Research*, 214, p. 114091. Available at: <https://doi.org/10.1016/j.envres.2022.114091>.
- Heidary, N. *et al.* (2020) “Disparity of Cytochrome Utilization in Anodic and Cathodic Extracellular Electron Transfer Pathways of *Geobacter sulfurreducens* Biofilms,” *Journal of the American Chemical Society*, 142(11), pp. 5194–5203. Available at: <https://doi.org/10.1021/jacs.9b13077>.
- Hembach, N. *et al.* (2019) “Dissemination prevention of antibiotic resistant and facultative pathogenic bacteria by ultrafiltration and ozone treatment at an urban wastewater treatment plant,” *Scientific Reports*, 9(1). Available at: <https://doi.org/10.1038/s41598-019-49263-1>.
- Hermosillo-Ochoa, E., Picos-Corrales, L.A. and Licea-Claverie, A. (2021) “Eco-friendly flocculants from chitosan grafted with PNVCL and PAAc: Hybrid materials with enhanced removal properties for water remediation,” *Separation and Purification Technology*, 258, p. 118052. Available at: <https://doi.org/10.1016/j.seppur.2020.118052>.
- Hiruy, A.M. *et al.* (2022) “Spatiotemporal variation in urban wastewater pollution impacts on river microbiomes and associated hazards in the Akaki catchment, Addis Ababa, Ethiopia,” *Science of the Total Environment*, 826, p. 153912. Available at: <https://doi.org/10.1016/j.scitotenv.2022.153912>.
- Honda, R. *et al.* (2020) “Estimated discharge of antibiotic-resistant bacteria from combined sewer overflows of urban sewage system,” *Npj Clean Water*, 3(1). Available at: <https://doi.org/10.1038/s41545-020-0059-5>.
- Hoque, S.A. *et al.* (2023) “Genotype Diversity of Enteric Viruses in Wastewater Amid the COVID-19 Pandemic,” *Food and Environmental Virology* [Preprint]. Available at: <https://doi.org/10.1007/s12560-023-09553-4>.
- HOXHA, V. *et al.* (2022) “Determination of Different Forms of Phosphorus in Waters of the Wastewater Treatment Plant in Durrës, Before and After Treatment,” *Proceedings of the 8th World Congress on Mechanical, Chemical, and Material Engineering* [Preprint]. Available at: <https://doi.org/10.11159/iccpe22.116>.
- Hu, Y. *et al.* (2020) “The mechanism of nitrate-Cr(VI) reduction mediated by microbial under different initial pHs,” *Journal of Hazardous Materials*, 393, p. 122434. Available at: <https://doi.org/10.1016/j.jhazmat.2020.122434>.
- Huang, G.-Y. *et al.* (2019) “Endocrine disrupting effects in western mosquitofish *Gambusia affinis* in two rivers impacted by untreated rural domestic wastewaters,” *Science of the Total Environment*, 683, pp. 61–70. Available at: <https://doi.org/10.1016/j.scitotenv.2019.05.231>.

- Huang, H. *et al.* (2020) “Sulfidogenic anaerobic digestion of sulfate-laden waste activated sludge: Evaluation on reactor performance and dynamics of microbial community,” *Bioresource Technology*, 297, p. 122396. Available at: <https://doi.org/10.1016/j.biortech.2019.122396>.
- Huang, J. *et al.* (2019) “The development and evaluation of a microstill with conductance detection for low level ammonia monitoring in chloraminated water,” *Talanta*, 200, pp. 256–262. Available at: <https://doi.org/10.1016/j.talanta.2019.03.043>.
- Huang, J. *et al.* (2021) “Occurrence of heterotrophic nitrification-aerobic denitrification induced by decreasing salinity in a halophilic AGS SBR treating hypersaline wastewater,” *Chemical Engineering Journal*, 431, p. 134133. Available at: <https://doi.org/10.1016/j.cej.2021.134133>.
- Iannacone, F. *et al.* (2019) “Effect of carbon-to-nitrogen ratio on simultaneous nitrification denitrification and phosphorus removal in a microaerobic moving bed biofilm reactor,” *Journal of Environmental Management*, 250, p. 109518. Available at: <https://doi.org/10.1016/j.jenvman.2019.109518>.
- Insel, G. *et al.* (2023) “Model-based evaluation of simultaneous nitrification and denitrification in aerobic granular sludge systems,” *Environmental Science and Pollution Research* [Preprint]. Available at: <https://doi.org/10.1007/s11356-023-25252-w>.
- Izydorczyk, G. *et al.* (2021) “Agricultural and non-agricultural directions of bio-based sewage sludge valorization by chemical conditioning,” *Environmental Science and Pollution Research*, 28(35), pp. 47725–47740. Available at: <https://doi.org/10.1007/s11356-021-15293-4>.
- Jasim, N.A. (2020) “The design for wastewater treatment plant (WWTP) with GPS X modelling,” *Cogent Engineering*, 7(1), p. 1723782. Available at: <https://doi.org/10.1080/23311916.2020.1723782>.
- Jia, F. *et al.* (2021) “Metagenomic prediction analysis of microbial aggregation in anammox-dominated community,” *Water Environment Research*, 93(11), pp. 2549–2558. Available at: <https://doi.org/10.1002/wer.1529>.
- Jiang, J. *et al.* (2021) “Comparative Study on Advanced Nitrogen Removal of Landfill Leachate Treated by SBR and SBBR,” *Water*, 13(22), p. 3240. Available at: <https://doi.org/10.3390/w13223240>.
- Jiraprasertwong, A., Maitriwong, K. and Chavadej, S. (2019) “Production of biogas from cassava wastewater using a three-stage upflow anaerobic sludge blanket (UASB) reactor,”

- Renewable Energy*, 130, pp. 191–205. Available at: <https://doi.org/10.1016/j.renene.2018.06.034>.
- Jiwarungrueangkul, T. *et al.* (2023) “Modification and validation of an analytical method for the simple determination of nitrate in seawater by reduction to nitrite with zinc powder,” *Marine Chemistry*, 251, p. 104235. Available at: <https://doi.org/10.1016/j.marchem.2023.104235>.
- Johansen, J.L. *et al.* (2022) “Effects of long-term fertilization with contemporary Danish human urine, composted household waste and sewage sludge on soil nematode abundance and community structure,” *Science of the Total Environment*, 860, p. 160485. Available at: <https://doi.org/10.1016/j.scitotenv.2022.160485>.
- John, E.M., Krishnapriya, K. and Sankar, T.V. (2020) “Treatment of ammonia and nitrite in aquaculture wastewater by an assembled bacterial consortium,” *Aquaculture*, 526, p. 735390. Available at: <https://doi.org/10.1016/j.aquaculture.2020.735390>.
- Júnior, O.S. *et al.* (2021) “Decontamination and toxicity removal of an industrial effluent containing pesticides via multistage treatment: Coagulation-flocculation-settling and photo-Fenton process,” *Chemical Engineering Research & Design*, 147, pp. 674–683. Available at: <https://doi.org/10.1016/j.psep.2020.12.021>.
- Kalpy J., C. *et al.* (2020) “Resistance Profile of *Vibrio* spp. Strains Collected from Lagoon Bays and Wastewater in the City of Abidjan, Côte d’Ivoire, from January to June 2017,” *The Open Microbiology Journal*, 14(1), pp. 297–303. Available at: <https://doi.org/10.2174/1874434602014010297>.
- Karuppiah, T. *et al.* (2022) “Processing of electroplating industry wastewater through dual chambered microbial fuel cells (MFC) for simultaneous treatment of wastewater and green fuel production,” *International Journal of Hydrogen Energy*, 47(88), pp. 37569–37576. Available at: <https://doi.org/10.1016/j.ijhydene.2021.06.034>.
- Kasper, D., Amaral, J.H.F. and Forsberg, B.R. (2018) “The effect of filter type and porosity on total suspended sediment determinations,” *Analytical Methods*, 10(46), pp. 5532–5539. Available at: <https://doi.org/10.1039/c8ay02134a>.
- Kazadi Mbamba, C. *et al.* (2019) “Plant-wide model-based analysis of iron dosage strategies for chemical phosphorus removal in wastewater treatment systems,” *Water Research*, 155, pp. 12–25. Available at: <https://doi.org/10.1016/j.watres.2019.01.048>.
- Kékedy-Nagy, L. *et al.* (2022) “Electrochemical nutrient removal from natural wastewater sources and its impact on water quality,” *Water Research*, 210, p. 118001. Available at: <https://doi.org/10.1016/j.watres.2021.118001>.

- Khraisheh, M., Al-Ghouti, M.A. and Almomani, F. (2020) “P. putida as biosorbent for the remediation of cobalt and phenol from industrial waste wastewaters,” *Environmental Technology and Innovation*, 20, p. 101148. Available at: <https://doi.org/10.1016/j.eti.2020.101148>.
- Khumalo, S.M. *et al.* (2022) “Sequencing Batch Reactor Performance Evaluation on Orthophosphates and COD Removal from Brewery Wastewater,” *Fermentation*, 8(7), p. 296. Available at: <https://doi.org/10.3390/fermentation8070296>.
- Kim, J.H. *et al.* (2008) “Analysis of ammonia loss mechanisms in microbial fuel cells treating animal wastewater,” *Biotechnology and Bioengineering*, 99(5), pp. 1120–1127. Available at: <https://doi.org/10.1002/bit.21687>.
- Kong, Y. *et al.* (2022) “Analysis of aerobic granulation trigger driving mechanism under different organic substrate diffusibility based on microfluidic system,” *Journal of Water Process Engineering*, 49, p. 103166. Available at: <https://doi.org/10.1016/j.jwpe.2022.103166>.
- Konieczka, P. and Namieśnik, J. (2018) *Quality assurance and quality control in the Analytical Chemical Laboratory*, CRC Press eBooks. Available at: <https://doi.org/10.1201/9781315295015>.
- Korajkic, A. *et al.* (2022) “Effectiveness of two wastewater disinfection strategies for the removal of fecal indicator bacteria, bacteriophage, and enteric viral pathogens concentrated using dead-end hollow fiber ultrafiltration (D-HFUF),” *Science of the Total Environment*, 831, p. 154861. Available at: <https://doi.org/10.1016/j.scitotenv.2022.154861>.
- Kosar, S. *et al.* (2022) “Impact of primary sedimentation on granulation and treatment performance of municipal wastewater by aerobic granular sludge process,” *Journal of Environmental Management*, 315, p. 115191. Available at: <https://doi.org/10.1016/j.jenvman.2022.115191>.
- Krogh, J. *et al.* (2018) “Risks of hypoxia and acidification in the high energy coastal environment near Victoria, Canada’s untreated municipal sewage outfalls,” *Marine Pollution Bulletin*, 133, pp. 517–531. Available at: <https://doi.org/10.1016/j.marpolbul.2018.05.018>.
- Kumar Maurya, P. *et al.* (2019) “Haematological and histological changes in fish *Heteropneustes fossilis* exposed to pesticides from industrial waste water,” *Human and Ecological Risk Assessment: An International Journal*, 25(5), pp. 1251–1278. Available at: <https://doi.org/10.1080/10807039.2018.1482736>.

- Kurup, G.G., Adhikari, B. and Zisu, B. (2019) “Treatment performance and recovery of organic components from high pH dairy wastewater using low-cost inorganic ferric chloride precipitant,” *Journal of Water Process Engineering*, 32, p. 100908. Available at: <https://doi.org/10.1016/j.jwpe.2019.100908>.
- Kusmayadi, A. *et al.* (2022) “Integrating anaerobic digestion and microalgae cultivation for dairy wastewater treatment and potential biochemicals production from the harvested microalgal biomass,” *Chemosphere*, 291, p. 133057. Available at: <https://doi.org/10.1016/j.chemosphere.2021.133057>.
- Lagum, A.A. (2022) “Simultaneous nitrification and denitrification by controlling current density and dissolved oxygen supply in a novel electrically-induced membrane bioreactor,” *Journal of Environmental Management*, 322, p. 116131. Available at: <https://doi.org/10.1016/j.jenvman.2022.116131>.
- Lakshminarasimman, N. *et al.* (2018) “Biotransformation and sorption of trace organic compounds in biological nutrient removal treatment systems,” *Science of the Total Environment*, 640–641, pp. 62–72. Available at: <https://doi.org/10.1016/j.scitotenv.2018.05.145>.
- Lambert, N. *et al.* (2021) “Performance assessment of ultrasonic sludge disintegration in activated sludge wastewater treatment plants under nutrient-deficient conditions,” *Chemical Engineering Journal*, 431, p. 133979. Available at: <https://doi.org/10.1016/j.cej.2021.133979>.
- Lavrinovičs, A. *et al.* (2022) “Optimizing phosphorus removal for municipal wastewater post-treatment with *Chlorella vulgaris*,” *Journal of Environmental Management*, 324, p. 116313. Available at: <https://doi.org/10.1016/j.jenvman.2022.116313>.
- Layer, M. *et al.* (2019) “Organic substrate diffusibility governs microbial community composition, nutrient removal performance and kinetics of granulation of aerobic granular sludge,” *Water Research X*, 4, p. 100033. Available at: <https://doi.org/10.1016/j.wroa.2019.100033>.
- Lee, E., Rout, P.R. and Bae, J. (2021) “The applicability of anaerobically treated domestic wastewater as a nutrient medium in hydroponic lettuce cultivation: Nitrogen toxicity and health risk assessment,” *Science of the Total Environment*, 780, p. 146482. Available at: <https://doi.org/10.1016/j.scitotenv.2021.146482>.
- Leng, Y. and Soares, A.P. (2021) “The mechanisms of struvite biomineralization in municipal wastewater,” *Science of the Total Environment*, 799, p. 149261. Available at: <https://doi.org/10.1016/j.scitotenv.2021.149261>.

- Lens, P.N.L. and Reddy, G.K.K. (2018) “Aerobic granular sludge technology: Mechanisms of granulation and biotechnological applications,” *Bioresource Technology*, 247, pp. 1128–1143. Available at: <https://doi.org/10.1016/j.biortech.2017.09.131>.
- Leong, H.W. *et al.* (2019) “Impact of various microalgal-bacterial populations on municipal wastewater bioremediation and its energy feasibility for lipid-based biofuel production,” *Journal of Environmental Management*, 249, p. 109384. Available at: <https://doi.org/10.1016/j.jenvman.2019.109384>.
- Li, H. *et al.* (2020) “Electrochemical disinfection of secondary effluent from a wastewater treatment plant: Removal efficiency of ARGs and variation of antibiotic resistance in surviving bacteria,” *Chemical Engineering Journal*, 392, p. 123674. Available at: <https://doi.org/10.1016/j.cej.2019.123674>.
- Li, Y. *et al.* (2018) “The Composition and Implications of Polyphosphate-Metal in Enhanced Biological Phosphorus Removal Systems,” *Environmental Science & Technology*, 53(3), pp. 1536–1544. Available at: <https://doi.org/10.1021/acs.est.8b06827>.
- Liang, Y. *et al.* (2022) “Filamentous Bacteria and Stalked Ciliates for the Stable Structure of Aerobic Granular Sludge Treating Wastewater,” *International Journal of Environmental Research and Public Health*, 19(23), p. 15747. Available at: <https://doi.org/10.3390/ijerph192315747>.
- Lim, K., Evans, P.J. and Parameswaran, P. (2019) “Long-Term Performance of a Pilot-Scale Gas-Sparged Anaerobic Membrane Bioreactor under Ambient Temperatures for Holistic Wastewater Treatment,” *Environmental Science & Technology*, 53(13), pp. 7347–7354. Available at: <https://doi.org/10.1021/acs.est.8b06198>.
- Liu, Z. *et al.* (2023) “Enhanced ammonia nitrogen removal from actual rare earth element tailings (REEs) wastewater by microalgae-bacteria symbiosis system (MBS): Ratio optimization of microalgae to bacteria and mechanism analysis,” *Bioresource Technology*, 367, p. 128304. Available at: <https://doi.org/10.1016/j.biortech.2022.128304>.
- Liwarska-Bizukojc, E. and Olejnik, D. (2020) “Activated sludge community and flocs morphology in response to aluminum oxide particles in the wastewater treatment system,” *Journal of Water Process Engineering*, 38, p. 101639. Available at: <https://doi.org/10.1016/j.jwpe.2020.101639>.
- Lopes, C. *et al.* (2021) “Nitrogen removal from poultry slaughterhouse wastewater in anaerobic-anoxic-aerobic combined reactor: Integrated effect of recirculation rate and hydraulic retention time,” *Journal of Environmental Management*, 303, p. 114162. Available at: <https://doi.org/10.1016/j.jenvman.2021.114162>.

- López-Ramón, M.V. *et al.* (2019) “Removal of bisphenols A and S by adsorption on activated carbon clothes enhanced by the presence of bacteria,” *Science of the Total Environment*, 669, pp. 767–776. Available at: <https://doi.org/10.1016/j.scitotenv.2019.03.125>.
- Lu, X. *et al.* (2023) “Social network of filamentous Sphaerotilus during activated sludge bulking: Identifying the roles of signaling molecules and verifying a novel control strategy,” *Chemical Engineering Journal*, 454, p. 140109. Available at: <https://doi.org/10.1016/j.cej.2022.140109>.
- Ma, X. *et al.* (2020) “Impact of salinity on anaerobic microbial community structure in high organic loading purified terephthalic acid wastewater treatment system,” *Journal of Hazardous Materials*, 383, p. 121132. Available at: <https://doi.org/10.1016/j.jhazmat.2019.121132>.
- Machnicka, A. and Grübel, K. (2022) “The effect of pre-treatment and anaerobic digestion for pathogens reduction in agricultural utilization of sewage sludge,” *Environmental Science and Pollution Research*, 30(5), pp. 13801–13810. Available at: <https://doi.org/10.1007/s11356-022-23164-9>.
- Maia, F.M.M. *et al.* (2022) “Influence of aeration intermittency on nitrogen removal in a reactor with aerobic granular sludge treating wastewater,” *Journal of Water Process Engineering*, 45, p. 102529. Available at: <https://doi.org/10.1016/j.jwpe.2021.102529>.
- Marchlewicz, A. *et al.* (2023) “Evaluation of the Defined Bacterial Consortium Efficacy in the Biodegradation of NSAIDs,” *Molecules*, 28(5), p. 2185. Available at: <https://doi.org/10.3390/molecules28052185>.
- Martinez, F.J. *et al.* (2018) “Techno-economical assessment of coupling Fenton/biological processes for the treatment of a pharmaceutical wastewater,” *Journal of Environmental Chemical Engineering*, 6(1), pp. 485–494. Available at: <https://doi.org/10.1016/j.jece.2017.12.008>.
- Masloń, A. (2022) “Impact of Uneven Flow Wastewater Distribution on the Technological Efficiency of a Sequencing Batch Reactor,” *Sustainability*, 14(4), p. 2405. Available at: <https://doi.org/10.3390/su14042405>.
- Masoner, J.R. *et al.* (2019) “Urban Stormwater: An Overlooked Pathway of Extensive Mixed Contaminants to Surface and Groundwaters in the United States,” *Environmental Science & Technology*, 53(17), pp. 10070–10081. Available at: <https://doi.org/10.1021/acs.est.9b02867>.
- Matheus, M.C. *et al.* (2020) “Assessing the impact of hydraulic conditions and absence of pretreatment on the treatability of pesticide formulation plant wastewater in a moving bed

- biofilm reactor,” *Journal of Water Process Engineering*, 36, p. 101243. Available at: <https://doi.org/10.1016/j.jwpe.2020.101243>.
- Mavhungu, A. *et al.* (2021) “Environmental sustainability of municipal wastewater treatment through struvite precipitation: Influence of operational parameters,” *Journal of Cleaner Production*, 285, p. 124856. Available at: <https://doi.org/10.1016/j.jclepro.2020.124856>.
- Mbamba, C.K. *et al.* (2019) “Plant-wide model-based analysis of iron dosage strategies for chemical phosphorus removal in wastewater treatment systems,” *Water Research*, 155, pp. 12–25. Available at: <https://doi.org/10.1016/j.watres.2019.01.048>.
- Mecha, A.C. *et al.* (2019) “Modelling inactivation kinetics of waterborne pathogens in municipal wastewater using ozone,” *Environmental Engineering Research*, 25(6), pp. 890–897. Available at: <https://doi.org/10.4491/eer.2019.432>.
- Medeiros, R.C., Sammarro Silva, K.J. and Daniel, L.A. (2020) “Wastewater treatment performance in microbiological removal and (oo)cyst viability assessed comparatively to fluorescence decay,” *Environmental Technology*, 43(7), pp. 962–970. Available at: <https://doi.org/10.1080/09593330.2020.1811396>.
- Meena, M., Sonigra, P. and Yadav, G. (2021) “Biological-based methods for the removal of volatile organic compounds (VOCs) and heavy metals,” *Environmental Science and Pollution Research*, 28(3), pp. 2485–2508. Available at: <https://doi.org/10.1007/s11356-020-11112-4>.
- Mehdaoui, R. *et al.* (2022) “An optimized sono-heterogeneous Fenton degradation of olive-oil mill wastewater organic matter by new magnetic glutaraldehyde-crosslinked developed cellulose,” *Environmental Science and Pollution Research*, 30(8), pp. 20450–20468. Available at: <https://doi.org/10.1007/s11356-022-23276-2>.
- Menezes, R.O. *et al.* (2021) “Reactors and active biomass potential as inoculum for nitrogen removal,” *Bioresource Technology*, 336, p. 125334. Available at: <https://doi.org/10.1016/j.biortech.2021.125334>.
- Meng, J. *et al.* (2022) “Determining Factors for Nitrite Accumulation in an Acidic Nitrifying System: Influent Ammonium Concentration, Operational pH, and Ammonia-Oxidizing Community,” *Environ. Sci. Technol.*, 56(16), pp. 11578–11588. Available at: <https://doi.org/10.1021/acs.est.1c07522>.
- Merbouh, Ch. *et al.* (2022) “Physico-Chemical Characterization of an Urban Wastewater Effluent and Its Impact on the Receiving Environment: Oued Nfifikh (Morocco),” *Journal of Ecological Engineering*, 23(3), pp. 183–193. Available at: <https://doi.org/10.12911/22998993/145464>.

- Miller Gil, L. and Fábrega Duque, J. (2022) “Reuse of Treated Domestic Wastewater by Employing Artificial Wetlands in Panama,” *Air, Soil and Water Research*, 15, p. 117862212210744. Available at: <https://doi.org/10.1177/11786221221074401>.
- Mishra, S., Nayak, J.K. and Maiti, A. (2020) “Bacteria-mediated bio-degradation of reactive azo dyes coupled with bio-energy generation from model wastewater,” *Clean Technologies and Environmental Policy*, 22(3), pp. 651–667. Available at: <https://doi.org/10.1007/s10098-020-01809-y>.
- Miyake, M. *et al.* (2022) “Efficient aerobic granular sludge production in simultaneous feeding and drawing sequencing batch reactors fed with low-strength municipal wastewater under high organic loading rate conditions,” *Biochemical Engineering Journal*, 184, p. 108469. Available at: <https://doi.org/10.1016/j.bej.2022.108469>.
- Moh, L.G., Etienne, P.T. and Kuate, J.-R. (2021) “Seasonal Diversity of Lactic Acid Bacteria in Artisanal Yoghurt and Their Antibiotic Susceptibility Pattern,” *International Journal of Food Science*, 2021, pp. 1–12. Available at: <https://doi.org/10.1155/2021/6674644>.
- Morones-Esquivel, M.M. *et al.* (2022) “Bacterial Communities in Effluents Rich in Phenol and Their Potential in Bioremediation: Kinetic Modeling,” *International Journal of Environmental Research and Public Health*, 19(21), p. 14222. Available at: <https://doi.org/10.3390/ijerph192114222>.
- Mourão, J. *et al.* (2021) “Post-treatment of swine wastewater using aerobic granular sludge: Granulation, microbiota development, and performance,” *Bioresource Technology Reports*, 16, p. 100862. Available at: <https://doi.org/10.1016/j.biteb.2021.100862>.
- Moyano, A.J.S., Delforno, T.P. and Subtil, E.L. (2021) “Simultaneous nitrification-denitrification (SND) using a thermoplastic gel as support: pollutants removal and microbial community in a pilot-scale biofilm membrane bioreactor,” *Environmental Technology*, 43(28), pp. 4411–4425. Available at: <https://doi.org/10.1080/09593330.2021.1950843>.
- Mukimin, A. *et al.* (2022) “Electrocatalytic Reaction as Efficient Removal Method for Ammonia Pollutant in Textile Wastewater,” *Research Square* [Preprint]. Available at: <https://doi.org/10.21203/rs.3.rs-2244621/v1>.
- Muriuki, C. *et al.* (2020) “Mass loading, distribution, and removal of antibiotics and antiretroviral drugs in selected wastewater treatment plants in Kenya,” *Science of the Total Environment*, 743, p. 140655. Available at: <https://doi.org/10.1016/j.scitotenv.2020.140655>.
- Murrell, K.A. and Dorman, F.L. (2020) “Characterization and quantification of methyl-benzotriazoles and chloromethyl-benzotriazoles produced from disinfection processes in

- wastewater treatment,” *Science of the Total Environment*, 699, p. 134310. Available at: <https://doi.org/10.1016/j.scitotenv.2019.134310>.
- Nawkarkar, P. *et al.* (2019) “Life cycle assessment of *Chlorella* species producing biodiesel and remediating wastewater,” *Journal of Biosciences*, 44(4). Available at: <https://doi.org/10.1007/s12038-019-9896-0>.
- Naylor, C.N. *et al.* (2019) “Validation of Calibration Parameters for Trapped Ion Mobility Spectrometry,” *Journal of the American Society for Mass Spectrometry*, 30(10), pp. 2152–2162. Available at: <https://doi.org/10.1007/s13361-019-02289-1>.
- Ndao, A. *et al.* (2021) “Biopesticide production using *Bacillus thuringiensis kurstaki* by valorization of starch industry wastewater and effluent from aerobic, anaerobic digestion,” *Systems Microbiology and Biomanufacturing*, 1(4), pp. 494–504. Available at: <https://doi.org/10.1007/s43393-021-00043-x>.
- Nguyen, P.Y. *et al.* (2023) “The impact of pH on the anaerobic and aerobic metabolism of Tetrasphaera-enriched polyphosphate accumulating organisms,” *Water Research X*, 19, p. 100177. Available at: <https://doi.org/10.1016/j.wroa.2023.100177>.
- Nguyen, T.H.O. *et al.* (2019) “Investigation of the Relationship between Bacteria Growth and Lipid Production Cultivating of Microalgae *Chlorella Vulgaris* in Seafood Wastewater,” *Energies*, 12(12), p. 2282. Available at: <https://doi.org/10.3390/en12122282>.
- Nierychlo, M. *et al.* (2021) “Low Global Diversity of *Candidatus Microthrix*, a Troublesome Filamentous Organism in Full-Scale WWTPs,” *Frontiers in Microbiology*, 12. Available at: <https://doi.org/10.3389/fmicb.2021.690251>.
- Nikel, K.E. *et al.* (2021) “Fish living near two wastewater treatment plants have unaltered thermal tolerance but show changes in organ and tissue traits,” *Journal of Great Lakes Research*, 47(2), pp. 522–533. Available at: <https://doi.org/10.1016/j.jglr.2021.01.017>.
- Noguchi, M. *et al.* (2021) “Application of real treated wastewater to starch production by microalgae: Potential effect of nutrients and microbial contamination,” *Biochemical Engineering Journal*, 169, p. 107973. Available at: <https://doi.org/10.1016/j.bej.2021.107973>.
- Nunes, M.I. *et al.* (2021) “Hydrogen sulfide levels in the ambient air of municipal solid waste management facilities: A case study in Portugal,” *Case Studies in Chemical and Environmental Engineering*, 4, p. 100152. Available at: <https://doi.org/10.1016/j.cscee.2021.100152>.
- Nuramkhaan, M. *et al.* (2019) “Isolation of microalgal strain from algal-bacterial aerobic granular sludge and examination on its contribution to granulation process during

- wastewater treatment in respect of nutrients removal, auto-aggregation capability and EPS excretion,” *Bioresource Technology Reports*, 8, p. 100330. Available at: <https://doi.org/10.1016/j.biteb.2019.100330>.
- Nxumalo, N.L. (2021) *Development of paper-based microfluidic strips for quantification of ammonia*. Available at: <https://doi.org/10.51415/10321/3218>.
- O’Brien, J.W. *et al.* (2019) “A National Wastewater Monitoring Program for a better understanding of public health: A case study using the Australian Census,” *Environment International*, 122, pp. 400–411. Available at: <https://doi.org/10.1016/j.envint.2018.12.003>.
- Odedishemi Ajibade, F. *et al.* (2021) “Total nitrogen removal in biochar amended non-aerated vertical flow constructed wetlands for secondary wastewater effluent with low C/N ratio: Microbial community structure and dissolved organic carbon release conditions,” *Bioresource Technology*, 322, p. 124430. Available at: <https://doi.org/10.1016/j.biortech.2020.124430>.
- Oeschger, T.M. *et al.* (2021) “Early Warning Diagnostics for Emerging Infectious Diseases in Developing into Late-Stage Pandemics,” *Accounts of Chemical Research*, 54(19), pp. 3656–3666. Available at: <https://doi.org/10.1021/acs.accounts.1c00383>.
- Oliveira, G.A. *et al.* (2021) “Floating treatment wetlands in domestic wastewater treatment as a decentralized sanitation alternative,” *Science of the Total Environment*, 773, p. 145609. Available at: <https://doi.org/10.1016/j.scitotenv.2021.145609>.
- Omwene, P.I., Koby, M. and Can, O.T. (2018) “Phosphorus removal from domestic wastewater in electrocoagulation reactor using aluminium and iron plate hybrid anodes,” *Ecological Engineering*, 123, pp. 65–73. Available at: <https://doi.org/10.1016/j.ecoleng.2018.08.025>.
- Optimization of an electrocoagulation-flotation system for domestic wastewater treatment and reuse* (no date). Available at: <https://www.tandfonline.com/doi/full/10.1080/09593330.2019.1709905>.
- Orhon, D. and Sözen, S. (2020) “Reshaping the activated sludge process: has the time come or passed?,” *Journal of Chemical Technology & Biotechnology*, 95(6), pp. 1632–1639. Available at: <https://doi.org/10.1002/jctb.6290>.
- Osińska, A. *et al.* (2019) “Quantitative Occurrence of Antibiotic Resistance Genes among Bacterial Populations from Wastewater Treatment Plants Using Activated Sludge,” *Applied Sciences*, 9(3), p. 387. Available at: <https://doi.org/10.3390/app9030387>.

- Pachiega, R. *et al.* (2019) “Hydrogen bioproduction with anaerobic bacteria consortium from brewery wastewater,” *International Journal of Hydrogen Energy*, 44(1), pp. 155–163. Available at: <https://doi.org/10.1016/j.ijhydene.2018.02.107>.
- Paddock, M.B., Fernández-Bayo, J.D. and VanderGheynst, J.S. (2020) “The effect of the microalgae-bacteria microbiome on wastewater treatment and biomass production,” *Applied Microbiology and Biotechnology*, 104(2), pp. 893–905. Available at: <https://doi.org/10.1007/s00253-019-10246-x>.
- Padri, M. *et al.* (2022) “Application of *Aspergillus niger* F5 as an alternative technique to harvest microalgae and as a phosphorous removal treatment for cassava biogas effluent wastewater,” *Journal of Water Process Engineering*, 46, p. 102524. Available at: <https://doi.org/10.1016/j.jwpe.2021.102524>.
- Pajerski, W. *et al.* (2019) “Attachment efficiency of gold nanoparticles by Gram-positive and Gram-negative bacterial strains governed by surface charges,” *Journal of Nanoparticle Research*, 21(8). Available at: <https://doi.org/10.1007/s11051-019-4617-z>.
- Pan, Y. *et al.* (2012) “Effect of pH on N₂O reduction and accumulation during denitrification by methanol utilizing denitrifiers,” *Water Research*, 46(15), pp. 4832–4840. Available at: <https://doi.org/10.1016/j.watres.2012.06.003>.
- Papini, G. *et al.* (2022) “Boosting aerobic microbial protein productivity and quality on brewery wastewater: Impact of anaerobic acidification, high-rate process and biomass age,” *Bioresource Technology*, 368, p. 128285. Available at: <https://doi.org/10.1016/j.biortech.2022.128285>.
- Park, S.-E. and Seungdae, O. (2020) “Inhibitory mechanisms and fate of the analgesic drug acetaminophen in nitrifying activated sludge,” *Journal of Hazardous Materials*, 399, p. 123104. Available at: <https://doi.org/10.1016/j.jhazmat.2020.123104>.
- Parolini, M. (2020) “Toxicity of the Non-Steroidal Anti-Inflammatory Drugs (NSAIDs) acetylsalicylic acid, paracetamol, diclofenac, ibuprofen and naproxen towards freshwater invertebrates: A review,” *Science of the Total Environment*, 740, p. 140043. Available at: <https://doi.org/10.1016/j.scitotenv.2020.140043>.
- Pathiraja, G. *et al.* (2019) “Effective degradation of polychlorinated biphenyls by a facultative anaerobic bacterial consortium using alternating anaerobic aerobic treatments,” *Science of the Total Environment*, 659, pp. 507–514. Available at: <https://doi.org/10.1016/j.scitotenv.2018.12.385>.

- Pechaud, Y. *et al.* (2021) “Size of biological flocs in activated sludge systems: Influence of hydrodynamic parameters at different scales,” *Journal of Environmental Chemical Engineering*, 9(4), p. 105427. Available at: <https://doi.org/10.1016/j.jece.2021.105427>.
- Pelivano, B. *et al.* (2021) “Application of pyritic sludge with an anaerobic granule consortium for nitrate removal in low carbon systems,” *Water Research*, 209, p. 117933. Available at: <https://doi.org/10.1016/j.watres.2021.117933>.
- Pellegrini, L. (2020) *Digital Transition and Waste Management in Architecture, Engineering, Construction, and Operations Industry*. Available at: <https://www.frontiersin.org/articles/10.3389/fenrg.2020.576462/full> (Accessed: November 4, 2022).
- Pereira, A.S.A.D.P. *et al.* (2021) “Organomineral fertilizers pastilles from microalgae grown in wastewater: Ammonia volatilization and plant growth,” *Science of the Total Environment*, 779, p. 146205. Available at: <https://doi.org/10.1016/j.scitotenv.2021.146205>.
- Persson, T., Persson, K.M. and Åström, J. (2021) “Ferric Oxide-Containing Waterworks Sludge Reduces Emissions of Hydrogen Sulfide in Biogas Plants and the Needs for Virgin Chemicals,” *Sustainability*, 13(13), p. 7416. Available at: <https://doi.org/10.3390/su13137416>.
- Phanwilai, S. *et al.* (2020) “Nitrogen removal efficiencies and microbial communities in full-scale IFAS and MBBR municipal wastewater treatment plants at high COD:N ratio,” *Frontiers of Environmental Science & Engineering*, 14(6). Available at: <https://doi.org/10.1007/s11783-020-1374-2>.
- Phuong, T. *et al.* (2022) “Study on Leaching of Phosphate from Municipal Wastewater Treatment Plant’s Sewage Sludge and Followed by Adsorption on Mg-Al Layered Double Hydroxide,” *Journal of Nanomaterials*. Edited by G. Sharma, 2022, pp. 1–9. Available at: <https://doi.org/10.1155/2022/1777187>.
- Picos-Corrales, L.A. *et al.* (2020) “Environment-Friendly Approach toward the Treatment of Raw Agricultural Wastewater and River Water via Flocculation Using Chitosan and Bean Straw Flour as Bioflocculants,” *ACS Omega*, 5(8), pp. 3943–3951. Available at: <https://doi.org/10.1021/acsomega.9b03419>.
- Pluciennik-Koropczuk, E., Myszograj, M. and Myszograj, S. (2021) “The Influence of the Poles’ Lifestyle on the Quantity and Quality of Municipal Wastewater,” *Civil and Environmental Engineering Reports*, 31(3), pp. 265–275. Available at: <https://doi.org/10.2478/ceer-2021-0045>.

- Preisner, M. *et al.* (2021) “Application of activated sludge model for phosphorus recovery potential simulation,” *DESALINATION AND WATER TREATMENT*, 232, pp. 199–207. Available at: <https://doi.org/10.5004/dwt.2021.27231>.
- Purba, L.D.A. *et al.* (2020) “Various applications of aerobic granular sludge: A review,” *Environmental Technology and Innovation*, 20, p. 101045. Available at: <https://doi.org/10.1016/j.eti.2020.101045>.
- Qian, J. *et al.* (2023) “Insight into the formation mechanism of algal biofilm in soy sauce wastewater,” *Journal of Cleaner Production*, p. 136179. Available at: <https://doi.org/10.1016/j.jclepro.2023.136179>.
- Quoc, B.N. *et al.* (2021) “Aerobic granular sludge: Impact of size distribution on nitrification capacity,” *Water Research*, 188, p. 116445. Available at: <https://doi.org/10.1016/j.watres.2020.116445>.
- Rani, S. *et al.* (2021) “Microalga-Mediated Tertiary Treatment of Municipal Wastewater: Removal of Nutrients and Pathogens,” *Sustainability*, 13(17), p. 9554. Available at: <https://doi.org/10.3390/su13179554>.
- Regmi, P. *et al.* (2021) “Combining continuous flow aerobic granulation using an external selector and carbon-efficient nutrient removal with AvN control in a full-scale simultaneous nitrification-denitrification process,” *Water Research*, 210, p. 117991. Available at: <https://doi.org/10.1016/j.watres.2021.117991>.
- Restivo, V.E. *et al.* (2021) “Rainbow darter (*Etheostoma caeruleum*) from a river impacted by municipal wastewater effluents have altered gut content microbiomes,” *Science of the Total Environment*, 751, p. 141724. Available at: <https://doi.org/10.1016/j.scitotenv.2020.141724>.
- Roche, C. *et al.* (2021) “Biological process architecture in continuous-flow activated sludge by gravimetry: Controlling densified biomass form and function in a hybrid granule–floc process at Dijon WRRF, France,” *Water Environment Research*, 94(1). Available at: <https://doi.org/10.1002/wer.1664>.
- Rodriguez-Mozaz, S. *et al.* (2020) “Antibiotic residues in final effluents of European wastewater treatment plants and their impact on the aquatic environment,” *Environment International*, 140, p. 105733. Available at: <https://doi.org/10.1016/j.envint.2020.105733>.
- Rohyami, Y., Berliana, C.D. and Wati, D.A. (2022) *Verification method on determination of chemical oxygen demand for hospital wastewater*, *AIP Conference Proceedings*. American Institute of Physics. Available at: <https://doi.org/10.1063/5.0112736>.

- Rolewicz-Kalińska, A., Lelicińska-Serafin, K. and Manczarski, P. (2021) “Volatile organic compounds, ammonia and hydrogen sulphide removal using a two-stage membrane biofiltration process,” *Chemical Engineering Research and Design*, 165, pp. 69–80. Available at: <https://doi.org/10.1016/j.cherd.2020.10.017>.
- Rongsayamanont, C. *et al.* (2020) “Inhibitory effect of phenol on wastewater ammonification,” *Bioresource Technology*, 309, p. 123312. Available at: <https://doi.org/10.1016/j.biortech.2020.123312>.
- Roots, P. *et al.* (2020) “Integrated shortcut nitrogen and biological phosphorus removal from mainstream wastewater: process operation and modeling,” *Environmental Science: Water Research & Technology*, 6(3), pp. 566–580. Available at: <https://doi.org/10.1039/c9ew00550a>.
- Rossi, L. *et al.* (2018) “RAVITA Technology – new innovation for combined phosphorus and nitrogen recovery,” *Water Science and Technology*, 78(12), pp. 2511–2517. Available at: <https://doi.org/10.2166/wst.2019.011>.
- Ruas, G. *et al.* (2021) “Removal of pathogens from domestic wastewater by microalgal-bacterial systems under different cultivation conditions,” *International Journal of Environmental Science and Technology*, 19(10), pp. 10177–10188. Available at: <https://doi.org/10.1007/s13762-021-03820-2>.
- Russel, M. *et al.* (2020) “Investigating the potentiality of *Scenedesmus obliquus* and *Acinetobacter pittii* partnership system and their effects on nutrients removal from synthetic domestic wastewater,” *Bioresource Technology*, 299, p. 122571. Available at: <https://doi.org/10.1016/j.biortech.2019.122571>.
- Sadek, A.H., Asker, M.S. and Abdelhamid, S.A. (2021) “Bacteriostatic impact of nanoscale zero-valent iron against pathogenic bacteria in the municipal wastewater,” *Biologia*, 76(9), pp. 2785–2809. Available at: <https://doi.org/10.1007/s11756-021-00814-w>.
- Saikia, R., Chetia, D. and Bhattacharyya, K.G. (2021) “Estimation of uranium in groundwater and assessment of age-dependent radiation dose in Nalbari district of Assam, India,” *SN Applied Sciences*, 3(1). Available at: <https://doi.org/10.1007/s42452-020-04071-5>.
- Salehiziri, M. *et al.* (2020) “Investigating the influences of quorum quenching and nutrient conditions on activated sludge flocs at a short-time scale,” *Chemosphere*, 248, p. 125917. Available at: <https://doi.org/10.1016/j.chemosphere.2020.125917>.
- Salmi, P. *et al.* (2021) “Particle balance and return loops for microplastics in a tertiary-level wastewater treatment plant,” *Water Science and Technology*, 84(1), pp. 89–100. Available at: <https://doi.org/10.2166/wst.2021.209>.

- Sanin, D. and Vesilind, P.A. (2000) “Bioflocculation of Activated Sludge: The Role of Calcium Ions and Extracellular Polymers,” *Environmental Technology* [Preprint]. Available at: <https://doi.org/10.1080/09593332208618170>.
- Sarma, S.J., Tay, J.-H. and Chu, A.C. (2017) “Finding Knowledge Gaps in Aerobic Granulation Technology,” *Trends in Biotechnology*, 35(1), pp. 66–78. Available at: <https://doi.org/10.1016/j.tibtech.2016.07.003>.
- Sarvajith, M. and Lens, P.N.L. (2022) “Concurrent tellurite reduction, biogenesis of elemental tellurium nanostructures and biological nutrient removal in aerobic granular sludge sequencing batch reactor,” *Journal of Environmental Chemical Engineering*, 10(6), p. 108511. Available at: <https://doi.org/10.1016/j.jece.2022.108511>.
- Sbahi, S. *et al.* (2020) “Neural network and cubist algorithms to predict fecal coliform content in treated wastewater by multi-soil-layering system for potential reuse,” *Journal of Environmental Quality*, 50(1), pp. 144–157. Available at: <https://doi.org/10.1002/jeq2.20176>.
- Scholes, R.C., Prasse, C. and Sedlak, D.L. (2019) “The Role of Reactive Nitrogen Species in Sensitized Photolysis of Wastewater-Derived Trace Organic Contaminants,” *Environmental Science & Technology*, 53(11), pp. 6483–6491. Available at: <https://doi.org/10.1021/acs.est.9b01386>.
- Scott, I.S.P.C. and Penn, C.J. (2021) “Estimating the variability of steel slag properties and their influence in phosphorus removal ability,” *Chemosphere*, 276, p. 130205. Available at: <https://doi.org/10.1016/j.chemosphere.2021.130205>.
- Searle, P.L. (1984) “The berthelot or indophenol reaction and its use in the analytical chemistry of nitrogen. A review,” *Analyst*, 109(5), p. 549. Available at: <https://doi.org/10.1039/an9840900549>.
- Sedlacek, C.J. *et al.* (2020) “Transcriptomic Response of *Nitrosomonas europaea* Transitioned from Ammonia- to Oxygen-Limited Steady-State Growth,” *MSystems*, 5(1). Available at: <https://doi.org/10.1128/msystems.00562-19>.
- Sedlacek, P. *et al.* (2019) “PHA granules help bacterial cells to preserve cell integrity when exposed to sudden osmotic imbalances,” *New Biotechnology*, 49, pp. 129–136. Available at: <https://doi.org/10.1016/j.nbt.2018.10.005>.
- Seghiri, R., Kharbach, M. and Essamri, A. (2019) “Functional Composition, Nutritional Properties, and Biological Activities of Moroccan *Spirulina* Microalga,” *Journal of Food Quality*, 2019, pp. 1–11. Available at: <https://doi.org/10.1155/2019/3707219>.

- Seviour, R.J., Mino, T. and Onuki, M. (2003) “The microbiology of biological phosphorus removal in activated sludge systems,” *Fems Microbiology Reviews*, 27(1), pp. 99–127. Available at: [https://doi.org/10.1016/s0168-6445\(03\)00021-4](https://doi.org/10.1016/s0168-6445(03)00021-4).
- Sgroi, M. *et al.* (2018) “Modeling emerging contaminants breakthrough in packed bed adsorption columns by UV absorbance and fluorescing components of dissolved organic matter,” *Water Research*, 145, pp. 667–677. Available at: <https://doi.org/10.1016/j.watres.2018.09.018>.
- Shahid, A. *et al.* (2021) “Characterization of a newly isolated cyanobacterium *Plectonema terebrans* for biotransformation of the wastewater-derived nutrients to biofuel and high-value bioproducts,” *Journal of Water Process Engineering*, 39, p. 101702. Available at: <https://doi.org/10.1016/j.jwpe.2020.101702>.
- Shameem, K.S. and Chacko, S.P. (2023) “A Review on the Stability, Sustainability, Storage and Rejuvenation of Aerobic Granular Sludge for Wastewater Treatment,” *Water*, 15(5), p. 950. Available at: <https://doi.org/10.3390/w15050950>.
- Shao, X.-T. *et al.* (2021) “Spatial analysis of metformin use compared with nicotine and caffeine consumption through wastewater-based epidemiology in China,” *Ecotoxicology and Environmental Safety*, 208, p. 111623. Available at: <https://doi.org/10.1016/j.ecoenv.2020.111623>.
- Sharma, B. and Shukla, P. (2021) “A comparative analysis of heavy metal bioaccumulation and functional gene annotation towards multiple metal resistant potential by *Ochrobactrum intermedium* BPS-20 and *Ochrobactrum ciceri* BPS-26,” *Bioresource Technology*, 320, p. 124330. Available at: <https://doi.org/10.1016/j.biortech.2020.124330>.
- Sheik, A., Seepana, M.M. and Rao, A.S. (2021) “Supervisory control configurations design for nitrogen and phosphorus removal in wastewater treatment plants,” *Water Environment Research*, 93(8), pp. 1289–1302. Available at: <https://doi.org/10.1002/wer.1512>.
- Sher, F. *et al.* (2021) “Coupling of electrocoagulation and powder activated carbon for the treatment of sustainable wastewater,” *Environmental Science and Pollution Research*, 28(35), pp. 48505–48516. Available at: <https://doi.org/10.1007/s11356-021-14129-5>.
- Shi, Y.-Q. *et al.* (2022) “Enhanced denitrification of sewage via bio-microcapsules embedding heterotrophic nitrification-aerobic denitrification bacteria *Acinetobacter pittii* SY9 and *com cob*,” *Bioresource Technology*, 358, p. 127260. Available at: <https://doi.org/10.1016/j.biortech.2022.127260>.
- Shrestha, S. *et al.* (2019) “Unravelling the influences of sewer-dosed iron salts on activated sludge properties with implications on settleability, dewaterability and sludge rheology,”

- Water Research*, 167, p. 115089. Available at: <https://doi.org/10.1016/j.watres.2019.115089>.
- Singh, P. *et al.* (2021) “Utilization of wastewater as nutrient media and biomass valorization in marine Chrysophytes- Chaetoceros and Isochrysis,” *Energy Conversion and Management: X* [Preprint]. Available at: <https://doi.org/10.1016/j.ecmx.2020.100062>.
- Sinlapacheewa, P., Sriariyanun, M. and Pornwongthong, P. (2023) “Effects of total dissolved solids and organic loadings on the chemical oxygen demand removal by yeast-activated sludge system,” *IOP Conference Series*, 1146(1), p. 012001. Available at: <https://doi.org/10.1088/1755-1315/1146/1/012001>.
- Smoliński, A. *et al.* (2019) “The Bioconversion of Sewage Sludge to Bio-Fuel: The Environmental and Economic Benefits,” *Materials*, 12(15), p. 2417. Available at: <https://doi.org/10.3390/ma12152417>.
- Sobczyk, M. *et al.* (2021) “Multivariate analysis of activated sludge community in full-scale wastewater treatment plants,” *Environmental Science and Pollution Research*, 28(3), pp. 3579–3589. Available at: <https://doi.org/10.1007/s11356-020-10684-5>.
- Soroosh, H., Otterpohl, R. and Hanelt, D. (2022) “Influence of hydraulic retention time on municipal wastewater treatment using microalgae-bacteria flocs in sequencing batch reactors,” *Bioresource Technology Reports*, 17, p. 100884. Available at: <https://doi.org/10.1016/j.biteb.2021.100884>.
- Spencer-Williams, I. *et al.* (2022) “Exploring the Impacts of Full-Scale Distribution System Orthophosphate Corrosion Control Implementation on the Microbial Ecology of Hydrologically Connected Urban Streams,” *Microbiology Spectrum* [Preprint]. Edited by J.A. Gralnick. Available at: <https://doi.org/10.1128/spectrum.02158-22>.
- Standard Methods Committee of the American Public Health Association, American Water Works Association, and Water Environment Federation. (2018) *4500-NO₃ – NITROGEN (NITRATE)*. Available at: <https://www.standardmethods.org/doi/10.2105/SMWW.2882.089> (Accessed: March 16, 2023).
- Standard Methods Committee of the American Public Health Association, American Water Works Association, and Water Environment Federation. *4500-p phosphorus In: Standard Methods For the Examination of Water and Wastewater*. Lipps WC, Baxter TE, Braun-Howland E (ed.) (2018) *4500-P PHOSPHORUS*. Available at: <https://www.standardmethods.org/doi/10.2105/SMWW.2882.093> (Accessed: March 25, 2023).

- Stiborova, H. *et al.* (2020) “Diversity and phylogenetic composition of bacterial communities and their association with anthropogenic pollutants in sewage sludge,” *Chemosphere*, 238, p. 124629. Available at: <https://doi.org/10.1016/j.chemosphere.2019.124629>.
- Strubbe, L. *et al.* (2022) “Continuous aerobic granular sludge plants: Better settling versus diffusion limitation,” *Chemical Engineering Journal*, 428, p. 131427. Available at: <https://doi.org/10.1016/j.cej.2021.131427>.
- Struk-Sokołowska, J. *et al.* (2022) “Analysis of 1H-benzotriazole removal efficiency from wastewater in individual process phases of a sequencing batch reactor SBR,” *Water Resources and Industry*, 28, p. 100182. Available at: <https://doi.org/10.1016/j.wri.2022.100182>.
- Štumpf, S. *et al.* (2020) “Generation Times of E. coli Prolong with Increasing Tannin Concentration while the Lag Phase Extends Exponentially,” *Plants*, 9(12), p. 1680. Available at: <https://doi.org/10.3390/plants9121680>.
- Subhashree Devasena, S. *et al.* (2020) “Assessment of fish scale biosorbent in the treatment of seafood processing plant wastewater,” *Journal of Chemical Technology & Biotechnology*, 96(3), pp. 723–731. Available at: <https://doi.org/10.1002/jctb.6585>.
- Sudiarto, S.I.A., Renggaman, A. and Choi, H.L. (2019) “Floating aquatic plants for total nitrogen and phosphorus removal from treated swine wastewater and their biomass characteristics,” *Journal of Environmental Management*, 231, pp. 763–769. Available at: <https://doi.org/10.1016/j.jenvman.2018.10.070>.
- Sun, H. *et al.* (2022) “Aerobic starvation treatment of activated sludge enhances the degradation efficiency of refractory organic compounds,” *Water Research*, 224, p. 119069. Available at: <https://doi.org/10.1016/j.watres.2022.119069>.
- Sun, Y.-X. *et al.* (2021) “Physical pretreatment of petroleum refinery wastewater instead of chemicals addition for collaborative removal of oil and suspended solids,” *Journal of Cleaner Production*, 278, p. 123821. Available at: <https://doi.org/10.1016/j.jclepro.2020.123821>.
- Sur, D.H. and Mukhopadhyay, M. (2019) “Role of zinc oxide nanoparticles for effluent treatment using *Pseudomonas putida* and *Pseudomonas aureofaciens*,” *Bioprocess and Biosystems Engineering*, 42(2), pp. 187–198. Available at: <https://doi.org/10.1007/s00449-018-2024-y>.
- Suryawan, I.W.K. *et al.* (2021) “NH₃-N and COD Reduction in Endek (Balinese Textile) Wastewater by Activated Sludge under Different DO Condition with Ozone Pretreatment,”

- Walailak Journal of Science and Technology*, 18(6). Available at: <https://doi.org/10.48048/wjst.2021.9127>.
- Sutherland, D.L. *et al.* (2021) “Ammonia, pH and dissolved inorganic carbon supply drive whole pond metabolism in full-scale wastewater high rate algal ponds,” *Algal Research*, 58, p. 102405. Available at: <https://doi.org/10.1016/j.algal.2021.102405>.
- Symonds, E.M., Rosario, K. and Breitbart, M. (2019) “Pepper mild mottle virus: Agricultural menace turned effective tool for microbial water quality monitoring and assessing (waste)water treatment technologies,” *PLOS Pathogens*. Edited by K.R. Spindler, 15(4), p. e1007639. Available at: <https://doi.org/10.1371/journal.ppat.1007639>.
- Tadda, M.A. *et al.* (2021) “Enhancement of nitrite/ammonia removal from saline recirculating aquaculture wastewater system using moving bed bioreactor,” *Journal of Environmental Chemical Engineering*, 9(5), p. 105947. Available at: <https://doi.org/10.1016/j.jece.2021.105947>.
- Tamayo, L. *et al.* (2020) “Does Bacterial Elasticity Affect Adhesion to Polymer Fibers?,” *ACS Applied Materials & Interfaces*, 12(12), pp. 14507–14517. Available at: <https://doi.org/10.1021/acsami.9b21060>.
- Thanh-Nho, N. *et al.* (2022) *Interfering ions and controlling their effects on the direct analysis of total dissolved ammonia nitrogen in aquacultural wastewater using molecular absorption spectrophotometry, Nucleation and Atmospheric Aerosols*. American Institute of Physics. Available at: <https://doi.org/10.1063/5.0099821>.
- Thiruchelva, S.R. *et al.* (2020) “<i>ASSESSMENT OF ENVIRONMENTAL IMPACTS IN THE UNTREATED URBAN WASTEWATER IRRIGATED SITES – A CASE STUDY</i>,” *2020 ASABE Annual International Virtual Meeting, July 13-15, 2020* [Preprint]. Available at: <https://doi.org/10.13031/aim.202001193>.
- Thomas, B.J. *et al.* (2022) “Decentralized high-strength wastewater treatment using a compact aerobic baffled bioreactor,” *Journal of Environmental Management*, 305, p. 114281. Available at: <https://doi.org/10.1016/j.jenvman.2021.114281>.
- Thompson, J.R. *et al.* (2020) “Making waves: Wastewater surveillance of SARS-CoV-2 for population-based health management,” *Water Research*, 184, p. 116181. Available at: <https://doi.org/10.1016/j.watres.2020.116181>.
- Tirkey, V. *et al.* (2022) “Short sludge age denitrification as alternative process for energy and nutrient recovery,” *Bioresource Technology*, 366, p. 128184. Available at: <https://doi.org/10.1016/j.biortech.2022.128184>.

- Trego, A.C., Mills, S. and Collins, G. (2021) “Granular biofilms: Function, application, and new trends as model microbial communities,” *Critical Reviews in Environmental Science and Technology*, 51(15), pp. 1702–1725. Available at: <https://doi.org/10.1080/10643389.2020.1769433>.
- Udaiyappan, A.F.M. *et al.* (2020) “Microalgae-bacteria interaction in palm oil mill effluent treatment,” *Journal of Water Process Engineering*, 35, p. 101203. Available at: <https://doi.org/10.1016/j.jwpe.2020.101203>.
- Uma, V.S. *et al.* (2023) “Development of marine activated algal-bacterial granule: A novel replacement to the conventional algal remediation processes,” *Algal Research-Biomass Biofuels and Bioproducts*, 69, p. 102914. Available at: <https://doi.org/10.1016/j.algal.2022.102914>.
- Umezawa, K. *et al.* (2020) “Disproportionation of inorganic sulfur compounds by a novel autotrophic bacterium belonging to Nitrospirota,” *Systematic and Applied Microbiology*, 43(5), p. 126110. Available at: <https://doi.org/10.1016/j.syapm.2020.126110>.
- Van Gijn, K. *et al.* (2021) “Optimizing biological effluent organic matter removal for subsequent micropollutant removal,” *Journal of Environmental Chemical Engineering*, 9(5), p. 106247. Available at: <https://doi.org/10.1016/j.jece.2021.106247>.
- Vecino, X. *et al.* (2019) “Liquid fertilizer production by ammonia recovery from treated ammonia-rich regenerated streams using liquid-liquid membrane contactors,” *Chemical Engineering Journal*, 360, pp. 890–899. Available at: <https://doi.org/10.1016/j.cej.2018.12.004>.
- Verma, M., Borah, R., *et al.* (2022) “Capturing of inorganic and organic pollutants simultaneously from complex wastewater using recyclable magnetically chitosan functionalized with EDTA adsorbent,” *Process Safety and Environmental Protection*, 167, pp. 56–66. Available at: <https://doi.org/10.1016/j.psep.2022.09.009>.
- Verma, M., Lee, I., *et al.* (2022) “Multifunctional β -Cyclodextrin-EDTA-Chitosan polymer adsorbent synthesis for simultaneous removal of heavy metals and organic dyes from wastewater,” *Environmental Pollution*, 292, p. 118447. Available at: <https://doi.org/10.1016/j.envpol.2021.118447>.
- Verma, M. *et al.* (2023) “Co-Treatment of Stabilized Landfill Leachate and Municipal Wastewater In A Granular Activated Carbon-Sequencing Batch Reactor (GAC-SBR),” *Chemical Engineering Research & Design* [Preprint]. Available at: <https://doi.org/10.1016/j.psep.2023.04.015>.

- Vunain, E. *et al.* (2019) “Evaluation of coagulating efficiency and water borne pathogens reduction capacity of Moringa oleifera seed powder for treatment of domestic wastewater from Zomba, Malawi,” *Journal of Environmental Chemical Engineering*, 7(3), p. 103118. Available at: <https://doi.org/10.1016/j.jece.2019.103118>.
- Wang, S. *et al.* (2020) “Promising carbon utilization for nitrogen recovery in low strength wastewater treatment: Ammonia nitrogen assimilation, protein production and microbial community structure,” *Science of the Total Environment*, 710, p. 136306. Available at: <https://doi.org/10.1016/j.scitotenv.2019.136306>.
- Wei, S.P. *et al.* (2021) “Partitioning of nutrient removal contribution between granules and flocs in a hybrid granular activated sludge system,” *Water Research*, 203, p. 117514. Available at: <https://doi.org/10.1016/j.watres.2021.117514>.
- Yan, T. *et al.* (2018) “Municipal Wastewater as a Microbial Surveillance Platform for Enteric Diseases: A Case Study for *Salmonella* and Salmonellosis,” *Environmental Science & Technology*, 52(8), pp. 4869–4877. Available at: <https://doi.org/10.1021/acs.est.8b00163>.
- Yekta, S.S. *et al.* (2019) “Molecular characterization of particulate organic matter in full scale anaerobic digesters: An NMR spectroscopy study,” *Science of the Total Environment*, 685, pp. 1107–1115. Available at: <https://doi.org/10.1016/j.scitotenv.2019.06.264>.
- Young, J.C. and Vanrolleghem, P.A. (2021) “Carbonaceous vs. total biochemical oxygen demand as a basis for WRRF design and performance monitoring,” *Water Environment Research*, 93(9), pp. 1510–1515. Available at: <https://doi.org/10.1002/wer.1541>.
- Yuan, K., Li, S. and Zhong, F. (2020) “Treatment of coking wastewater in biofilm-based bioaugmentation process: Biofilm formation and microbial community analysis,” *Journal of Hazardous Materials*, 400, p. 123117. Available at: <https://doi.org/10.1016/j.jhazmat.2020.123117>.
- Yulisa, A. *et al.* (2022) “Enhancement of Voting Regressor Algorithm on Predicting Total Ammonia Nitrogen Concentration in Fish Waste Anaerobiosis,” *Waste and Biomass Valorization*, 14(2), pp. 461–478. Available at: <https://doi.org/10.1007/s12649-022-01811-z>.
- Zafar, R. *et al.* (2021) “Occurrence and quantification of prevalent antibiotics in wastewater samples from Rawalpindi and Islamabad, Pakistan,” *Science of the Total Environment*, 764, p. 142596. Available at: <https://doi.org/10.1016/j.scitotenv.2020.142596>.
- Zaghloul, M.S. *et al.* (2020) “Comparison of adaptive neuro-fuzzy inference systems (ANFIS) and support vector regression (SVR) for data-driven modelling of aerobic granular sludge

- reactors,” *Journal of Environmental Chemical Engineering*, 8(3), p. 103742. Available at: <https://doi.org/10.1016/j.jece.2020.103742>.
- Zajac-Woźnialis, A. *et al.* (2023) “Efficiency of Diclofenac Removal Using Activated Sludge in a Dynamic System (SBR Reactor) with Variable Parameters of pH, Concentration, and Sludge Oxygenation,” *Materials*, 16(4), p. 1422. Available at: <https://doi.org/10.3390/ma16041422>.
- Zhang, L. *et al.* (2012) “Degradation of paracetamol by pure bacterial cultures and their microbial consortium,” *Applied Microbiology and Biotechnology*, 97(8), pp. 3687–3698. Available at: <https://doi.org/10.1007/s00253-012-4170-5>.
- Zhao, J. *et al.* (2020) “Anaerobic co-digestion of hydrolysate from anaerobically digested sludge with raw waste activated sludge: Feasibility assessment of a new sewage sludge management strategy in the context of a local wastewater treatment plant,” *Bioresource Technology*, 314, p. 123748. Available at: <https://doi.org/10.1016/j.biortech.2020.123748>.
- Zheng, K. *et al.* (2021) “Enhanced proteins and amino acids production based on ammonia nitrogen assimilation and sludge increment by the integration of bioadsorption with anaerobic-anoxic-oxic (AAO) process,” *Chemosphere*, 280, p. 130721. Available at: <https://doi.org/10.1016/j.chemosphere.2021.130721>.
- Zhou, L., Zhou, H. and Yang, X. (2019) “Preparation and performance of a novel starch-based inorganic/organic composite coagulant for textile wastewater treatment,” *Separation and Purification Technology*, 210, pp. 93–99. Available at: <https://doi.org/10.1016/j.seppur.2018.07.089>.
- Zhou, Y. *et al.* (2022) “Enhanced nitrogen removal of aquaculture wastewater in the combined biological aerated filter: the effect of GAC location setting,” *Journal of Chemical Technology & Biotechnology*, 97(9), pp. 2519–2527. Available at: <https://doi.org/10.1002/jctb.7112>.
- Zhou, Z., Qi, M. and Wang, H. (2020) “Achieving Partial Nitrification via Intermittent Aeration in SBR and Short-Term Effects of Different C/N Ratios on Reactor Performance and Microbial Community Structure,” *Water*, 12(12), p. 3485. Available at: <https://doi.org/10.3390/w12123485>.
- Zhao, J. (2017) Biodegradation of dihydroxybenzenes (hydroquinone, catechol and resorcinol) by granules enriched with phenol in an aerobic granular sequencing batch reactor. Available at: <https://doi.org/10.7298/x4jq0z1h>.

- Zhu, Z. *et al.* (2023) “Antibacterial performance of electrodeposited Cu@Cu₂O coatings on concrete using printed circuit board wastewater,” *Journal of Cleaner Production*, 383, p. 135373. Available at: <https://doi.org/10.1016/j.jclepro.2022.135373>.
- Ziajahromi, S. *et al.* (2021) “An audit of microplastic abundance throughout three Australian wastewater treatment plants,” *Chemosphere*, 263, p. 128294. Available at: <https://doi.org/10.1016/j.chemosphere.2020.128294>.
- Zorgani, A.E. *et al.* (2020) “Evaluation of South African Sand/Zero-Valent Iron Combinations for the Treatment of Nitrate-Contaminated Water: Kinetic and Effect of Competitive Ions,” *Water, Air, & Soil Pollution*, 231(6). Available at: <https://doi.org/10.1007/s11270-020-04643-6>.
- Zhang, X. *et al.* (2022) “Bacterial diversity evolution process based on physicochemical characteristics of sludge treating hydroquinone during acclimation,” *Environmental Science and Pollution Research [Preprint]*. Available at: <https://doi.org/10.1007/s11356-021-17325-5>.